# National assessment of chemicals associated with coal seam gas extraction in Australia

*Technical report number 4*

## Literature review: Hydraulic fracture growth and well integrity

This report was prepared by CSIRO

Australian Government
Department of the Environment and Energy
Department of Health
National Industrial Chemicals Notification and Assessment Scheme

CSIRO

The National assessment of chemicals associated with coal seam gas extraction in Australia was commissioned by the Department of the Environment and Energy and prepared in collaboration with NICNAS and CSIRO

# Copyright

© Copyright Commonwealth of Australia, 2017.

This report is licensed by the Commonwealth of Australia for use under a Creative Commons Attribution 4.0 International licence, with the exception of the Coat of Arms of the Commonwealth of Australia, the logo of the agencies involved in producing and publishing the report, content supplied by third parties, and any images depicting people. For licence conditions see: https://creativecommons.org/licenses/by/4.0/

For written permission to use the information or material from this site, please contact the Department of the Environment and Energy at e-mail http://www.environment.gov.au/webform/website-feedback or by phone on 1800 803 772. Alternatively, you can write requesting copyright information to:

Office of Water Science
Department of the Environment and Energy
GPO Box 787
CANBERRA ACT 2601
Australia

# Citation

This report should be cited as:

Jeffrey R, Wu B, Bunger A, Zhang X, Chen Z, Kear J and Kasperczyk D 2017, *Literature review: Hydraulic fracture growth and well integrity*, Project report, prepared by the Commonwealth Scientific and Industrial Research Organisation (CSIRO) as part of the National Assessment of Chemicals Associated with Coal Seam Gas Extraction in Australia, Commonwealth of Australia, Canberra.

# Acknowledgements

This report is one in a series prepared under the National Assessment of Chemicals Associated with Coal Seam Gas Extraction in Australia. It was prepared by the Commonwealth Scientific and Industrial Research Organisation (CSIRO). This literature review covers information available to the end of 2013. The review report was completed in 2013, with minor updates made between 2013 and 2016.

The report's authors gratefully acknowledge input from the Project Steering Committee, which comprised representatives from the National Industrial Chemicals Notification and Assessment Scheme (NICNAS), the Department of the Environment and Energy, the Commonwealth Scientific and Industrial Research Organisation (CSIRO), Geoscience Australia (GA), and an independent scientific member, Dr David Jones of DR Jones Environmental Excellence.

This report was subject to internal review processes during its development.

# Disclaimer

The information contained in this publication comprises general statements based on scientific and other research. Reasonable efforts have been made to ensure the quality of the information in this report. However, before relying on the information for a specific purpose, users should obtain appropriate advice relevant to their particular circumstances. This report has been prepared using a range of sources, including information from databases maintained by third parties, voluntary surveys, and data supplied by industry. The Commonwealth has not verified and cannot guarantee the correctness or completeness of the information obtained from these sources. The Commonwealth cannot guarantee and assumes no legal liability or responsibility for the accuracy, currency, completeness or interpretation of the information in this report, or for any loss or damage that may be occasioned directly or indirectly through the use of, or reliance on, the contents of this publication.

The material in this report may include the views or recommendations of third parties and does not necessarily reflect the views and opinions of the Australian Government, the Minister for the Environment and Energy, the Minister for Health and Aged Care, or the IESC; nor does it indicate a commitment to a particular course of action.

## Accessibility

The Commonwealth of Australia is committed to providing web accessible content wherever possible. If you are having difficulties with accessing this document please call the Department of the Environment and Energy on 1800 803 772 (free call).

## Reports in this series

The full set of technical reports in this series and the partner agency responsible for each is listed below.

| Technical report number | Title | Authoring agency |
|---|---|---|
| | ***Reviewing existing literature*** | |
| 1 | Literature review: Summary report | NICNAS |
| 2 | Literature review: Human health implications | NICNAS |
| 3 | Literature review: Environmental risks posed by chemicals used coal seam gas operations | Department of the Environment and Energy |
| 4 | Literature review: Hydraulic fracture growth and well integrity | CSIRO |
| 5 | Literature review: Geogenic contaminants associated with coal seam gas operations | CSIRO |
| 6 | Literature review: Identification of potential pathways to shallow groundwater of fluids associated with hydraulic fracturing | CSIRO |
| | ***Identifying chemicals used in coal seam gas extraction*** | |
| 7 | Identification of chemicals associated with coal seam gas extraction in Australia | NICNAS |
| | ***Modelling how people and the environment could come into contact with chemicals during coal seam gas extraction*** | |
| 8 | Human and environmental exposure conceptualisation: Soil to shallow groundwater pathways | CSIRO |
| 9 | Environmental exposure conceptualisation: Surface to surface water pathways | Department of the Environment and Energy |
| 10 | Human and environmental exposure assessment: Soil to shallow groundwater pathways – A study of predicted environmental concentrations | CSIRO |
| | ***Assessing risks to workers and the public*** | |
| 11 | Chemicals of low concern for human health based on an initial assessment of hazards | NICNAS |

| Technical report number | Title | Authoring agency |
|---|---|---|
| 12 | Human health hazards of chemicals associated with coal seam gas extraction in Australia | NICNAS |
| 13 | Human health risks associated with surface handling of chemicals used in coal seam gas extraction in Australia | NICNAS |
| ***Assessing risks to the environment*** | | |
| 14 | Environmental risks associated with surface handling of chemicals used in coal seam gas extraction in Australia | Department of the Environment and Energy |

# Foreword

## Purpose of the Assessment

This report is one in a series of technical reports that make up the *National Assessment of Chemicals Associated with Coal Seam Gas Extraction in Australia* (the Assessment).

Many chemicals used in the extraction of coal seam gas are also used in other industries. The Assessment was commissioned by the Australian Government in June 2012 in recognition of increased scientific and community interest in understanding the risks of chemical use in this industry. The Assessment aimed to develop an improved understanding of the occupational, public health and environmental risks associated with chemicals used in drilling and hydraulic fracturing for coal seam gas in an Australian context.

This research assessed and characterised the risks to human health and the environment from surface handling of chemicals used in coal seam gas extraction during the period 2010 to 2012. This included the transport, storage and mixing of chemicals, and the storage and handling of water pumped out of coal seam gas wells (flowback or produced water) that can contain chemicals. International evidence[1] showed the risks of chemical use were likely to be greatest during surface handling because the chemicals were undiluted and in the largest volumes. The Assessment did not consider the effects of chemical mixtures that are used in coal seam gas extraction, geogenic chemicals, or potential risks to deeper groundwater.

The Assessment findings significantly strengthen the evidence base and increase the level of knowledge about chemicals used in coal seam gas extraction in Australia. This information directly informs our understanding of which chemicals can continue to be used safely, and which chemicals are likely to require extra monitoring, industry management and regulatory consideration.

## Australia's regulatory framework

Australia has a strong framework of regulations and industrial practices which protects people and the environment from adverse effects of industrial chemical use. For coal seam gas extraction, there is existing legislation, regulations, standards and industry codes of practice that cover chemical use, including workplace and public health and safety, environmental protection, and the transport, handling, storage and disposal of chemicals. Coal seam gas projects must be assessed and approved under relevant Commonwealth, state and territory environmental laws, and are subject to conditions including how the companies manage chemical risk.

## Approach

Technical experts from the National Industrial Chemicals Notification and Assessment Scheme (NICNAS), the Commonwealth Scientific and Industrial Research Organisation (CSIRO), and the Department of the Environment and Energy conducted the Assessment. The Assessment drew on technical expertise in chemistry, hydrogeology, hydrology, geology, toxicology, ecotoxicology, natural resource management and risk assessment. The Independent Expert Scientific Committee on Coal Seam Gas and Large Coal Mining

[1] See Mallants et al. 2017; Adgate et al. 2014; Flewelling and Sharma 2014; DEHP 2014; Stringfellow et al. 2014; Groat and Grimshaw 2012; Vidic et al. 2013; Myers 2012; Rozell and Reaven 2012; The Royal Society and The Royal Academy of Engineering 2012; Rutovitz et al. 2011.

Development (IESC) provided advice on the Assessment. Experts from the United States Environmental Protection Authority, Health Canada and Australia reviewed the Assessment and found the Assessment and its methods to be robust and fit-for-purpose.

The Assessment was a very large and complex scientific undertaking. No comparable studies had been done in Australia or overseas and new models and methodologies were developed and tested in order to complete the Assessment. The Assessment was conducted in a number of iterative steps and inter-related processes, many of which needed to be done in sequence (Figure F.1). There were two separate streams of analysis – one for human health and one for the environment. The steps included for each were: literature reviews; identifying chemicals used in drilling and hydraulic fracturing for coal seam gas extraction; developing conceptual models of exposure pathways; models to predict soil, surface and shallow groundwater concentrations of identified chemicals; reviewing information on human health hazards; and identifying existing Australian work practices, to assess risks to human health and the environment.

The risk assessments did not take into account the full range of safety and handling precautions that are designed to protect people and the environment from the use of chemicals in coal seam gas extraction. This approach is standard practice for this type of assessment. In practice, safety and handling precautions are required, which means the likelihood of a risk occurring would actually be reduced for those chemicals that were identified as a potential risk to humans or the environment.

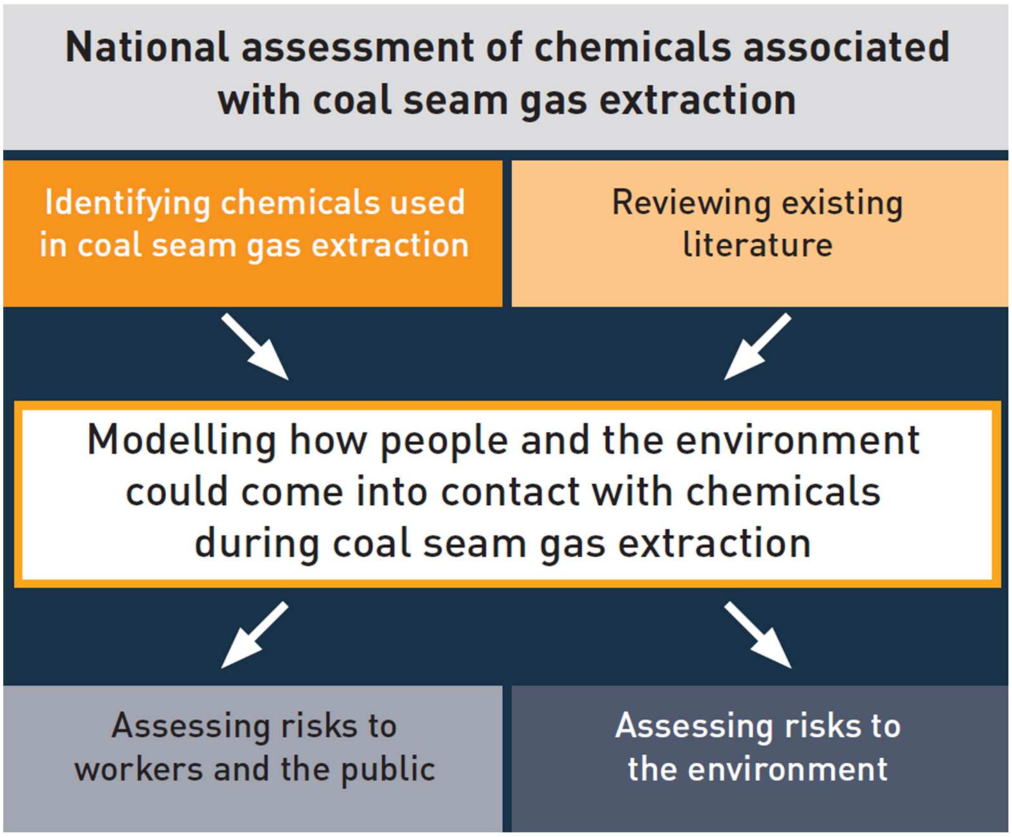


Figure F.1 Steps in the Assessment

## Collaborators

The Australian Government Department of the Environment and Energy designs and implements policies and programs, and administers national laws, to protect and conserve the environment and heritage, promote action on climate change, advance Australia's interests in the Antarctic, and improve our water use efficiency and the health of Australia's river systems.

Within the Department, the Office of Water Science is leading the Australian Government's efforts to improve understanding of the water-related impacts of coal seam gas and large coal mining. This includes managing the Australian Government's program of bioregional assessments and other priority research, and providing support to the Independent Expert Scientific Committee on Coal Seam Gas and Large Coal Mining Development (IESC). The IESC provides independent, expert scientific advice on coal seam gas and large coal mining proposals as requested by the Australian Government and state government regulators, and advice to the Australian Government on bioregional assessments and research priorities and projects.

The National Industrial Chemicals Notification and Assessment Scheme (NICNAS) is a statutory scheme administered by the Australian Government Department of Health. NICNAS aids in the protection of the Australian people and the environment by assessing the risks of industrial chemicals and providing information to promote their safe use.

CSIRO, the Commonwealth Scientific and Industrial Research Organisation, is Australia's national science agency and one of the largest and most diverse research agencies in the world. The agency's research is focused on building prosperity, growth, health and sustainability for Australia and the world. CSIRO delivers solutions for agribusiness, energy and transport, environment and natural resources, health, information technology, telecommunications, manufacturing and mineral resources.

## This report: *Literature review: Hydraulic fracture growth and well integrity*

This report presents a detailed review of the literature on hydraulic fracture growth during the stimulation of coal seams to increase water and gas production rates of coal seam gas wells. Information from over 250 papers and reports dealing with aspects of hydraulic fracture growth and well integrity has been incorporated into this review. The review covers information available to the end of 2013. The review was completed in 2013, with minor updates between 2013 and 2016.

Predicting hydraulic fracture growth is fundamental to designing and optimising fracture treatments. Likewise, well integrity is an issue that needs to be addressed during design, construction and operation phases.

This report includes a general introduction that provides an historical context and a generic description of hydraulic fracturing. This is included to provide background information and as an aid in understanding the rest of the report. The first part of this report forms the basis for an assessment of the pathways that a hydraulic fracture may provide for fracturing fluid to enter an aquifer. In a typical case, the aquifer lies above or below the seam and the hydraulic fracture must then grow through other rock layers to connect into the aquifer. The prediction of such an occurrence requires calculation of hydraulic fracture vertical growth (called height growth). The second part of the report covers well integrity issues and the potential mechanisms and pathways that they may provide if not correctly drilled and completed for fracturing fluids to enter an aquifer or other formation.

### *Hydraulic Fracturing*

Fracture growth is predominantly in the lateral and vertical direction. When considering growth of a vertical fracture, the lateral and vertical growth components of the fracture are coupled. Additional lateral growth will reduce the vertical growth and vice versa. Growth is affected by fluid loss (leak-off) into the permeable reservoir layers encountered. In coal or other fractured rock, leak-off is pressure dependent and non-linear, leading to larger fluid loss volumes than in unfractured reservoir rock of the same initial permeability. In addition, lateral growth is affected by natural fractures and occasional shear zones or faults that the hydraulic fracture encounters and with which it interacts. The interaction with natural fractures and faults can lead to the development of offsets and branches in the hydraulic fracture. As leak-off, branching, and offsetting increase, the fracture growth is slowed and the ultimate size is reduced.

Height growth is affected by the layering in the sedimentary rocks that the hydraulic fracture must grow through in order to extend vertically. These rock layers have different physical properties and carry different magnitudes of in-situ stress. In general, a hydraulic fracture that grows only in one zone or seam is called ‘contained’ while a fracture that grows out of a zone (or seam) is referred to as ‘uncontained’. Stress contrasts (i.e. the difference in the magnitude of the minimum horizontal stress existing in adjacent layers) between layers have the strongest effect on containment. Higher stress in bounding layers can work to effectively contain the hydraulic fracture to the lower stressed layer. In the case of the horizontal stress in the rock exceeding the vertical stress in magnitude, the hydraulic fracture will be completely contained. If the injection pressure is high enough to extend the fracture into this high stress zone, the fracture will reorient to grow horizontally, preventing further vertical growth.

Although stress contrast has the strongest effect on fracture height growth, such contrasts may be weak or not exist at some locations. The other main factors that affect hydraulic fracture lateral and height growth are listed below:

- **Fracture toughness.** Fracture toughness is a property of the rock. The pressure inside a hydraulic fracture opens it and increases the tensile stress at the leading edge of the fracture. The near-tip stress field is represented by the stress intensity factor. The fracture will extend when the stress intensity factor becomes equal to the rock fracture toughness. Different rock layers will have slightly different fracture toughness. A bounding layer with higher fracture toughness will act to slow fracture growth or even arrest the fracture.
- **Rock elastic stiffness.** Rock layers that are higher in elastic stiffness generally act to limit fracture growth. The fracture width is reduced in the stiffer layer, leading to more viscous fluid friction which reduces the fracture growth rate. The stress intensity at the tip of the hydraulic fracture is reduced as it approaches a stiff layer and, conversely, increased as it approaches a soft layer. Tectonic compressive strain will induce higher horizontal stress in the stiffer rock layers, producing stress contrasts that favour containment of the hydraulic fracture as discussed above.
- **Fluid gradient.** Fluid gradients (rate of pressure change with position) inside the hydraulic fracture are generated by viscous flow of the fracturing fluid through the hydraulic fracture channel. High gradients can exist where fluid is forced through an offset or tortuous pathway. Fracture growth is slowed by high fluid pressure gradients along the flow path. An obstruction in the fracture channel, such as provided by proppant plugging the fracture, can arrest fracture growth. Buoyant proppants have been developed to limit vertical growth of hydraulic fractures. Normal proppant that settles to the base of a vertical fracture act to limit downward growth by the same mechanism.

- **Permeability.** The rock layers above and below the seam can vary significantly in permeability. Hydraulic fracture growth occurs more rapidly through a rock with a lower permeability because less of the injected fluid is lost into the surrounding rock. High permeability layers or zones act to slow or blunt fracture growth.
- **Interfaces.** Interfaces include natural fractures, faults, shear zones and bedding interfaces. Interfaces are often weak in tension and shear and may have an initial permeability that allows the fracturing fluid to more easily penetrate into them. As the hydraulic fracture interacts with such interfaces, offsets and branches may form, which retard fracture growth. The interface between the coal and the rock is a feature into which the initially vertical hydraulic fracture is often diverted, resulting in a T-shaped fracture geometry and contained fracture growth.

## *Well integrity*

Well integrity for oil and gas wells is defined by the Standards Norway document NORSOK D.010 as the *Application of technical, operational and organizational solutions to reduce risk of uncontrolled release of formation fluids throughout the life cycle of a well*. Thus, any problem that occurs that allows fluid to move from the well into the surrounding rock or soil or air or allows fluid to move along the wellbore can be considered a well integrity issue.

A vertical well includes several steel casing strings that are cemented to seal the space between the outside of the casing and the rock. A liner is a casing string that does not extend to the surface. Liners can be cemented or left with an open annulus, serving to maintain an open production pathway.

A cement seal must be established and maintained between the casing and the rock along the wellbore. This seal is designed to prevent fluid migration from one level of the well to another, and in particular to prevent movement of the produced gas and water along the outside of the casing. Some key areas affecting well integrity are detailed below:

- **Wellbore condition.** The wellbore condition at the time of cementing affects the cementing operation and the quality of the cement seal. Portions of the well that are oversize because of failure of the rock during drilling must be minimised. Oversized sections result in a lower cement velocity during placement, which in turn can reduce the efficiency of drilling mud displacement by the cement and thereby the quality of the cement seal is reduced. If oversize sections are present, they must be factored into the design of the casing cementing operation.
- **Damaged / fractured rock.** Fracturing and failure of the rock may extend some distance into the rock behind the immediate wellbore wall. This damaged rock may be of enhanced permeability, allowing fluid to move along the wellbore in this damaged region. The vertical extent and continuity of damage can be limited by good drilling practices that eliminate or reduce wellbore failure. The existence of rock layers with different strengths that carry different stresses limit both the vertical extent and continuity of any such damage. No literature was found that reported leakage of fluid over significant distances along the well via a damaged zone in the rock.

The quality of the cement seal around the casing can be determined by several methods after the casing cementing operation is completed. A leak-off test (LOT) is routinely performed after each casing string is set. A LOT involves drilling a few metres of new hole beyond the casing string that has just been set and then pressurising this section to test that the cement will hold fluid pressure. If poor cement is found to exist, there are methods to repair the poorly cemented sections. In the extreme case, part of the well or the entire well can be plugged and abandoned to allow a new well to be drilled.

Other risks associated with wellbores concern the methods used to seal the entire well when it is plugged and abandoned. If the cementing during this phase is not done or if it is of poor quality, the wellbore provides a path for fluid movement from the coal seam to the surface. Abandoned and orphaned wells (either from petroleum, mining, or agricultural activities) may exist in a coal seam gas area and if not plugged correctly may provide pathways for fluid and gas movement.

Poor well integrity is a significant problem in the conventional oil and gas industry. A number of large-scale studies indicate that there is not full integrity in a significant percentage of all wells. In the Gulf of Mexico, US (United States), approximately 10 per cent of wells experienced sustained casing pressure (SCP) within one year of being completed, and this figure rose to 50 per cent after 15 years of production. This sustained casing pressure state indicates that there is a leakage path to pressurised reservoir fluids through one or more of the cement sheaths or cased intervals. According to the National Petroleum Safety Authority, in areas offshore of Norway, 18 per cent of the wells surveyed in a pilot study (more than 400 wells) had integrity failure issues or uncertainties, and seven per cent of these were shut in because of well integrity issues. In Canada, 4.6 per cent of 316 439 wells in the database collected by the Energy Resources Conservation Board (ERCB) had leakage issues with gas migration outside casing or surface casing vent flow (SCVF) from wellbore annuli.

It should be noted that completed and producing conventional oil and gas wells are constructed with multiple well barriers. Individual well barrier failure rates are often one to two orders of magnitude higher than well integrity failure rates. Well integrity failure is reached when all well barriers in a protection sequence fail and pollution to environment either could occur or has already occurred.

Comparable statistics for leakage of coal seam gas wells in Australia were not found during this review.

## *Findings and gaps in knowledge*

The main findings from the review of fracture growth and well integrity are listed below:

- Hydraulic fracture growth in coal and growth in height into layers above and below a coal seam are affected by the rock properties and in-situ stresses. Interactions with bedding planes, faults and natural fractures often strongly affect the fracture growth. The processes that control whether these features slow, arrest or divert hydraulic fracture growth require further investigation to facilitate their incorporation into fracture design models.
- The nature and size of the fractures formed by coal seam gas treatments are fairly well characterised because many have been mapped after mining, both in Australia and in the US. The fractures have been documented to contain branches and offsets and to sometimes form as T-shaped geometries with a large horizontal fracture overlying a vertical one.
- Complex branched and offset fracture geometry occurs along a main backbone hydraulic fracture and this exact geometry is a challenge for existing models to simulate. However, existing planar fracture models can be reliably used to provide upper limits for both lateral and vertical fracture extent because the branching and offsetting acts to retard the fracture growth, with the effect that the more complex fractures are less extensive than what is predicted by a planar model. Recently

developed models that simulate the growth of a network-like fracture can be applied to coal seam gas stimulation design, but these models currently are not able to reproduce the geometries documented by mined fracture studies. There is an apparent gap in knowledge relating to this, as coal seam gas fracture design models are still lacking in their ability to account for T-shaped fracture development and growth. This is in addition to other aspects of fracture growth in naturally fractured reservoir material, such as pressure-dependent leak-off, offsetting and branching, and interaction with the stiffer roof and floor rock layers.

- In any case, careful site characterisation is required to design and accurately predict fracture growth during coal seam gas stimulations. Monitoring of fracture growth by microseismic and tiltmeter instrumentation, and by employing other technologies such as tracers, is important during early phases of development of new areas. This monitoring serves to calibrate modelling and verify that designs are producing the fractures intended. There is a gap in monitoring which would be filled by development of lower cost but reliable fracture monitoring methods.
- The wellbore provides a possible pathway along which fluids can move between zones in a coal seam gas well or from the subsurface to the surface. Application of correct drilling and completion practice effectively limits the risk of such fluid movement. Overseas studies indicate that well integrity may be a general problem, reinforcing the idea that the wellbore is the main risk of a leakage pathway developing between the reservoir and aquifers and the surface. Statistical data describing historical Australian coal seam gas well integrity experience were not found.
- Characterisation of the stress and rock properties is required as part of the well design process. The drilling operation and drilling fluids used can then be designed to limit the risk of lost fluids or wellbore breakout.
- Casing cementing operations must be designed to account for any oversized and damaged sections of the wellbore to ensure removal of drilling fluids during cement displacement. The integrity of the cement and casing sheath can be verified by geophysical logging tools. Remediation of poorly cemented sections can be undertaken.
- Plugging and abandonment procedures must be designed and carried out using good engineering practice. Pre-existing wells and boreholes that have not been plugged correctly pose a risk for vertical fluid movement and gas entering aquifers or venting at the surface.

# Abbreviations

| General abbreviations | Description |
|---|---|
| API RP | American Petroleum Institute Recommended Practice |
| APLNG | Australia Pacific Liquefied Natural Gas |
| APPEA | Australian Petroleum Production and Exploration Association |
| BHA | Bottom hole assembly |
| BTC | Buttress thread casing |
| CBL | Cement bond log |
| CBM | Coal bed methane |
| CSG | Coal seam gas |
| CSM | Coal seam methane |
| CSIRO | Commonwealth Scientific and Industrial Research Organisation |
| dB | Decibel |
| DD | Displacement discontinuity |
| DST | Drill Stem Test, a type of well test used to measure reservoir permeability and pressure |
| DTS | Distributed temperature sensor |
| ECD | Equivalent circulation mud weight |
| ERCB | Energy Resources Conservation Board |
| FIT | Formation Integrity Test |
| $g_{fi}$ | Fracture initiation gradient |
| $g_{fpr}$ | Fracture propagation gradient |
| GM | Gas migration |
| HF | Hydraulic Fracture |
| IESC | Independent Expert Scientific Committee on Coal Seam Gas and Large Coal Mining Development |
| KGD | Fracture growth model developed by Khristianovic and Zheltov, and Geertsma and de Klerk |
| kHz | KiloHertz |
| LCM | Lost circulation material |
| LOP | Leak-off point |
| LOT | Leak-off test |
| LWD | Logging While Drilling |

| General abbreviations | Description |
|---|---|
| MMS | Minerals Management Service |
| mV | Millivolts |
| NICNAS | National Industrial Chemicals Notification and Assessment Scheme |
| NORSOK | Norwegian Petroleum Standards document |
| NSW | New South Wales |
| PHPA | Partially Hydrolysed Polyacrylamide |
| PKN | Model developed by Perkins, Kern and Nordgren |
| ROP | Rate of Penetration |
| SCP | Sustained Casing Pressure |
| SCVF | Surface Casing Vent Flow |
| SIS | Surface to In-Seam |
| SLG | Solid-Liquid-Gas |
| UAC | Uniform asymptotic solution |
| US | United States of America |
| USBM | United States Bureau of Mines |
| US EPA | United States Environment Protection Agency |
| USI | Ultrasonic imaging |
| VDL | Variable density log |
| VSP | Vertical seismic profiles |
| XLOT | Extended leak-off test |

| Units, chemicals and symbols | Description |
|---|---|
| C | Celsius – temperature scale |
| ft | Foot or feet |
| KCl | Potassium chloride |
| kPa | KiloPascal |
| MPa | MegaPascal |
| m | Metres |
| mm | Millimetres |
| ppg | Pounds per gallon |
| psi | Pounds per square inch |

| Units, chemicals and symbols | Description |
|---|---|
| Tcf | Trillion cubic feet |

# Glossary

| Term | Description |
| --- | --- |
| Accelerometers | A sensor that measures acceleration and is used to detect microseismic events |
| Annulus | The gap between tubing and casing or between two casing strings or between the casing and the wellbore. The annulus between the tubing and casing is the primary path for producing gas from coal seam gas wells |
| Azimuth | The angle in degrees measured clockwise from grid north or magnetic north |
| Borehole | A hole drilled for purposes other than production of oil, gas or water (e.g. a mineral exploration borehole) |
| Bottom hole | A measurement, usually temperature or pressure, made at a specified depth in a well |
| Boussinesq solution | The solution for stresses and displacements caused by a point force acting on a half-space |
| Casing | Steel or fibreglass pipe used to line a well and support the rock. Casing extends to the surface and is sealed by a cement sheath between the casing and the rock |
| Casing shoe | A short adaptor that fits on the downhole end of the casing string that facilitates insertion of the casing into the well |
| Coal seam gas | A form of natural gas (generally 95 to 97% pure methane, $CH_4$) typically extracted from permeable coal seams at depths of 300 to 1 000 m. Also called coal seam methane (CSM) or coalbed methane (CBM) |
| Effective stress | Stress transmitted by the solid matrix materials of rocks and soils. The effective stress in a reservoir or coal seam is the total stress minus the pore pressure |
| Elastic modulus | A material parameter that relates stress to strain or strain to strain for an elastic material |
| Filter cake | A deposit of fine particles left on the rock surface as a fluid leaks off. The build-up of the filter cake reduces further loss of fluid |
| Formation pore pressure | The pressure in the porous rock around the well |
| Geogenic | A naturally occurring chemical originating, for example, from geological formations |
| Geophones | A sensor that detects ground movement or velocity and is often used to detect and locate microseismic events |
| Geophysical wireline logging | A method of recording the response of a well logging tool that involves running the tool in and out of the well on a cable and recording the signal at the surface |
| Gravitational potential | The potential energy per unit mass |
| Half-space | A domain in solid mechanics defined by the material lying on one side of a flat infinite surface |

| Term | Description |
|---|---|
| Height growth | Vertical growth (upwards or downwards) of a vertical hydraulic fracture |
| Hydraulic fracturing | Also known as ‘fracking’, ‘fraccing’, ‘fracture stimulation’ or ‘fluid-driven fractures’, is the process by which hydrocarbon (oil and gas) bearing geological formations are ‘stimulated’ to enhance the flow of hydrocarbons and other fluids towards the well. The process involves the injection of fluids, gas, proppant and other additives under high pressure into a geological formation to create a fracture connecting the well to the reservoir. The fracture acts as a high conductivity channel through which the gas, and any associated water, can flow to the well |
| Hydrostatic pressure | The theoretical pore pressure that would be expected purely from the weight of water in a column running from the depth of interest to the surface |
| In-situ stress | The stress acting in the rock. Contrasts in the magnitude of the minimum principal stress strongly affect hydraulic fracture height growth |
| Leak-off | The process that results in loss of fluid during a hydraulic fracture treatment by diffusion from the fracture into the surrounding rock |
| Leak-off test (LOT) | A test performed during drilling to measure the pressure at which a hydraulic fracture will initiate from the wellbore |
| Liner | Steel or fibreglass pipe used to line a well and support the rock. Liners are essentially the same as casing, but do not extend to the surface |
| Macerals | Components of coal that have a role similar to minerals in making up rock |
| Non-linear leak-off | Enhanced leak-off caused by pore pressure increase interacting with natural fracture permeability in the coal reservoir around the hydraulic fracture |
| Non-Newtonian fluid | A fluid that possesses a non-Newtonian rheology. The viscosity of such a fluid is a function of the shear rate rather than being a constant, which is the case for Newtonian fluids |
| Openhole | An un-cased section of the well |
| Overburden | Material of any nature, consolidated or unconsolidated, that overlies a deposit of useful materials such as ores or coal, especially those deposits that are mined from the surface by open-cut methods |
| Overburden formations | Named rock layers in the overburden |
| Payzone | The rock layer or layers containing hydrocarbons and that is the intended zone targeted for hydraulic fracture stimulation |
| Production interval | The section of rock from which hydrocarbons are being produced |
| Proppant | A component of the hydraulic fracturing injected fluid comprised of sand, ceramics or other granular material that ‘prop’ open fractures to prevent them from closing when the injection is stopped |
| Screen out | Proppant bridging in the wellbore or in the hydraulic fracture that restricts further fluid flow |
| Slick water | A fracturing fluid consisting of water containing a friction reducer additive |
| Spacer | A spacer is a viscous fluid used to aid removal of drilling fluids before a primary cementing operation. By coating the wellbore with a reactive spacer that reacts with cement, a small filter cake is formed that prevents |

| Term | Description |
|---|---|
| | cement from invading the formation. A non-reactive spacer should then be run between the reactive spacer and cement slurry to prevent premature setting of the slurry |
| Treating pressure | The injection pressure during hydraulic fracturing |
| Tubing | Steel pipe that is hung inside the casing. The tubing string may have a pump installed at its lower end and, for pumped wells, is a primary path for producing fluids from coal seam gas wells |
| Well | As used in this report: a completed wellbore, typically including casing and tubing strings and possibly a pump |
| Well integrity | A measure of the ability of the well and wellbore system to allow access to the reservoir while controlling fluid movement along the well or from the well into or out of the surrounding rock |
| Well logging | The process of acquiring and recording a signal from a geophysical tool run into a well |
| Wellbore | The hole in the Earth produced by drilling, with the final intended purpose being for production of oil, gas or water |
| Workover | Repair and maintenance work, such as cleaning a tubing string or replacing a pump, undertaken on a well |

# Contents



## Tables

# Figures

WORKING DRAFT
DO NOT DISTRIBUTE OR CITE

# 1 Introduction

## 1.1 This literature review

This literature review covers information available to the end of 2013. The review report was completed in 2013, with minor updates made between 2013 and 2016. It presents a compilation of data on hydraulic fracture growth in Australian coals, considering growth within the coal seam and growth out of seam (height growth). A comprehensive literature review on the topic of hydraulic fracture growth in coal and factors that control fracture growth out of seam is included. The review also extends to an appraisal of published risk assessments.

Hydraulic fracturing has been applied to stimulation of oil and gas wells in Australia for over 40 years. The first hydraulic fracturing for stimulation in Australia was carried out in the Cooper Basin of South Australia in 1969 in a tight gas reservoir (McGowen et al. 2007). Fracturing of coal for testing of production coal seam gas in Australia began in 1976 (Geoscience Australia 2012) and fracturing trials aimed at gas drainage for coal mining started in the early 1980s (Stewart and Barro 1982).

Coal seam gas production in the United States began in the 1970s with the objective of reducing gas levels in coal mines. A few years later with the aid of government incentives, it developed into a profitable industry targeting the gas as the primary commodity (US EPA 2004). By 2008 the US coal seam gas industry (in the US, gas produced from coal for sale is called coalbed methane or CBM) consisted of more than 55 000 wells being operated by more than 250 operators working in 13 basins and producing 2 trillion cubic feet (Tcf) of gas per year, or just under 10 per cent of the US domestic gas production (US EPA 2010). By comparison, Australian coal seam gas totalled 0.2 Tcf (234 PJ) in 2010-2011 from under 600 wells (Queensland Government 2012), accounting for about 13 per cent of Australia's gas production (Energy Information Administration 2011).

A typical lifespan for a coal seam gas well is five to 15 years, with maximum gas production achieved within a few months of the start of water production (US EPA 2010; Saulsberry et al. 1996). The need for stimulation by hydraulic fracturing varies by region. In the US, for example, hydraulic fracturing is common in some regions and seldom used in others (US EPA 2010). Locally, Australia Pacific LNG (APLNG) has estimated that future development of their leases in Australia will result in 30 per cent of their new wells being stimulated by hydraulic fracturing (Origin et al. 2013).

## 1.2 Pathways for groundwater contamination

Chemicals associated with coal seam gas operations may escape from coal seams and cause groundwater contamination. The migration pathway may be through:

- propagation of hydraulic fractures out of the target zones and into adjacent groundwater bearing layers
- the intersection of induced fractures with natural fracture zones that lead to adjacent aquifers
- abandoned and improperly plugged oil and gas wells

- poorly cemented production wells that may lead to upward migration in the wellbore or along the annulus between the wellbore and the casing.

Figure 1.1 shows three types of fluid migration pathways that could occur during hydraulic fracturing. Case 1 illustrates a fracture contained in height to the coal seam growing into a well that penetrates the coal seam itself. Case 2a illustrates a fracture intersecting a fault, which then allows fluid to pass into an aquifer and potentially into a water well, and Case 2b illustrates a fracture growing in height to eventually penetrate into an aquifer above the coal seam. Coloured regions in the hydraulic fracture shown in Figure 1.1 are used to indicate the fracture size at early (red), intermediate (orange) and late (yellow) times.

It is important to note that fluid flow is directed toward the coal seam gas well after fracturing is completed because gas and water enter the low pressure wellbore during production. After cessation of production, hydraulic gradients will gradually return to their pre-extraction levels. Overall, this process will involve flow from the surrounding rock layers into the coal seam, representing a recharge of the seam since the coal is de-pressurised by the production process. However, local gradients may exist that result in reverse flows out of the coal seam and potentially into adjacent groundwater aquifers. Similar possible contamination pathways – involving growth out of the zone and subsequent stranding of hydraulic fracturing fluid during production – are discussed in a recent report by the US Environmental Protection Agency (2004).

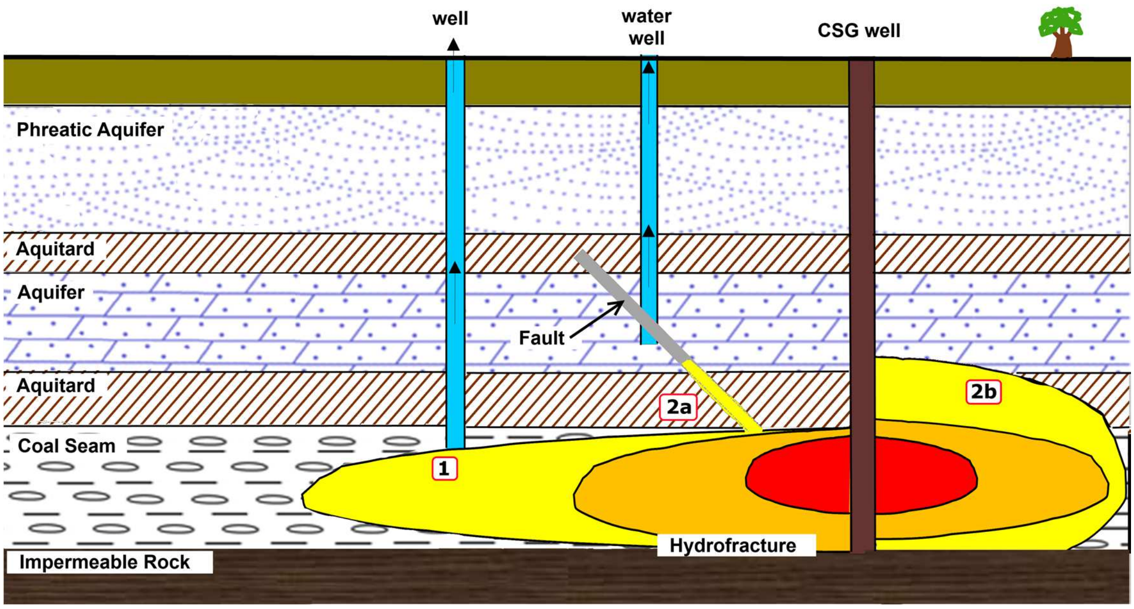


Figure 1.1 Profile sketch (not to scale) of three possible contaminant migration pathways between a coal seam hydraulic fracture and an aquifer

# 2 Hydraulic fracturing for coal seam gas

Targeted coal zones for hydraulic fracturing in Australia are typically located at depths that range between 300 to 1000 m below the surface and are usually separated by aquitards (low permeable shales, siltstones, sandstones and clays) and barriers to fracture growth (e.g. frictionally weak sub-horizontal planes, high stress layers) (Enever et al. 2000; Van Eekelen 1982). The fracture treatments are designed to grow only in the zone of rock that contains coal seams because growth out of the coal seam gas containing layers increases the cost and reduces the effectiveness of the treatment (Nolte and Smith 1981; Van Eekelen 1982). Each site must be characterised by measuring rock properties and local stress so that the potential for fracture growth can be assessed. Remote monitoring can be employed during treatments to measure fracture growth after the fact or as the treatment occurs.

## 2.1 Hydraulic fracture growth in coal

### *2.1.1 Introduction*

The characteristics of coal as a material, of coal as a lithological unit, and of the sedimentary basins in which coal occurs all contribute to the nature of hydraulic fracture growth in coal. Table 2.1 summarises some of the most striking characteristics of coal and in particular Australian coal basins with an assessment of the impact that these have on hydraulic fracture growth. The listed characteristics and impacts provide motivation to modelling considerations briefly described in this section.

The interested reader is also referred to US Environmental Protection Agency (2004) for a detailed overview of hydraulic fracture modelling for coal seam reservoirs.

Table 2.1 Summary of characteristics of typical coal seam gas reservoir rocks and the associated impact on hydraulic fracturing

| Characteristic | Impact on hydraulic fracture growth |
|---|---|
| Coal occurs in sedimentary basins. The minimum principal stress in the coal is typically horizontally-directed, but in Australia this stress is often the vertical stress in surrounding stiffer rock layers. | The main component of hydraulic fractures is typically vertically oriented in the coal, so as to be opposed by the least principal stress (Figure 2.9 in Section 2.9.1.1). T-shaped fractures may form if the overlying rock carries high horizontal stresses or if fracture growth out of the coal is blunted. |
| Coal is heavily naturally fractured. | Fracture path branching and offsetting (non-planar growth) results in high injection pressure and can make proppant placement more difficult. High injection pressure can promote height growth or lead to T-shaped fractures with a horizontal component at the coal-roof rock interface. |
| Competent and stiffer bounding layers exist, with weak interfaces. The pressure to propagate a single vertical fracture in the coal may increase with its length. | An initially vertical hydraulic fracture forms and as pressure increases a horizontal component may grow along the roof and / or base of the coal seam (Jeffrey et al. 1992). |
| Natural fracture permeability is stress sensitive, leading to permeability that varies | Leak-off of fluid to the formation is significantly underestimated by models that assume constant |

| Characteristic | Impact on hydraulic fracture growth |
|---|---|
| with formation stress and fluid pressure. | coal permeability with pore pressure change. |
| Drilling, fracturing, proppant placement and production can all lead to mechanical failure of coal. | Coal chips and fines plugging perforations can substantially inhibit longevity of the hydraulic fracture stimulation. Wells require workover from time to time to clean coal from pump and well. |
| Coal is a soft rock. | Proppant embedment can reduce effectiveness of the hydraulic fracture stimulation. |

### 2.1.2 Planar hydraulic fracture growth

Table 2.1 lists a number of coal seam and hydraulic fracture characteristics that result in fundamentally non-planar fracture growth, including T-shaped growth, branching and offsetting through natural fractures and cleat. However, while it is a coarse approximation in many cases, planar models are still capable of providing estimates of important geometric features such as fracture length and width and the propensity for a fracture to grow in height in the presence of layer and interfaces.

Figure 2. shows an idealised progression of a hydraulic fracture growing from a vertical well that is completed in a reservoir bounded by high stress barriers (Nolte 1991). In the absence of T-shaped growth and offsetting, which are discussed below, this gives a useful and widely accepted illustration of hydraulic fracture behaviour that is relevant to a range of reservoir types including coal seams.

The progression consists of three stages of hydraulic fracture growth (Nolte and Smith 1981; Nolte 1991). Stage 1 is characterised by a decreasing pressure trend that is nuanced depending on whether the well is uncased across the zone or perforated across the entire zone (line source) or at a limited interval within the zone (point source). The initial geometry is approximated, then, as either plane strain ("KGD" after the names of early developers of the model (Khristianovic and Zheltov 1955; Geertsma and De Klerk 1969) or radial, respectively. Growth of both KGD and radial fractures produce a trend of decreasing pressure with time.

Once the hydraulic fracture reaches the barrier, its height growth is suppressed and it begins to grow with a blade-like geometry ("PKN", again after the names of early developers of the model (Perkins and Kern 1961; Nordgren 1972). Most importantly, the PKN geometry is associated with an increasing injection pressure trend required to sustain its growth. Hence the fluid pressure increases throughout Stage 2.

As the fluid pressure increases, the effectiveness of the barrier layers at preventing height growth diminishes. Stage 3, then, is characterised by the injection pressure reaching a plateau that is similar in magnitude to the minimum stress in the barrier layers. Factors affecting and approaches to predicting height growth are discussed in Section 2.2.

Alternatively, in conditions common for coal seam reservoirs, the hydraulic fracture could start to grow along the interface at the top or bottom of the coal forming a so-called 'T-shaped' hydraulic fracture. The behaviour of and approach to modelling this particular form of non-planar hydraulic fracture are discussed in Section 2.1.3.

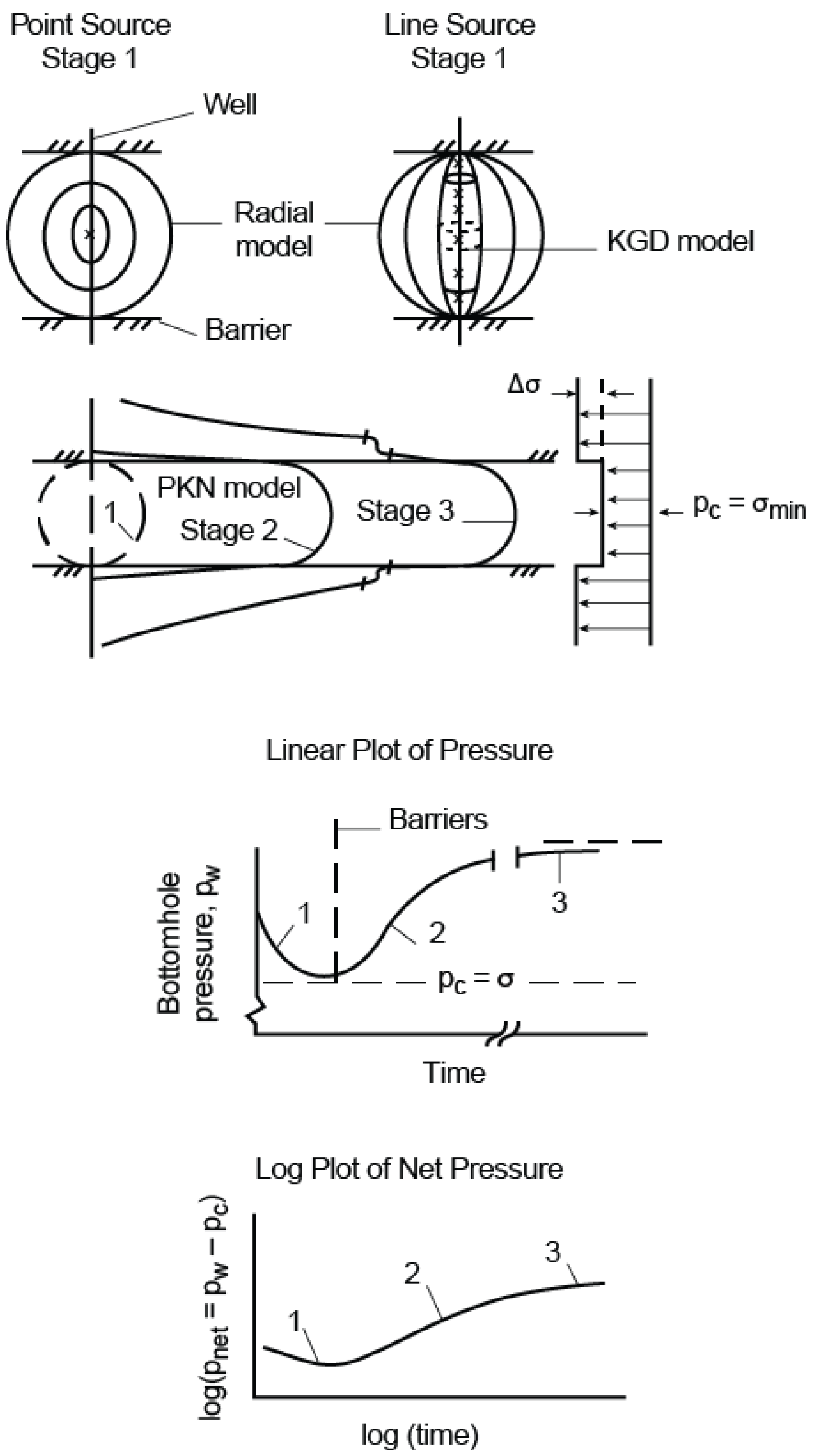


*Source: Nolte (1991)*[2]

Figure 2.1 Hydraulic fracture growth/shape evolution and the associated pressure response

[2] Copyright 1991, SPE. Reproduced with permission of SPE. Further reproduction prohibited without permission

#### 2.1.2.1 Height versus length growth – fracture shape

The need to predict hydraulic fracture height growth has been recognised as important since the first attempts to model vertical fractures. The early two-dimensional models (KGD and PKN) separated this calculation from the model. In setting up a 2D model, the user must select the fixed height based on what is known about the properties of potential barriers to growth above and below the targeted payzone interval (Perkins and Kern 1961). The model could be re-run with a different assumed height to decide what impact this would have on the other treatment parameters and on the ultimate length of the fracture produced. It was recognised that a model that could solve for height growth along with length growth was desirable and such models were developed in the late 1970s and early 1980s (Barree 1983; Cleary 1980; Clifton and Abou-Sayed 1981; Meyer 1989; Settari and Cleary 1984; Sousa et al. 1993; Touboul et al. 1986; Vandamme and Curran 1989). The pseudo three-dimensional models became the industry standard design tool by the late 1980s with planar 3D and even non-planar 3D models developed in parallel. However, the 3D models required more computer time to run and imposed restrictions on the type of problem that could be solved. For example, they typically could not consider layered rock sequences (Clifton and Abou-Sayed 1981; Vandamme and Curran 1989).

#### 2.1.2.2 Fluid loss, fracture orientation, natural fractures and interfaces

As has been mentioned above, coal is a naturally fractured reservoir rock. The existence of natural fractures changes the growth behaviour of a hydraulic fracture because the loss of fluid from the hydraulic fracture into the surrounding coal is greater than it would be in a sandstone reservoir that is not naturally fractured (Jeffrey and Settari 1998). The permeability of a natural fracture is sensitive to the effective normal stress acting across it. The effective normal stress is reduced in proportion with the increase in pore pressure in the natural fracture. The loss of fluid from the hydraulic fracture causes the pore pressure in the natural fractures around the hydraulic fracture to increase, increasing the permeability of these natural fractures which in turn increases the rate of fluid loss (or leak-off) from the hydraulic fracture. This positive feedback process results in non-linear leak-off behaviour. The additional fluid lost into the coal is not then available to extend the hydraulic fracture and this slows the rate of fracture growth (Barree and Mukherjee 1996; Jeffrey and Settari 1998; Jeffrey et al. 1999). Interfaces, such as bedding planes, can act in a similar way to natural fractures (Zhang et al. 2007a) and the fluid lost into them results in a slowing of the fracture growth rate.

Hydraulic fractures can be arrested or slowed by growth into high permeability faults or shear zones. In the most extreme cases, the fluid in the hydraulic fracture enters the permeability feature and all of it is lost so that no volume remains to extend the hydraulic fracture. Less extreme cases can allow the fracture to cross the feature; but as fluid loss occurs into it, the permeability of the feature may increase by the process described above (non-linear leak-off) and this will progressively slow the hydraulic fracture growth rate (Zhang et al. 2007a).

The hydraulic fracture may grow into natural fractures or interfaces and it often crosses these features by exiting in the direction it initially was growing in. This results in an offset in the fracture path which produces a section of the fracture with reduced width (Daneshy 2003; Jeffrey et al. 2009). The reduced width will in turn result in higher treating pressures in order to force fluid through it. The higher excess pressure in the fracture channel upstream of each restriction then results in wider fracture opening and this additional width and fluid volume stored produces a slower fracture growth rate (Jeffrey et al. 2009; Zhang et al. 2008, 2007b).

#### 2.1.2.3 Planar 3D hydraulic fracture models

As has been done in the above sections, a distinction is made here between design and research models. There are more research models available than design models because certain aspects of the practical problem, such as proppant transport, pumping of multiple stages of fluid, and flow of fluid with non-Newtonian rheology are often ignored in a research model that is concentrating, for example, on developing new fracture propagation algorithms. This section consists of a list of models and a brief description of the models' capabilities and limitations. It should be noted that this list is not comprehensive, and some of the models are no longer actively being used.

**Terra Frac:** This planar 3D model was developed by Terra Tek in the 1980s (Clifton and Abou-Sayed 1981). It is based on a boundary element method which is implemented using a variational formulation as is common in finite element methods. The model solves the problem on a unit square mesh and maps this to the physical mesh to obtain the fracture geometry. Terra Frac was developed into the first 3D design model available to industry and included non-Newtonian fluid flow, proppant transport, fluid leak-off and stress layering.

**Touboul model:** A planar 3D boundary element model was developed by Touboul and Ben Naceur in the 1980s (Naceur and Touboul 1990; Touboul et al. 1986). The formulation was similar to the variational method used by Clifton and Abou-Sayed (1981) but included terms that could be used to allow for out-of-plane fracture growth and interaction with natural fractures. The model was proprietary to Dowell Schlumberger and was therefore only used by the developers.

**Vandamme model**: This 3D model was an early effort to consider out-of-plane fracture growth (Vandamme and Curran 1989). The model was based on boundary element displacement discontinuity methods and used higher order shape functions with square root shape tip elements. It included leak-off by implementing a 1D leak-off coefficient approach. This model required considerable computational effort to obtain solutions to problems of interest, especially considering the limited processing power of computers available in the 1980s.

**HyFranc3D:** This 3D model was developed by the Cornell Fracturing Group in the 1980s (Sousa et al. 1993). The model uses boundary elements and can consider out-of-plane fracture growth. It has been applied to fracture initiation and reorientation from a wellbore among other problems. It has been found to require considerable computational effort.

**Planar3D**: This Schlumberger proprietary 3D model has been developed in the past 10 years and uses a fixed grid to implement a boundary element based model. Horizontal layering for stress and mechanical properties is supported, as are non-Newtonian fluids, proppant transport and fluid leak-off (Peirce et al. 2009; Siebrits and Peirce 2002). Only planar fracture growth is considered.

**GOHFER:** The GOHFER 3D model calculates the fracture width based on superposition of displacements found by integrating the Boussinesq solution for a point force applied to the surface of a half-space (Barree 1983). The model uses a fixed grid and is a full design model that supports non-Newtonian fluids, proppant transport, layering and leak-off. The model is limited to planar fractures.

**StimPlan**: The StimPlan 3D model is based on the finite element method and offers full design capability with support for layers, non-Newtonian fluids, proppant transport and leak-off (NSI Technologies 2012). The model is limited to planar fracture geometries.

A number of other 3D models have been developed but are not included here as most are research-only models that are currently only available to their authors.

### *2.1.3 Non-planar hydraulic fracture growth*

Hydraulic fractures become non-planar when they grow in regions where the stress field is modified by pre-existing geological structures such as faults, bedding, or man-made wellbores or where the fracture propagation becomes energetically easier for a direction that is not a straight extension of the current fracture direction (Daneshy 2003). Reorientation may occur at a frictionally weak interface because it takes less energy for the fracture to grow along the interface than it does to cross it. In many cases, the reorientation involves both a change in the local stress direction and a change in the energy required for fracture growth. The stress change induced by the fracture itself may contribute to the local stress field and affect the fracture path (e.g. when frictional sliding on a pre-existing natural fracture or fault occurs). The main causes of non-planar hydraulic fracture growth are reviewed in the following sections.

#### 2.1.3.1 Early 2D hydraulic fracture models

Adopting the classic Sneddon plane strain crack solution (Sneddon and Elliott 1946), Perkins and Kern developed the so-called PK model (Perkins and Kern 1961). Later, Nordgren (1972) extended the PK model to formulate the PKN model, which considered the effects of fluid loss. Khristianovic and Zheltov (1955) and Geertsma and de Klerk (1969) developed the so-called KGD plane strain hydraulic fracture model. Design versions of these models were in use in the 1970s and 1980s (Daneshy 1973; Settari 1988) The PKN model is applicable to long fractures of constant height with an elliptical vertical cross-section, whereas the KGD model for width calculation is height independent, and is strictly applicable for either short fractures that extend to large height along the wellbore or to cases where a low friction strength horizontal interface allows slip at the top and bottom of the fracture to occur. In these cases the plane strain assumption built into the KGD model can be used (Nolte 1991).

Simonson et al. (1978) considered height growth for a symmetric hydraulic fracture growing in a central reservoir or payzone layer and contained by layers above and below. Their work was a starting point for analysis of height growth (see also Nolte and Smith 1981), and soon after, height calculations were integrated into hydraulic fracturing models, such as the so-called pseudo 3D (P3D) models (see, for example, Figure 2.2), which eventually were developed for non-symmetric multi-layer cases (e.g. Settari and Cleary 1984; Meyer 1989; Fung et al. 1987).

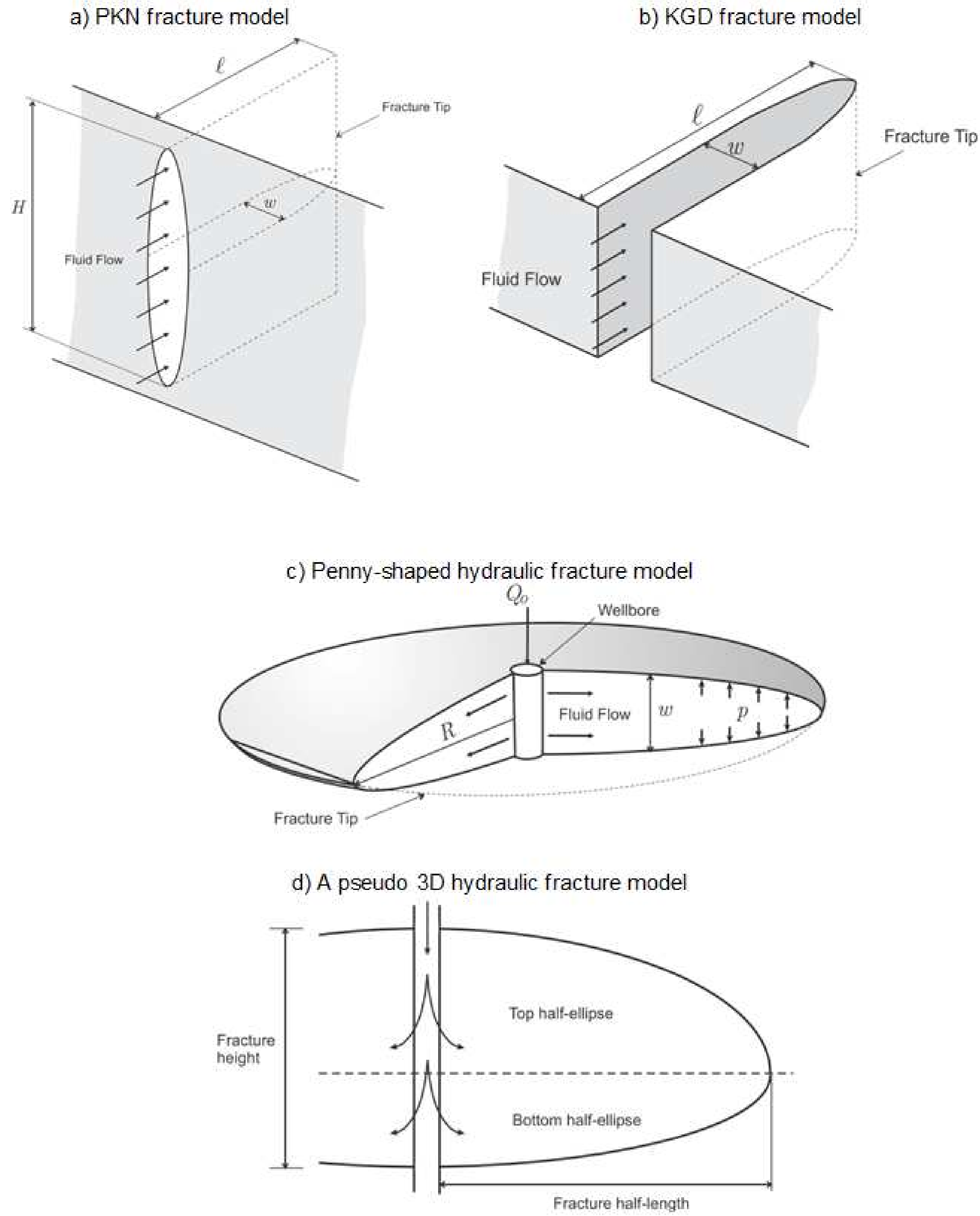


*Source: Adachi et al. (2007)*[3]

Figure 2.2  Fracture geometry represented in PKN, KGD, penny-shaped and pseudo 3D hydraulic fracture models

[3] Reprinted from International Journal of Rock Mechanics and Mining Sciences, 44, J. Adachi, E. Siebrits, A. Peirce, J. Desroches, Computer simulation of hydraulic fractures, 741-742, Copyright (2007), with permission from Elsevier

A number of authors have used dimensional analysis in developing more efficient and accurate methods to model hydraulic fractures and for design of laboratory experiments (Cleary 1980; de Pater et al. 1994). Much of the more recent effort has been in employing dimensional analysis methods, as described by Barenblatt (1996), to define important non-dimensional parameter groups that control hydraulic fracture growth (Detournay 2004). The simpler 2D models described above have been the main focus of this analytical and semi-analytical work, but the results obtained, which describe the near-tip fracture behaviour (e.g. the development and size of the fluid lag region and the asymptotic shape of the near-tip region) and relationships that apply to hydraulic fracture growth (e.g. viscous dissipation versus toughness as the dominant process consuming energy), have direct application to 3D modelling. Following the method originally proposed by Spence and Sharp (1985), Adachi (2001) and Adachi and Detournay (2002) have developed approximate self-similar solutions for the KGD hydraulic fracture geometry. Following the approach used for the KGD fracture, Savitski and Detournay (2002) developed approximate self-similar solutions for the penny-shaped hydraulic fractures. These results have been reviewed and summarised by Detournay (2004).

Different numerical simulators have been developed for application to research issues around modelling of the propagation of a plane strain KGD or penny-shaped hydraulic fractures. Many such models have been developed for particular purposes (Bunger et al. 2007; Weng 1993; Chen and Jeffrey 2009; Chen 2012; Peirce and Detournay 2008; Zhang et al. 2002; de Pater et al. 1996; Cherny et al. 2009)

### 2.1.3.2 Branching and offsetting

Branching and offsetting have been recorded in mine-through experiments where hydraulic fractures are placed into a rock and then mapped after mining (Diamond and Oyler 1987; Jeffrey et al. 2009; Steidl 1993; Warpinski 1985). Branching and offsetting have also been noted in a number of laboratory experimental results (Beugelsdijk et al. 2000; Daneshy 1973; Meng and de Pater 2011). When the fracture consists of a vertical and horizontal fracture branch, it is usually referred to as T-shaped, because the horizontal fracture often forms at the upper limit of the vertical fracture. This type of geometry is relatively frequently produced by fracture stimulations of coal seams, partly because of the strong contrast between the coal mechanical properties and the floor and roof rock properties. The stress conditions in Australian seams are often such that a vertical hydraulic fracture is formed in the coal (Enever et al. 2000) but, because of higher horizontal stress in the rock above and below the seam, the fracture cannot extend into these rock layers and a horizontal fracture may then form at the roof rock and coal interface.

Offsets along the fracture path are produced as the hydraulic fracture interacts with and crosses natural fractures and faults (Daneshy 1973; Jeffrey et al. 2009; Warpinski 1985). The offsets can have a strong effect on the fracture width and the fracturing pressure, with the offsets being sections of reduced fracture width, leading to higher fracturing pressures (Daneshy 2003; Jeffrey et al. 2009). In coal, higher fracturing pressures required to extend a vertical fracture can lead to the formation of a horizontal branch, producing a T-shaped overall geometry. High pressures may also lead to height growth, which is then reflected in declining treating pressure with time (Nolte and Smith 1981).

### 2.1.3.3 Multiple fractures and segmentation

Multiple sub-parallel fractures have been mapped in several mine back experiments (Warpinski 1985). Many of these parallel fractures represent a slice through a hydraulic fracture that contains branches and, if the mapping is carried out over a wider area, the secondary branches will often be found to not extend far. In other cases, parallel fractures have been mapped to extend over a considerable distance (Steidl 1993) but evidence can be found in some cases for these having been formed sequentially rather than growing simultaneously (Jeffrey et al. 1998). Sequential growth of parallel, closely spaced hydraulic fractures is supported by the analysis provided by Bunger et al. (2012). In such cases, an early fracture may screen out causing a second branch to grow parallel to the first propped fracture (Jeffrey et al. 1998). Further evidence for multiple parallel fracture growth was presented in Warpinski et al. (1993) where multiple fractures were found in a core from a well drilled through a hydraulic fracture placed in a tight gas research well.

#### 2.1.3.4 Network fracture models

Shale gas stimulations have been frequently monitored by recording microseismic events during the treatments. This monitoring has shown that events occur over a region around the hydraulic fracture and indications for a network of fractures forming are seen in some of the monitoring data (Fisher et al. 2004). The service industry has therefore developed network hydraulic fracture models to be better able to analyse and design such fracture growth.

**UFM:** This proprietary model has been developed by Schlumberger in recent years to serve as a design tool for shale gas fracture stimulation. The model is able to propagate hydraulic fractures through a pre-existing set of natural fractures, generating a network-like hydraulic fracture (Kresse et al. 2012; Weng et al. 2011). Proppant transport and non-Newtonian fluid properties are included.

**Meyer DFN:** This model considers growth and interaction in a network of pseudo 3D fractures. The fractures grow along two or three pre-defined orthogonal planes aligned with each of the principal stresses. Proppant transport is included in the model (Meyer and Bazan 2011).

**FracMan:** Golder and Associates have modified their discrete fracture network FracMan model to include aspects of hydraulic fracturing. The hydraulic fracture growth is simulated by considering mass balance between injected volume and volume leaking off and contained to the hydraulic fracture. Elastic coupling of pressure and fracture opening is not considered (Dershowitz et al. 2010). Fracture growth is limited to occur along pre-existing fracture paths.

**UDEC:** This commercial distinct element model is available from Itasca and has been applied to modelling of hydraulic fracture growth in naturally fractured rock masses, including mapping of shear deformation during the injection (Nagel et al. 2012). The model only allows fracture growth along a pre-defined natural fracture. Fractures can deform in aperture and shear in response to far-field stress and fluid pressure change. UDEC has been used by a number of researchers to investigate aspects of hydraulic fracture mechanics. For example, Choi and Shin (2001) used UDEC to study the fracture closure process from microfracturing used for in-situ stress measurements. The 3D version of UDEC, called 3DEC, has been applied to injections into naturally fractured rock for the purpose of simulating induced shear deformation (Damjanac et al. 2010).

**PFC:** A hydraulic fracturing model has been developed within the framework of Itasca's PFC Discrete Element Model. This particle-based model includes natural fractures as planes of defined strength and conductivity, and models fluid flow by pipes connecting pore volumes (Damjanac et al. 2010; Han et al. 2012).

### *2.1.4 Hydraulic fracture growth monitoring*

#### 2.1.4.1 Microseismic event detection

Microseismic events are generated by rock failure, usually associated with shear movement on pre-existing natural fractures or faults, in response to changes in the effective stress acting on them. The stress change is, in this case, produced by the growing hydraulic fracture. The increase in pore pressure around the hydraulic fracture, which results from leak-off of fracturing fluid, is the primary mechanism that results in generation of microseismic events (Warpinski 2013). The leak-off process results in an increase in the pore pressure in the rock on either side of the hydraulic fracture. This increased pore pressure acts to reduce the effective normal stress acting across pre-existing natural fractures and as a result these may undergo shear failure, with an associated release of energy and generation of a microseismic event. The elastic stress change in the rock around the fracture, produced by the physical opening of the fracture, is a second but less important mechanism. The empirical observation is that the microseismic events tend to cluster around the plane of the hydraulic fracture and locating these events is a useful method of mapping the fracture orientation and extent (Warpinski et al. 2010; Fisher et al. 2004).

An array of geophones or accelerometers is used to locate microseismic events. The array can be located in a number of boreholes spread across the surface or along a string that is run into an offset well, ideally located 100 to 300 m from the well to be fractured. The sensors are used to detect the arrival of the compression and shear waves from the event. Knowing the wave velocity in the rock allows the event's location to be determined, provided arrivals from at least six sensors are recorded. Accelerometers also provide the direction of first movement associated with the compression wave which gives a direction from the sensor to the event. A typical array for monitoring might contain eight to 16 sensors and can typically locate events to within 10 to 20 m of their true position. The accuracy of event locations depends on site-specific conditions including the instrumentation array details and the knowledge of rock seismic velocity for various rock layers at the site (Zimmer et al. 2009).

#### 2.1.4.2 Tiltmeter monitoring

Tiltmeters are extremely accurate measuring devices that typically use electrolytes with bubble sensors to measure, at their position, the changes of inclination with respect to vertical in two orthogonal directions. Several types of tilt sensor exist but the most common are electrolyte level sensors which convert changes of tilt angle to changes of resistance. When applied to monitoring hydraulic fractures, the resolution of these tiltmeters is typically in the nanoradian range (e.g. approximately $5\times10^{-9}$ radians or less). Usually for geotechnical applications, tiltmeters are located in shallow boreholes (6 to 12 m deep) in order to reduce the ambient noise.

The opening and propagation of a pressurised fracture produces elastic (more or less) deformations in the surrounding rock mass which, in turn, result in a change in inclination at the position of the tiltmeter. During the monitoring operations, the inclination change is sampled sequentially in time at each tiltmeter and an array of tiltmeters is used to obtain tilts at different locations remote from the hydraulic fracture. The tiltmeters can be located in shallow boreholes on the surface (surface tiltmeter array) or in a vertical well (downhole tiltmeter array), as illustrated in Figure 2..The use of tiltmeters to monitor hydraulic fractures is an established geophysical technique, which can be traced back to the paper of Sun (1969). Since then, this technique has been used to monitor deformations associated with the formation of both shallow and deep hydraulic fractures. Monitoring using a surface array has been undertaken for fractures at depths up to 3 000 m (Wright et al. 1998b). Surface tiltmeters have been employed to map hydraulic fractures for over three decades, but the downhole application of this technology is more recent (Warpinski 2006; Wright et al. 1998a).

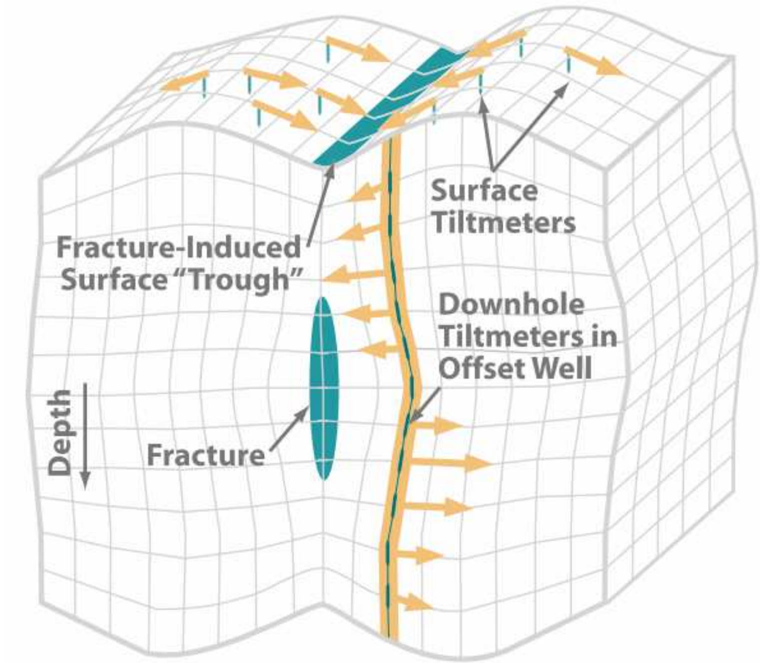


*Source: Wright and Weijers (2001), with permission*

Figure 2.3 Tiltmeter monitoring of hydraulic fracture

### *Inverse modelling of tilt data*

Models for evaluating the deformations (displacement and tilt) produced by a planar hydraulic fracture, as part of the inverse modelling associated with analysis of tiltmeter data, have generally been obtained from either elastic crack solutions (e.g. Sneddon 1946; Sun 1969; Pollard and Holzhausen 1979; Warpinski 2000) or dislocation solutions (Converse and Comninou 1975; Okada 1992, 1985; Press et al. 1986; Rongved and Frasier 1958; Rongved and Hill 1957; Yang and Davis 1986). The most common and efficient forward methods for evaluating the deformations induced by hydraulic fractures use a distribution of Displacement Discontinuities (DD) on a planar surface representing the fracture. In addition, analytical expressions for simple geometric shapes, such as the penny-shaped crack (Sneddon 1946), are useful as forward models. The validity of these types of models and their applications has been extensively discussed (Davis 1983; Evans 1983; Warpinski 2000).

By applying the Sneddon solution, Sun (1969) developed an approximate solution for a penny-shaped crack embedded in a semi-infinite elastic medium, with the crack plane parallel to the boundary (ground) surface. He derived analytical expressions for the surface displacement by superimposing an image solution and a stress function on the Sneddon solution. The solution given by Sun is valid only when the crack is deep in comparison with its radius. For a crack near the surface, modifications must be made (Davis 1983). Pollard and Holzhausen (1979) derived a solution for near surface, two-dimensional cracks, which satisfies the free surface and crack surface boundary conditions simultaneously by using a numerical method of successive approximations. A rigorous numerical solution for a penny-shaped hydraulic fracture parallel to the free-surface of an elastic half-space was derived by Zhang et al. (2002).

Because the Sneddon (1946) model is for a penny-shaped crack in an infinite medium, the Sun model is valid only for a deep penny-shaped crack with the crack plane parallel to the ground surface, and the Pollard-Holzhausen model is two-dimensional and numerical, the application of the elastic crack solutions is limited. There is a need for more general, efficient three-dimensional models for iterative inverse analyses.

Dislocation solutions based on the distributed displacement discontinuity (DD) technique provide a convenient method for constructing 3D fracture models for hydraulic fracture tiltmeter mapping. The most common models are a rectangular DD with constant opening (Converse and Comninou 1975; Okada 1992, 1985; Press et al. 1986; Rongved and Frasier 1958; Rongved and Hill 1957; Yang and Davis 1986). Because of their simplicity, the Davis (1983) and Okada (1985) formulations are particularly convenient for the estimation of surface deformation. Yang and Davis (1986) gave the full solution for a dipping rectangular tension crack extending throughout the medium. Okada (1992) presented a complete set of closed analytical expressions for the internal displacements and strains arising from inclined shear and tensile faults in a half-space for both point and finite rectangular fractures. Those expressions provide powerful tools both for the observational and theoretical analyses of static deformation fields associated with hydraulic fractures.

In order to efficiently carry out the inversion process, a number of different types of forward models are typically available in the analysis software and the engineer can try different models for the problem being analysed (Lecampion et al. 2004; Wright et al. 1994).

In addition to the closed-form analytical expressions for both point and finite rectangular DD sources, the distributed DD technique also provides an efficient numerical method for the prediction of the deformation associated with a more complex planar fracture. In a more

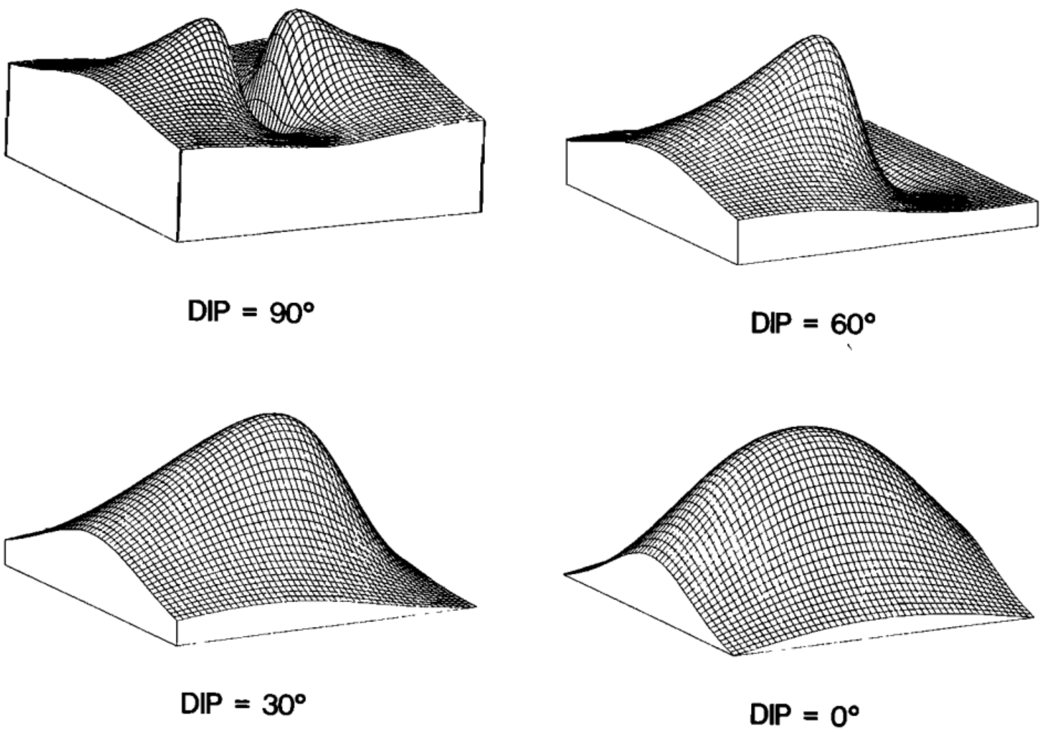


*Source: Davis (1983), with permission*

Figure 2.4 Characteristic surface uplifting patterns produced by fractures with four different orientations (using a dislocation model for the fracture) whose geometry differs only in dip

general way, DD singularities can be used as fundamental building blocks to construct elastic solutions for any geometry of finite fractures, by superposition (Olson et al. 1997).

Hydraulic fractures produce a well-defined tilt signature in a predictable manner that can be inverted using an appropriate model to infer fracture geometry parameters. Figure 2. and Figure 2.5 illustrate the characteristic surface deformation patterns for fractures of several geometries.

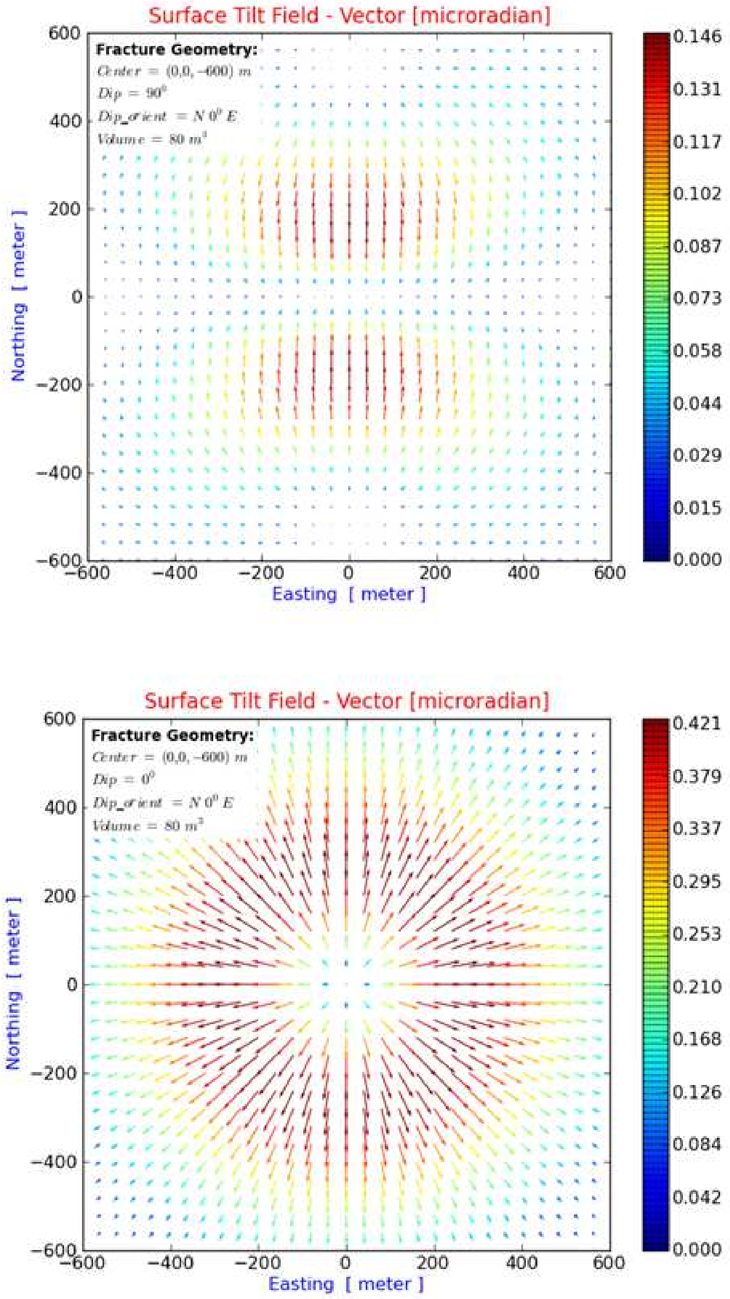


*Source: CSIRO (unpublished study). Tilt vectors are drawn to point downhill. The vector length is proportional to the tilt magnitude which is also indicated by colour according to the scale in microradians.*

Figure 2.5 Calculated tilt vectors for vertical and horizontal hydraulic fractures

The dependence of the surface deformation field on fracture dimensions is weak in comparison to the influence of strike, dip, depth to centre, and total fracture volume. The surface tilt data provide only smoothed information regarding the distribution of fracture opening displacements and are inherently insensitive to details in cross-sectional geometry.

Only mean aperture can be determined from the surface tilt data (Evans 1983), so a map of surface tilt deformation allows robust and unambiguous estimation of the azimuth, dip and volume of the fracture. Depth to fracture-centre and fracture offset due to asymmetric growth can also be determined, though with somewhat less precision (Wright and Weijers 2001). The greatest limitation of surface tilt mapping is the inability to accurately resolve fracture dimensions. Mapping fracture dimensions requires either downhole tilt mapping or microseismic imaging.

Based on practical experience, Cipolla and Wright (2000) list some of the fracture quantities resolvable by surface or downhole tilt mapping (see, for example Table 2.2). Based on theoretical analysis, a proper limit for the resolution of fracture dimensions depending on the measurements configuration (spatial relationship between the tiltmeters and the treatment well) has been obtained (Lecampion et al. 2005). The loss of resolution when the tiltmeters are far from the fracture with respect to fracture length is crucial in practice.

Tiltmeter monitoring has proved to be a reliable technique of hydraulic fracture mapping for shallow to medium depths, with reported success at great depths (Smith et al. 1986). Surface tiltmeter monitoring has been used to evaluate hydraulic fracture effectiveness in a coal seam gas reservoir by Johnson et al. (2010b). Tiltmeter monitoring together with stress change monitoring (Mills and Jeffrey 2004; Mills et al. 2004) can provide more detailed information about the hydraulic fracture such as the fracture growth rate and mode of growth, and the asymmetric growth of a hydraulic fracture (Jeffrey et al. 1995). The use of hybrid tiltmeter / microseismic arrays can provide high-resolution monitoring of hydraulic fracture growth and behaviour (Warpinski 2006) such as the fracture height growth in sedimentary environments (Warpinski 2011). According to Warpinski (2011), vertical propagation of a hydraulic fracture across layers is very inefficient and it is difficult to obtain extensive vertical growth in such rock. In shale projects where large fluid volumes are injected, different diagnostic measurements have consistently shown that fractures remain thousands of feet deeper than the aquifers.

Table 2.2 Capabilities and limitations of fracture diagnostics

| **Group** | **Fracture diagnostic method** | **Main limitations** | **Ability to estimate** | | | | | | | |
|---|---|---|---|---|---|---|---|---|---|---|
| | | | **Length** | **Height** | **Asymmetry** | **Width** | **Azimuth** | **Dip** | **Volume** | **Conductivity** |
| Far field, during fracturing | Surface tiltmeter mapping | Cannot resolve individual and complex fracture dimensions.<br>Mapping resolution decreases with depth (fracture azimuth ±30 at 3000.ft depth and ±100 at 10 000.ft depth. | # | # | # | ^ | * | * | * | ^ |
| | Downhole tiltmeter mapping | Resolution in fracture length and height decreases as monitoring-well distance increases. | * | * | * | # | # | ^ | * | ^ |

| Group | Fracture diagnostic method | Main limitations | Ability to estimate | | | | | | | |
|---|---|---|---|---|---|---|---|---|---|---|
| | | | Length | Height | Asymmetry | Width | Azimuth | Dip | Volume | Conductivity |
| | | Limited by the availability of potential monitoring wells.<br>No information about proppant distribution and effective fracture geometry. | | | | | | | | |
| | Microseismic mapping | Limited by the availability of potential monitoring wells.<br>Dependent on velocity-model correctness.<br>No information about proppant distribution and effective fracture geometry. | * | * | * | ^ | * | # | ^ | ^ |
| Near wellbore, after fracturing | Radioactive tracers | Measurement in near-wellbore volume.<br>Provides only a lower limit for fracture height if fracture and well path are not aligned. | ^ | # | ^ | # | # | ^ | ^ | ^ |
| | Temperature logging | Thermal conductivity of different formations can vary, skewing temperature log results.<br>Post-treatment log requires multiple passes within 24 hours after the treatment.<br>Provides only a lower limit for fracture height if fracture and well path are not aligned. | ^ | # | ^ | ^ | ^ | ^ | ^ | ^ |
| | Production | Provides only information about | ^ | # | ^ | ^ | ^ | ^ | ^ | ^ |

| Group | Fracture diagnostic method | Main limitations | Ability to estimate | | | | | | | |
|---|---|---|---|---|---|---|---|---|---|---|
| | | | Length | Height | Asymmetry | Width | Azimuth | Dip | Volume | Conductivity |
| | logging | zone or perforation contributing to production in cased-hole applications. | | | | | | | | |
| | Wellbore imaging logging | Run only in open hole.<br>Provides fracture orientation only near the wellbore. | ^ | # | ^ | # | # | # | ^ | ^ |
| | Downhole video | Run mostly in cased holes and provides information only about zones and perforation contributing to production.<br>May have open hole applications. | ^ | # | ^ | ^ | ^ | ^ | ^ | ^ |
| Model based | Net-pressure fracture analysis | Results depend on model assumptions and reservoir description.<br>Requires "calibration" with direct observations. | # | # | ^ | # | ^ | ^ | # | # |
| | Well testing | Results depend on model assumptions.<br>Requires accurate permeability and reservoir pressure estimates. | # | ^ | ^ | # | ^ | ^ | ^ | # |
| | Production analysis | Results dependent on model assumptions.<br>Requires accurate permeability and reservoir pressure estimates. | # | ^ | ^ | # | ^ | ^ | ^ | # |

*Note: * Techniques can be determined; # techniques may be determined; ^ techniques that cannot be determined*

*Source: Bennett et al. (2005), Table copyright Schlumberger. Used with permission*

### 2.1.4.3 Fracture pressure analysis

The earliest but still very useful method to obtain information about fracture growth is by analysis of the pressure recorded during the injection and falloff periods (Nolte and Smith 1981). Pressure analysis includes recording and analysing information about the injection rate and stages of fluids and proppant pumped, as these parameters strongly affect the pressure. Pressure for analysis is best obtained from bottom-hole gauges, which are not affected by the fluid friction pressure in the wellbore and tubing strings or by the need to account for pressure gained from gravitational potential and the density of the fluid.

#### *Pressure and rate measured at the injection well*

Monitoring and recording pressure and injection rate at the pump or downhole at the injection well is a universal practice in the oil and gas industry (Gidley et al. 1989). When the pressure response is viewed in light of simple hydraulic fracture models, useful inferences about fracture growth can be made (Nolte and Smith 1981; Nolte 1991). For example, the pressure recorded in time, as illustrated in Figure 2. in Section 2.1.2 provides information about fracture height growth. Once height growth is estimated, the hydraulic fracture model is constrained and an improved estimate of fracture length growth is obtained. Fracture treatments are often analysed by a numerical hydraulic fracture model in real time as the treatment is being carried out. The model can accept pressure and rate data from instrumentation at the well site and produces a fracture geometry that is constrained to match the data input.

#### *Pressure measured at offset wells*

Occasionally, offset wells can be monitored to obtain information about hydraulic fracture growth during stimulation of a targeted well. If the offset wells are used in this way, they are usually shut in and pressure is monitored either at the wellhead or downhole. It is also sometimes feasible to monitor deformation or temperature in the offset well, but this is usually only applied in detailed research projects (see for example Jeffrey and Settari 1998). Pressure response at the offset wells is an indication of the hydraulic fracture approaching the well or even intersected it, providing useful constraint on the fracture growth and orientation.

### 2.1.4.4 Logging methods

#### *Radioactive tracers*

Small amounts of radioactive isotopes, such as Scandium 46, Iridium 192 and Antimony 124 are used, typically by applying them in resin coating onto proppant or by integrating them into specially manufactured proppant grains (Holditch et al. 1993). The radioactive tagged proppant is pumped as part of the overall proppant stage and later located by well logging to determine where in a wellbore the various stages of proppant entered the reservoir. This is useful when a number of perforations are present over an interval of the well or when the well section in the targeted area is uncased. The tracers can be detected through casing and then provide an indication of fracture height growth along the wellbore (McDaniel et al. 2007; Rahim and Al-qahtani 2001). Different isotopes are used to tag different stages during the treatment and these are then detected by geophysical wireline logging after the fracture treatment has been placed and flowed back. Non-radioactive tracers have recently been introduced that are activated by a neutron source on the logging tool. After being activated, these materials produce radioactive emissions for a few seconds that can be detected and recorded by the same tool (McDaniel et al. 2007) but are otherwise non-radioactive, enhancing safety and simplifying transport, handling and disposal.

### *Optical and acoustic image logs and resistivity image logs*

Wireline logging tools are available that provide an image of the wellbore wall with a resolution high enough to detect and map natural and hydraulic fractures (Palmer and Sparks 1991; Smith et al. 1982). These logging methods do require an uncased wellbore and this limits their application in mapping fractures because many wells are cased before being treated by hydraulic fracturing. An image of a propped hydraulic fracture in a coal seam in New South Wales (NSW), obtained with a digital video wellbore camera, is contained in Figure 2.6. The optical image shown in Figure 2.6 indicates that the fracture did not grow vertically in height into the rock above or below the seam. This was later confirmed when the fracture was mapped after mining.

### *Production logs and temperature logs*

Production logging involves running a tool into the well that records the fluid flow in the wellbore. By continuously logging this flow rate as the tool is run into or out of the well, the change in flow rate with position can be interpreted to give the flow into (or out of) the wellbore at various locations. Thus the locations and extent of conductive fractures, including propped hydraulic fractures can be established (Matsunaga and Tenma 1995).

Temperature logging can be done before and after the hydraulic fracture treatment with a temperature anomaly created by the warm fluid in the fracture returning to the cooled wellbore after the fracture is placed. This type of survey can establish the approximate top and bottom of a vertical fracture (Gidley et al. 1989). More recently, fibre optic temperature sensors have been used to install a distributed temperature sensor (DTS) array along a wellbore. Logging the temperature and noting the cooled areas during the fracturing injection then provides information on which perforations or parts of the wellbore are accepting fluid. After the end of the treatment, the warm fracturing fluid can be detected returning to the wellbore, providing another indication of the zones that were fractured. This monitoring method has gained popularity in horizontal shale gas wells where long intervals are treated (Huckabee 2009), but installing such systems remains fairly expensive, which limits the frequency of use.

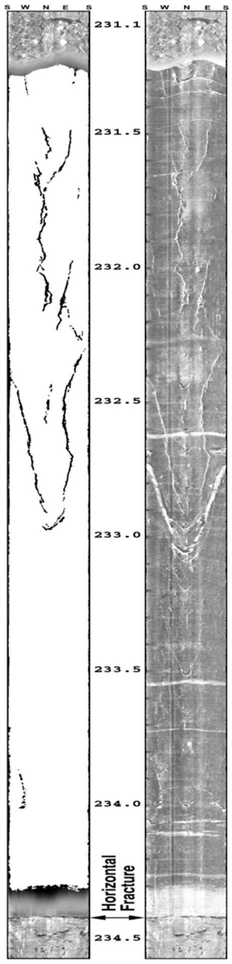


*Source: Jeffrey et al. (1998)[4]. Greyscale image is shown on the right and a processed image on the left. The fracture was interpreted to be an inverted T-shape.*

Figure 2.6 Wellbore optical video log showing a propped hydraulic fracture in a coal seam in NSW

### 2.1.5 Mining and mapping fractures

Hydraulic fractures have been mined and mapped in a number of rock types, but the largest database of mined fractures exists for coal seams. Hydraulic fracturing is undertaken in coal both for gas drainage ahead of mining and for coal seam gas extraction. Fractures that are placed into the seams for these reasons are often mined, but not always well documented. Early work on mapping such fractures was undertaken by the US Bureau of Mines (USBM) in order to determine if the hydraulic fractures presented any risk to eventual mining of the seam (Elder and Deul 1975). The US Bureau of Mines Report of Investigation 9083 documents 22 of these mined and mapped fractures located at sites in Pennsylvania, Virginia, West Virginia, Alabama, Utah and Illinois (Diamond and Oyler 1987). This report states that approximately half of the fractures mined had both vertical and horizontal branches. The fractures were generally shorter than the design models suggested, but one vertical fracture was mapped to a distance of 630 feet (192 m) and the maximum extent of a horizontal fracture was 265 feet (81 m). This USBM work was added to by several mine back projects carried out under sponsorship of the Gas Research Institute for the purpose of gaining a better understanding of the growth and extent of hydraulic fractures placed for

[4] Copyright 1998, SPE. Reproduced with permission of SPE, further reproduction prohibited without permission

stimulation of coalbed methane wells (Steidl 1993). Early efforts in Australia to use hydraulic fracturing for mine gas drainage resulted in mining through a number of fractures at Appin coal mine in NSW and at Leichhardt coal mine in Queensland (Stewart and Barro 1982). The mine back projects in these cases were intended to assess the effect of the fractures on mining so that no details of the fracture geometry were reported. Finally, between 1991 and 1998, the CSIRO carried out a program of research that resulted in mining and mapping of hydraulic fractures at nine different sites in Queensland and NSW (Jeffrey et al. 1995, 1992). The CSIRO work was designed to study hydraulic fracture growth in coal and compare the mapped fracture geometry and extent with predictions from numerical modelling.

One full-size hydraulic fracture, which was placed in the German Creek seam in Queensland, was mapped by Jeffrey et al. (1992). This fracture was designed to test vertical wells as a method for gas drainage in advance of mining. This fracture was T-shaped with a large horizontal component at the coal-roof rock interface that extended to a maximum propped distance of 120 m to the north-east. The vertical fracture was not detected beyond the extent of the horizontal fracture and both fracture branches were contained to the seam. Figure 2.7 shows a vertical section drawing of the fracture at a location 15 m from the wellbore, showing the T-shaped geometry with no penetration of the fracture into the roof rock.

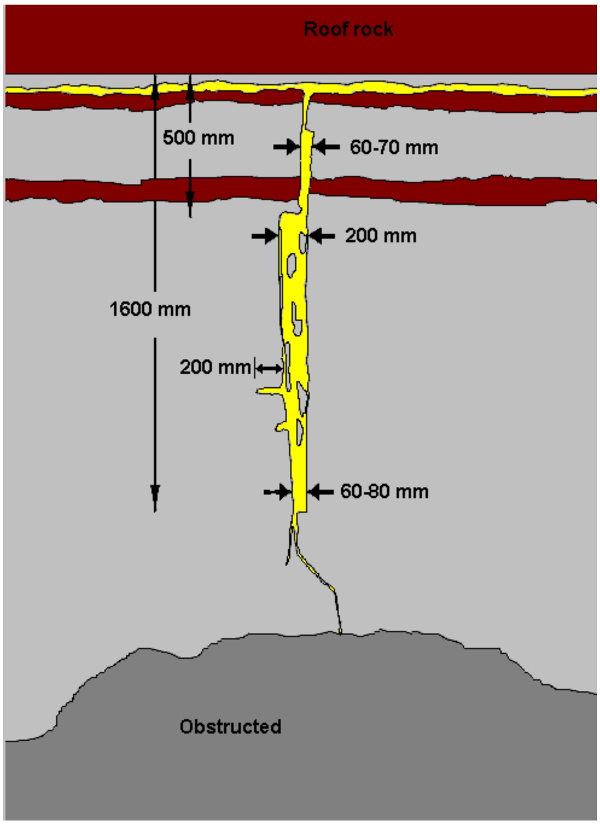


*Source: Jeffrey et al. (1992)[5]. The treatment screened out at the end and it is probable that the large propped fracture widths in the vertical fracture were generated during that event.*

Figure 2.7 A drawing of the mapped T-shaped hydraulic fracture exposed by mining of the treatment in well ECC90 in the German Creek coal seam

A map view of the fracture resulting from the treatment in well ECC90 is shown in Figure 2.8. The vertical section view in Figure 2.7 is located at point c in this figure. The yellow coloured

[5] Copyright 1992, SPE. Reproduced with permission of SPE, further reproduction prohibited without permission.

portion was propped with sand while the dashed line around the outside of this region indicates the limits of the zone where water and gas were seen to be produced at higher than normal rates from the roof-rock coal interface.

If the dotted line is taken as the maximum extent of the horizontal fracture, its length in the north-east direction is nearly 150 m. The solid black line running north-east to south-west from the well is the trace of the propped vertical fracture. The hydraulic fracture treatment in well ECC90 used a borate cross-linked guar gel pumped at 26 to 29 barrels per minute (4.1 to 4.6 $m^3$ per minute). By comparison, in Australia today, hydraulic fracture coal seam gas treatments might be pumped at up to approximately twice these injection rates but often use thinner fluids, including water with minor additives.

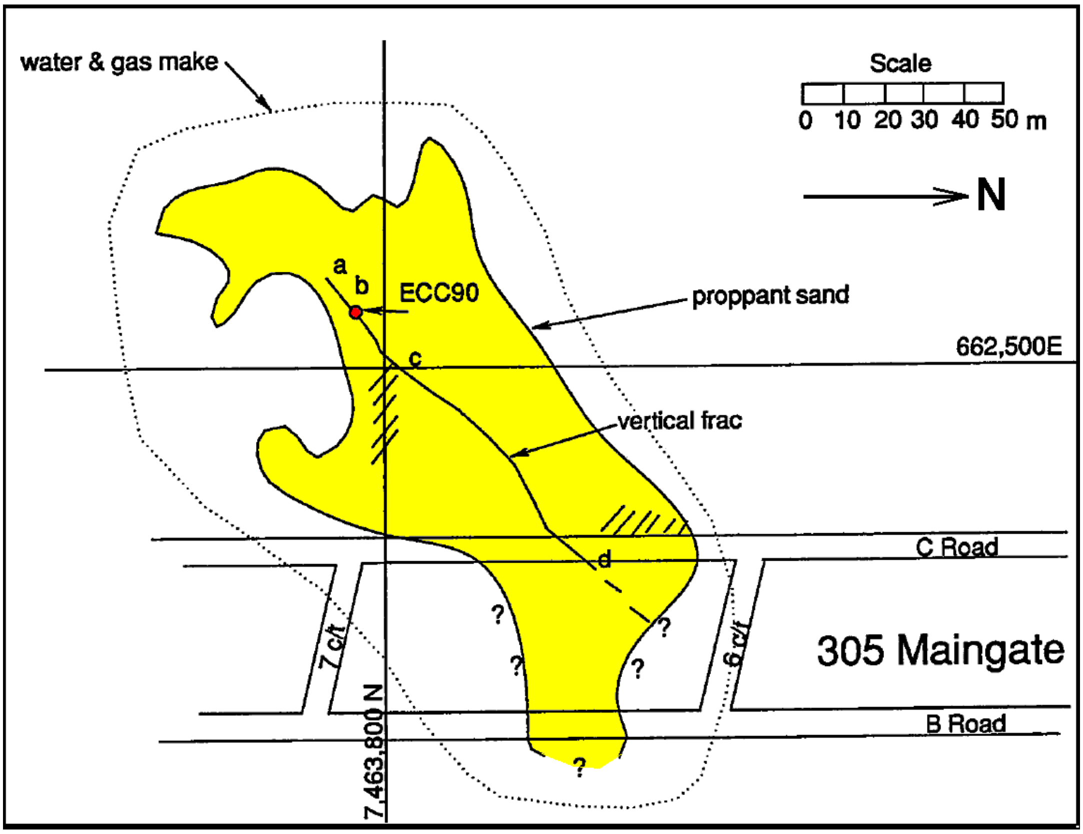


*Source: Jeffrey et al. (1992)[6]. The well (ECC90) is denoted by the red circle. The yellow colour indicates the mapped extent of the propped horizontal fracture.*

Figure 2.8 The extent and shape of the fracture mapped in the German Creek seam

### 2.1.6 Conclusions

Perhaps the most important consideration for designing effective hydraulic fracture stimulation in coal is ensuring that the fracture grows in the desired zone. Fortunately, in many if not most coal seams, the geology favours the formation of barriers to unwanted fracture height growth (see Section 2.2 for a discussion of factors affecting height growth). The existing planar hydraulic fracture models are useful for the relevant predictions and the industry has more than 30 years of experience in applying so-called pseudo 3D and 3D models to design of hydraulic fractures. Planar models will also provide an upper limit for extent of the fracture when compared to predictions made that consider branching, offsets,

---

[6] Copyright 1992, SPE. Reproduced with permission of SPE, further reproduction prohibited without permission.

and pressure-dependent leak-off. The non-planar models, by their nature, often have a statistical basis embedded into them describing the natural fracture orientations, sizes, and frequency. This statistical component adds a degree of freedom that can result in predictions of fracture growth varying between different models, perhaps suggesting that there is an uncertainty in understanding the growth. However, including branching and other non-planar and non-linear processes can slow fracture growth and reduce the ultimate size of the fracture generated. Therefore, the planar models provide a useful tool for establishing an upper limit for fracture growth.

One of the features of hydraulic fractures in coal is the propensity for secondary fracture sections to grow with a horizontal orientation along the contact between the coal and the roof and / or floor rock. Predicting this so-called T-shaped hydraulic fracture growth is beyond the reach of the current suite of models, which rely on an assumption of planar geometry in order to make the mathematical/numerical problem tractable.

Finally, there are a variety of diagnostic methods that have been applied to ascertain features of hydraulic fracture growth in coal. For example, well pressure and offset well pressure records can be used to infer whether the hydraulic fractures are likely to have grown in a vertical or horizontal orientation – or perhaps with a combination of both. Additionally, microseismic monitoring is often used to estimate the extent of the region mechanically impacted by the fracturing process and tiltmeter monitoring is an effective method to estimate the orientation of the hydraulic fracture and to constrain the proportion of injected fluid that leaks off into the formation during fracture propagation.

There are, however, some important caveats associated with the monitoring methods. One is that a microseismic event can be produced through a number of mechanisms and its occurrence is not necessarily indicative of a hydraulic fracture reaching that point, let alone the proppant. Another is that monitoring adds a cost to the stimulation that is often significant, and as a result methods such as microseismic and tiltmeter monitoring are most often used for only a few wells early in the development of a field and not as a standard source of data during the development of an entire field. From a risk management perspective, this indicates that reliance on expensive monitoring methods is probably not consistent with economic constraints.

## 2.2 Fracture height growth

### *2.2.1 Introduction*

Hydraulic fracture shape is determined by the variation in the parameters that affect fracture growth. These parameters include the properties of the rock, such as elastic modulus and permeability, and of the pore pressure, stress, and system compressibility. A change in a parameter in one region of the rock that acts to slow or arrest fracture growth will often lead to some redirection of growth into other parts of the rock mass. In an isotropic and homogeneous rock with uniform pressure and stress, a hydraulic fracture initiated from a point source will grow as a planar fracture with a circular shape.

### *2.2.2 Factors affecting height growth*

The prediction of height growth of a hydraulic fracture is a critical aspect of the fracture design process. The penetration of the fracture laterally into the reservoir rock layer will depend strongly on height growth, which includes growth upwards and downwards in the reservoir rock itself and in rocks lying above and below the reservoir.

### 2.2.2.1 Stress and pore pressure contrasts and gradients

It is generally accepted that stress contrasts between the reservoir and the bounding layers are the most important factors in determining height growth (Warpinski and Teufel 1987; Nolte and Smith 1981). Laboratory experiments (Jeffrey and Bunger 2007; Jeffrey et al. 2009) illustrate the striking contrast between cases with higher stress barrier layers and cases with lower stress layers bounding the reservoir. When the bounding layers have higher stress, they act as barriers. Figure 2.9 shows parameters and a chart for estimating fracture height growth into symmetric high stress layers, assuming the fracture is long compared to its height and that the fluid pressure in any cross section is uniform. Figure 2.9a shows a sequence of development as the fracture extends in length into the reservoir and eventually starts to grow vertically in height. A typical cross section of this fracture is shown in Figure 2.9b and Figure 2.9c shows the height growth as it depends on the ratio $\frac{P_{net}}{\Delta\sigma}$. If a lower stress region exists above or below the hydraulic fracture, the fracture will tend to heavily favour growth into this low stress zone (Wu et al. 2004).

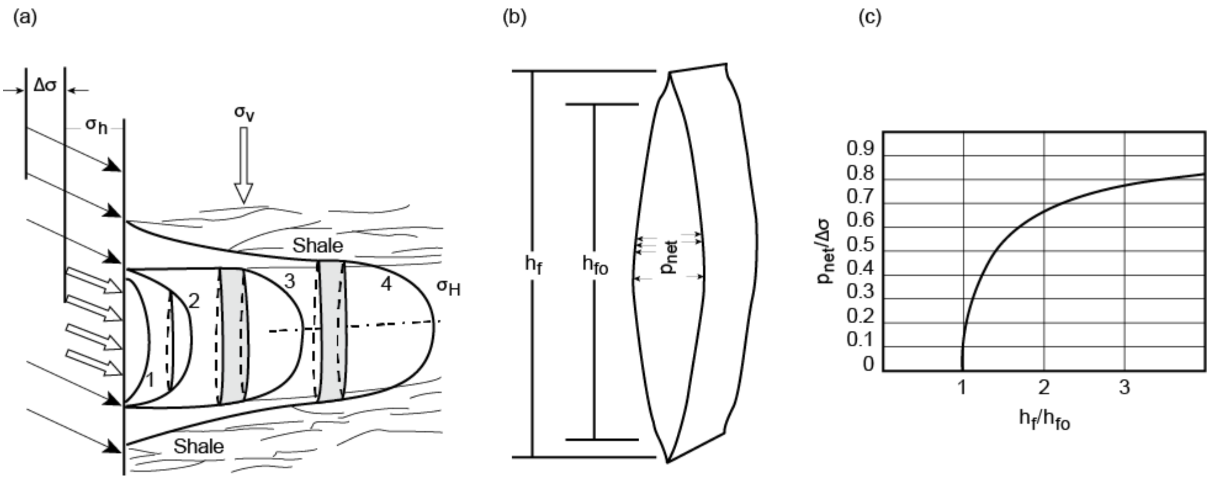


*Source: Economides and Nolte (2000)*[7]

Figure 2.9 Hydraulic fracture height growth in the presence of stress contrast barriers

However, as is clearly illustrated by experiments (Jeffrey and Bunger 2007), some height growth can occur even in the presence of high stress barriers. Simonson et al. (1978) and Economides and Nolte (2000) provide the classical treatment of height growth in the presence of high stress barriers.

Referring to the discussion of pressure increase from Section 2.1.2, the calculations contained in Figure 2.10 predict height growth of about 10 per cent when the difference between the confining stress in the barrier and injection pressure reaches about 65 per cent of the jump in stress between the reservoir and the barrier layers. If hydraulic fracture growth continues such that the injection pressure continues to increase, the height of the fracture is predicted to double when the difference in confining stress and pressure is ~30 per cent of the stress jump and triple when this difference is ~20 per cent of the stress jump. Hence, the analysis demonstrates that the propensity for height growth depends strongly on the difference in the stress between the reservoir and the bounding layers compared to the value of the fracture pressure.

[7] Reservoir Stimulation, 3rd edition by Michael J. Economides and Kenneth G. Nolte. 2000, Wiley. Reproduced with permission of John Wiley and sons.

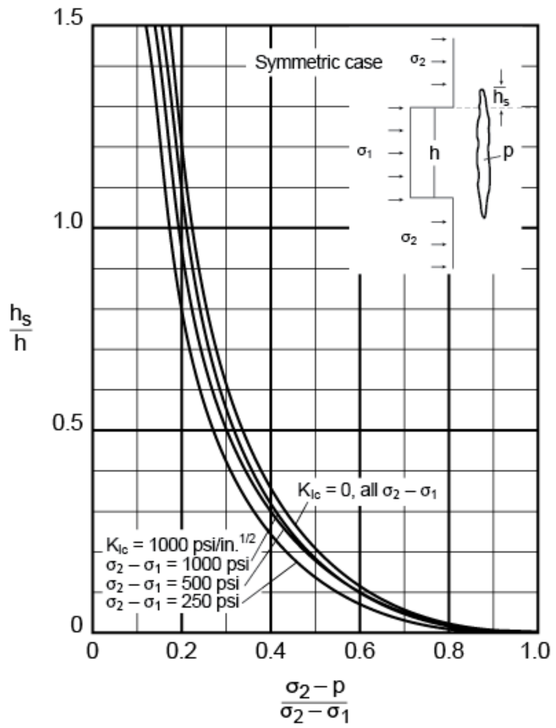


*Source: Economides and Nolte (2000)*

Figure 2.10 Hydraulic fracture height growth for barriers with contrasts in stress and fracture toughness

### 2.2.2.2 Fracture toughness contrasts and fracture pressure shielding

So far we have discussed height growth in terms of the contrasting stresses between layers only. In the presence of a stress barrier, however, there is always some height growth according to this model – that is, it might be small but it is always non-zero. Furthermore, the model so far only allows for limitation of height growth inasmuch as the engineer modifies the fluid properties and injection rate so as to manipulate the fluid pressure in the hydraulic fracture.

Taking a first enhancement of the stress contrast model, one can consider the barriers to not only be defined as presenting an increase in the stress, but also as having a certain resistance to crack growth, typically quantified as the so-called fracture toughness. When toughness is considered, height growth is reduced and, furthermore, it is zero until the net fluid pressure in the hydraulic fracture reaches a critical value that increases proportionately to the fracture toughness and is inversely proportional to the square root of the height of the fracture (Economides and Nolte 2000; Simonson et al. 1978).

To this point, we have only considerations that allow the engineer to limit height growth through manipulating the fluid net pressure via the injection conditions. However, engineers also make use of a technique called fracture pressure shielding to limit unwanted height growth. In this technique, the proppant is used to plug the lower and / or upper leading edge of the hydraulic fracture to some degree, hence modifying the near-tip pressure. Downward growth is often affected by proppant settling. Lightweight, buoyant proppants have been used to mitigate upward growth (Mukherjee et al. 1995).

#### 2.2.2.3 Permeability contrasts

When height growth impinges on a high permeability bounding layer, the fluid loss from the vicinity of the growing hydraulic fracture tip causes it to slow down (e.g. Quinn, 1994). Hence, high permeability layers can serve as effective barriers to height growth, provided that the contrast is sufficient relative to the reservoir. For example, one experimental investigation has suggested that a permeability contrast of a factor of 3 to 4 is sufficient to arrest height growth in some cases (de Pater and Dong 2009).

In summary, it is generally accepted that high permeability layers can provide effective barriers to height growth. However, this comes with the obvious caveat that a high permeability bounding layer tends to increase the leak-off of hydraulic fracturing fluid outside of the reservoir. It should also be pointed out that mechanical barriers to growth, which also give rise to stress contrasts, are often low permeability. High permeability layers essentially provide a mechanism for arrest of height growth when a mechanical barrier is not present.

#### 2.2.2.4 Stiffness contrasts

All coal seams occur within layered geological systems wherein the layers each have a different stiffness. The impact of these stiffness contrasts is two-fold. Firstly, when a layered system is subject to a remote tectonic loading, the stiffer layers tend to be more highly stressed. In this regard, stiff layers can provide barriers to height growth because they represent a contrastingly larger stress (Prats and Maraven 1981). Secondly, when the fracture toughness of the rock is limiting height growth, the stress intensity at the tip of the hydraulic fracture can be reduced as it approaches a stiff layer and, conversely, increased as it approaches a soft layer (Simonson et al. 1978). Hence, stiff layers can provide barriers to height growth not only because of their tendency to be more highly stressed, but also because they can reduce the propensity for crack growth. In addition, fracture growth through a stiffer layer results in additional fluid pressure loss because of the narrower hydraulic fracture channel produced in the higher elastic modulus rock (Van Eekelen 1982). This effect decreases as the rate of height growth is decreased and essentially disappears when height growth is arrested. However, besides these impacts, it is generally considered that stiffness contrasts alone do not have a strong impact on the inhibition of height growth (Gu and Siebrits 2008; Naceur and Touboul 1990).

#### 2.2.2.5 Interfaces

There are four typical fracture growth patterns in the presence of interfaces, as discussed by Thiercelin et al. (1987) and Zhang et al. (2007b). Fractures can penetrate through the bedding contacts without any diversion of the fracture path and vertical fluid flow. This type of crossing is what is implicitly assumed to occur by all current planar hydraulic fracture design models. In the opposite extreme case, the hydraulic fracture may be arrested or blunted at the bedding contact due to slip along the contact. Between these above two extremes, a potential intermediate state is that the fracture and the fluid flow are deflected into the bedding plane, producing a branched fracture. If the interface is free of flaws, the fluid will invade it in the same way as an opening-mode hydraulic fracture growing along the horizontal bedding plane, so that the vertical fracture is effectively terminated at the bedding plane, becoming a T-shaped fracture. Moreover, if there are flaws on the interface, potential re-initiation of a new fracture from one flaw will leave a step-over or offset in the hydraulic fracture path at the bedding interface.

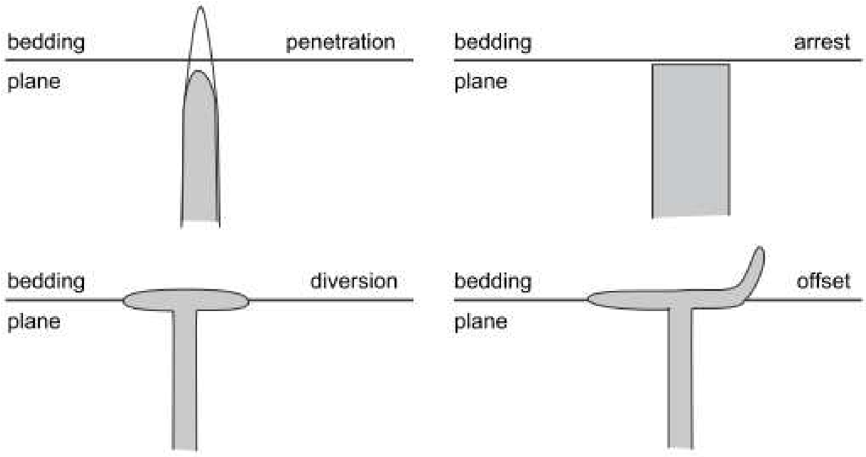


*Source: Zhang et al. (2007b)*[8]

Figure 2.11 Four fracture patterns in the presence of a single interface or bedding plane

A direct effect of an interface is the potential for frictional shear failure along it and the subsequent slip. The slip can blunt the fracture tip and contain the fracture growth in one layer, thus producing a wider fracture. However, this can also lead to a higher fluid pressure which may lead to new fracture initiation or opening of cross cutting fissures, natural fractures and faults. On the other hand, in contrast to a tensile fracture, the fluid flow and associated fluid pressure variations along the interface play a key role in final fracture pattern development. These interfaces with fluid flow not only tend to fail in shear more easily since the effective normal compressive stress is reduced, but also act as a conduit in transporting fluid to any new fractures.

Gu et al. (2008) considered a blunted crack-tip terminated at the interface. In their P3D models, the zero displacement requirement at the intersection is relaxed, in contrast to PKN models, with the interface replaced by distributed linear springs. The bedding plane interfacial slip is a direct result of the numerical solution based on a shear stiffness to relate the interfacial slip and the shear resistance force. Of course, a more compliant fracture geometry can hold more fluid and the pressure level is reduced. The inclusion of interfacial hydraulic fracture was found to be in good agreement with observed measurement in fracture height, length and pressure (Gu et al. 2008).

As described previously, the fracture may reorient and deflect into the interface to create interfacial hydraulic fractures (Daneshy 2009; Zhang et al. 2007a). A T-shaped fracture would be likely generated by hydraulic fractures growing into a weak discontinuity. This geometry has been identified by mapping, but not explicitly dealt with in most studies (Gudmundsson and Brenner 2001; Cooke and Underwood 2001). One important factor affecting the interfacial hydraulic fracture growth is the coefficient of friction of the interface. Zhang et al. (2007a) found that this parameter only plays a role in early time development, as shown in Figure 2.12. The lower the coefficient of friction, the more difficult the fluid penetration along the interface is. Of course, the confining stress across the interface is another important factor as hydraulic fracture growth along the interface requires a certain fracture conductivity, which can only be realised by overcoming the overburden stress. An interesting result is the formation of a pinch point near the intersection point between the hydraulic fracture and the interface due to the asymmetric deformation of the interface walls.

---

[8] Reprinted from Journal of Structural Geology,29, Xi Zhang, Robert Jeffrey, Marc Thiercelin, Deflection and propagation of fluid-driven fractures at frictional bedding interfaces: A numerical investigation, 397, Copyright (2007), with permission from Elsevier

The pinch point would be one reason for the observed fluid pressure increase during the fracture stimulation of naturally fractured reservoirs.

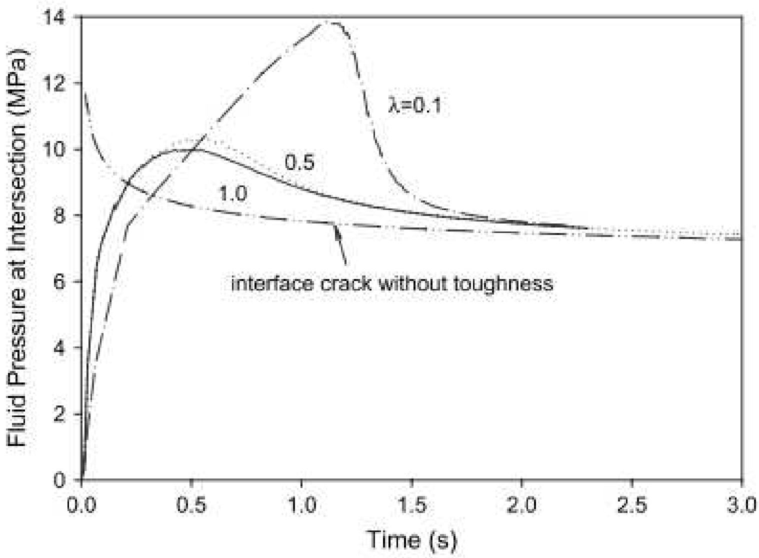


*Source: Zhang et al. (2007b)*[9]

Figure 2.12 Effect of coefficient of friction on injection pressure

Fracture crossing of the interface without offset or penetration of the fracture into the interface is possible and often results in a lower fluid pressure to extend the fracture compared to other interaction modes. When a hydraulic fracture approaches an interface, the interaction may change the interface-parallel normal stress on the other side of the interface. The normal stress can become tensile under certain conditions and this may lead to fracture initiation or nucleation. In addition, the kinematics of the displacement between interface slip driven by far-field stresses and the fracture opening of a new fracture extending from the far side of the natural fracture may assist in growth of this new fracture. In order to predict the conditions under which the hydraulic fracture will cross an interface, the problem of determining a reliable and accurate method to predict fracture nucleation must be solved. Ultimately, the nucleation criterion must be verified against experimental data. One widely used new fracture initiation criterion is based on the inception of interface slip presented by Renshaw and Pollard (1995). Although the kinematic transfer of deformations can facilitate the growth of the new fracture, its continuous growth requires that fluid enter and pressurise it.

Zhang and Jeffrey (2008) used a numerical method to investigate fracture initiation based on using a tensile strength crack nucleation criterion. In this study, the hydraulic fracture approached perpendicular to an interface between two rock layers. A minimum new fracture size was used to evaluate the normal stress and this flaw length is assumed to be an inherent parameter in the criterion. The authors found that as the fluid penetrates the interface, the value of the peak interface-parallel normal stress became less tensile. The numerical results provided the range of this normal stress for some specific conditions. Figure 2.13 illustrates the location of initiation of the new fracture and continued growth of the

---

[9] Reprinted from Journal of Structural Geology,29, Xi Zhang, Robert Jeffrey, Marc Thiercelin, Deflection and propagation of fluid-driven fractures at frictional bedding interfaces: A numerical investigation, 406, Copyright (2007), with permission from Elsevier

hydraulic fracture as a function of the specified tensile strength of the upper sandstone layer. If this tensile strength is high and if the interface is of low frictional strength, the hydraulic fracture will deflect into the interface instead of crossing it. Moreover, if the modulus and toughness contrasts on either side of the interface are too high, these newly created fractures cannot propagate further in the upper rock layer.

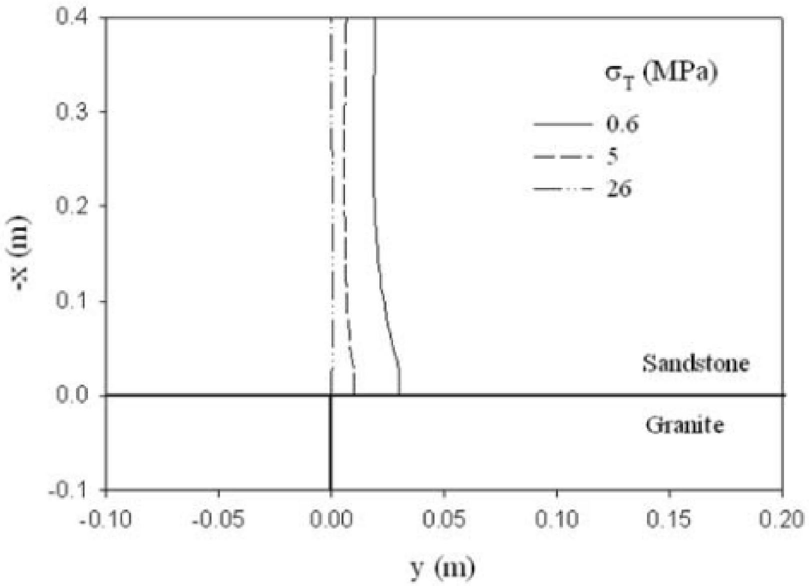


*Source: Zhang and Jeffrey (2008), with permission*

Figure 2.13 Fracture paths for newly created fractures as a function of different tensile strengths

Another nucleation criterion that is based on the dual conditions of strength and toughness was presented by Leguillon (2002). The minimum new fracture length can be obtained in terms of the strength and the toughness. Recent research on this issue by Chuprakov and Melchaeva (2013) showed consistency between the numerical model predictions and the experimental observations on fracture crossing and deflection.

The jogged or offset path of the hydraulic fracture created as it crosses an interface can be attributed either to the dual-lobed stress distributions induced by the fracture in the rock on the far side of the interface before the main hydraulic fracture reaches the interface, or to some pre-existing small flaws distributed along the interface. In cases where fracture penetration is prevented by the local stress and flow barriers, the fluid pressure that penetrates along the interface and into pre-existing flaws may be sufficient to cause them to extend. It is clear that to extend the fracture past the offset, a higher injection fluid pressure is required (Zhang et al. 2008; Jeffrey and Zhang 2008). Also, along the offset portion on the interface, the fracture conductivity is significantly reduced. This area of restricted fracture width and associated reduced hydraulic conductivity leads to the high pressure requirement and may lead to proppant bridging during slurry injection.

Interface shear strength may include cohesion which will resist initial interface slip, thus helping fractures cross without offsets. This effect has not been considered in the existing models, but it may be important under some circumstances.

### 2.2.2.6 Composite and laminated rock effects

Fracture containment can be provided by thinner, softer laminates existing between thicker layers. In composite man-made materials, such systems are typically produced by glue or adhesive (soft layers) between the stiffer structural layers. The fracturing of such composite systems has been studied (Gudmundsson and Brenner 2001; Helgeson and Aydin 1991; Peirce and Siebrits 2001; Peirce et al. 2009) and the fracture mechanics of such layered systems can be applied to layered rocks. Gudmundsson and Brenner (2000) and Helgeson and Aydin (1991) explicitly discussed the effect of a jointed layer on ascending hydraulic fractures, finding that a thin soft layer with a strong modulus and stress contrast was an effective barrier to fracture height growth. Figure 2.14 shows the stress contours ahead of a hydraulic fracture growing towards such a layer. Layer C is much softer than layer B with a modulus contrast of 1:100. The soft layer acts to dissipate most of the crack-tip tensile stress and this low stress zone results in arrest of the growth of hydraulic fractures. The change of hydraulic fracture into a T-shaped fracture is encouraged thereafter.

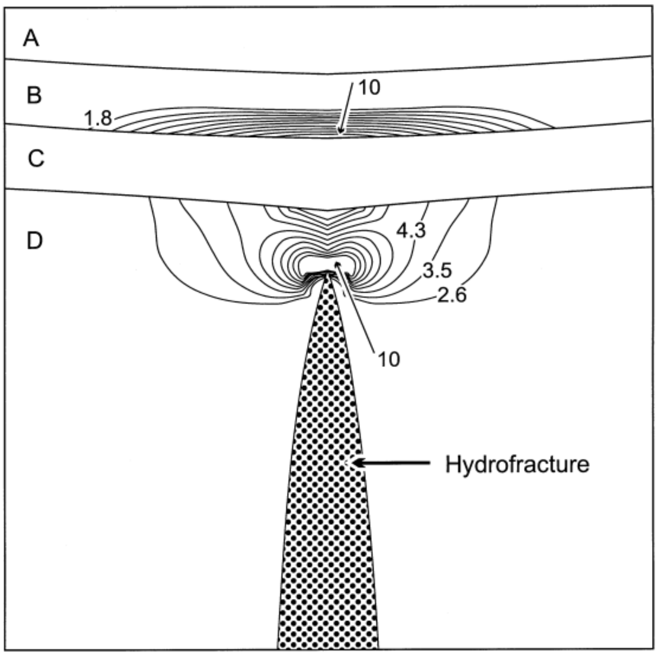


*Source: Gudmundsson and Brenner (2001)*[10]

Figure 2.14 Contours of maximum principal stresses in layered rocks. Layers A and C (Young's modulus, E=1 GPa) are much softer than layers B and D (100 GPa)

On the other hand, the soft layer could fail in compression or become thinner and be filled with microdefects at the high stress level. With the decrease in the thickness of the soft layer, the stress concentration of the upper stiff layer increases (Gudmundsson and Brenner 2001). The stress concentration transfer from one stiff layer to another can occur if the hydraulic fracture terminates or propagates in the softer layer. Rationally, the soft interlayer then can be treated as a weak plane, instead of a finite-thickness layer. The direct effect of stress transfer can potentially initiate a new crack at the upper stiffer layer, as discussed by Helgeson and Aydin (1991).

[10] Copyright © 2001, Blackwell Science Ltd

Apart from the modulus contrast, the stress jump among layers is another important issue for hydraulic fracture vertical growth. Numerical simulation has been carried out by Peirce and Siebrits (2001) and Peirce et al. (2009). The frictional behaviour of interfaces is modelled using linear springs in Peirce et al. (2009). The proposed Uniform Asymptotic Solution (UAC) has been implemented in their Planar3D hydraulic fracture model. Although the horizontal bedding plane fractures are not captured in their code, the simulator can produce crack arrest and interface frictional slip. The calculated bottom hole pressure becomes higher when fracture arrest occurs and the model can provide results for vertical fracture growth in the layers with modulus and stress contrasts.

Higher treating pressure associated with fracture arrest and slip caused by soft layers and weak interfaces and by interaction with natural fractures in fracture reservoirs has been described in the literature. Barree and Winterfeld (1998) and others have emphasised the effect of shear slip and stress jumps on fracture containment (Barree et al. 2010).

### *2.2.3 Conclusions*

Predicting height growth is one of the most important considerations in hydraulic fracture design in general and specifically for coal seam gas extraction. This issue is not new, nor is it uniquely aimed at mitigating risk to groundwater. Rather, it is fundamental to maximising recovery and therefore return on investment. Commensurately, industry and industry-driven research has produced many contributions in this area. Overall, the current tools are sufficient to support the industry’s activities, as demonstrated by more than 20 years of successful coal seam gas stimulation making use of these existing predictive models. Still, this review demonstrates that a number of important areas in the science could be strengthened to improve our ability to predict the conditions under which height is expected to grow; and conversely, to help design hydraulic fracturing treatments that avoid unwanted height growth. These areas are listed below.

- Numerical hydraulic fracture models should include multiple layers and three-dimensional effects, such as T-shaped growth and offsetting of the fracture path.
- The influence of the properties of the interface formed by the contact between the coal and the bounding layers needs to be better understood experimentally and numerically.
- Marginal barriers to growth, i.e. those that are thin or that have only a small contrast in stress or material properties with the coal seam, need to be better understood.
- Hydraulic fracture growth in coal and growth in height into layers above and below a coal seam are affected by the rock properties and in-situ stresses. Interactions with bedding planes, faults and natural fractures often strongly affect the fracture growth.
- The nature and size of the fractures formed by coal seam gas treatments are fairly well characterised because many have been mapped after mining, both in Australia and in the US. The fractures have been documented to contain branches and offsets and to sometimes form as T-shaped geometries with a large horizontal fracture overlying a vertical one.
- The complex branched and offset structure is limited to form along a main backbone fracture and this exact geometry is a challenge for existing models to simulate. However, planar fractures can be reliably used to provide upper limits for both lateral and vertical fracture extent because the branching and offsetting acts to retard the fracture growth, with the effect that the more complex fractures are less extensive than what is predicted by a planar model. Recently developed models that simulate the growth of a network-like fracture can be applied to coal seam gas stimulation design,

but these models currently are not able to reproduce the geometries documented by mined fracture studies.

- In any case, careful site characterisation is required to design and accurately predict fracture growth during coal seam gas stimulations. Monitoring of fracture growth by microseismic and tiltmeter instrumentation and by employing other technologies such as tracers, is important during early phases of development of new areas. This monitoring serves to calibrate modelling and verify that designs are producing the intended fractures.

# 3 Review of well integrity

## 3.1 Introduction

This section reviews and discusses the risk scenarios and mechanisms of losing well integrity related to coal seam gas well drilling, casing and cementing, and de-watering and production. In addition, the technologies for evaluating zonal isolation, well abandonment and remediating poor well integrity are briefly reviewed and discussed.

### *3.1.1 Defining well integrity*

Well integrity for oil and gas wells is defined by NORSOK D.010 (Standards Norway 2004) as the *Application of technical, operational and organizational solutions to reduce risk of uncontrolled release of formation fluids throughout the life cycle of a well*. A definition specific to coal seam gas well integrity was not found by this review. Since the coal seam gas industry in Australia is generally regulated in the same way as other onshore petroleum upstream activity through the relevant state and territory petroleum and gas acts, this definition of well integrity for oil and gas wells will be adopted in this review.

This definition is very broad and covers various facets of well integrity, including organisational, technical and operational solutions and processes. This review addresses some of the technical and operational issues critical to coal seam gas well integrity.

### *3.1.2 Typical coal seam gas well configuration*

The coal seam gas well configurations have evolved significantly since the first coal wells were drilled in the 1970s as the drilling technology has progressed and a variety of coal reservoir conditions have been encountered. Coal has a number of unique properties that must be considered in designing the well. The variety of these unique reservoir and geological characteristics has resulted in a range of problems and associated solutions applied to drilling coal seam gas wells.

Currently, coal seam gas production well designs in Australia can be broken down into two categories, vertical and horizontal (Cunnington and Hedger 2010; Bennett 2012). The vertical production wells (Figure 3.1) are normally designed to commingle production from multiple coal seams (e.g. up to 22 seams in the Surat Basin). In the Surat Basin, the production interval is often under-reamed (enlarged) with pre-slotted liner installed across the interval using mechanical-tension multizone external-casing packers (Bennett 2012).

The horizontal production wells, also termed surface to in-seam wells (SIS) (Figure 3.1), are drilled horizontally in the coal seam and are steered to intersect a vertical well. The vertical well is drilled first and under-reamed in the target seam. The horizontal well or wells are then drilled within the coal seam to intersect the vertical well. The in-seam section is lined with high-density polyethylene, instead of the steel casing, to enable future longwall mining of the coal seam without loss of production or increased safety risk.

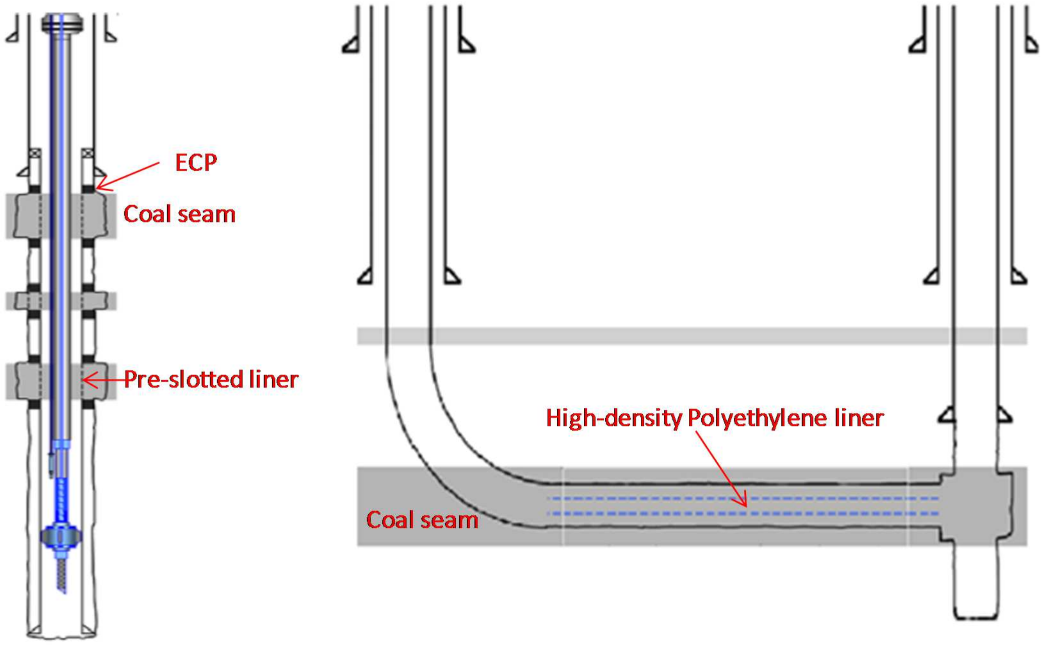


*Source: modified from Bennett (2012)*[11]

Figure 3.1 Typical coal seam gas production well configuration; vertical commingled well (left) and surface to in-seam (SIS) wells (right)

### 3.1.3 Consequences of loss of well integrity

As will be described in later sections of this report, in the majority of cases, petroleum wells are constructed and abandoned according to designs and procedures based on relevant industry standards and guidelines (such as provided by American Petroleum Institute Recommended Practice API RP). For these cases, well integrity is a minor issue. However, there are other cases where the well was either not constructed or abandoned according to the standard procedures (e.g. legacy wells), or casing corrosion and / or cement degradation occurs, which results in the well integrity being compromised.

There are a range of potential impacts on environments resulting from poor coal seam gas well integrity (Commonwealth of Australia 2014a), such as:

- impact on groundwater:
  - contamination of shallow and deep aquifers is a risk associated with coal seam gas drilling, stimulation and production activities. For example, drilling and hydraulic fracturing fluids can enter aquifers during drilling and stimulation
  - localised hydraulic connectivity between isolated aquifers along a well trajectory can occur because of failed casing, poor cementing or generally poor well construction, decommissioning or abandonment practices
- fugitive gas emissions:
  - localised gas leakage to both the atmosphere and into aquifers from coal seam

[11] Copyright 2012, IADC/SPE Asia Pacific Drilling Technology Conference and Exhibition. Reproduced with permission of IADC/SPE, further reproduction prohibited without permission.

gas wells can occur because of equipment failure or poor coal seam gas well construction and abandonment practices

- gas leakage to the atmosphere and into aquifers from existing non-CSG wellbores intersecting coal seams may occur when these wells are affected by de-watering. Coal seam gas is held in the coal seams by water pressure. As water is pumped from the coal seams, the pressure is decreased and the gas is desorbed and produced. When the target coal seam is de-pressurised, the surrounding aquifers and other minor coal seams will also be de-pressurised to some extent and gases may be released from any coal affected by the lower pressure. There could be many water wells and coal mining exploration boreholes in the same region as the coal seam gas wells. If these boreholes intersect the coal seams that are affected by de-watering and are not abandoned or have been abandoned inappropriately, gases from the coal seams may be released into the groundwater and atmosphere via these non-CSG wellbores and boreholes (Johnson et al. 2006).

## 3.2 Risks and mechanisms of losing well integrity while drilling

Coal seam gas wells are required by the coal seam gas industry and are critical to the processes of exploring for, testing and producing coal seam gas (Australian Petroleum Production and Exploration Association (APPEA) Factsheet, no date). Drilling is the first step in constructing a coal seam gas well, and this step contains a number of risks to well integrity. During drilling, the primary well barrier is the drilling fluid column, in particular the drilling fluid pressure exerted on the rock because of the density of the fluid. The secondary well barrier includes the drilling blowout preventer, casing and cement, wellhead and in-situ rock formation (Standards Norway 2004). Furthermore, drilling fluid plays a vital role in maintaining wellbore stability of the openhole section prior to a casing being cemented.

Before a drill bit penetrates a rock formation, the rock at depth is in a state of mechanical, thermal and chemical equilibrium. A wellbore is drilled by cutting and removing the rock inside the hole and replacing it with a column of drilling fluid. Due to the inherent differences in mechanical (physical) properties, temperature and chemistry between the drilling fluid and the formation rock, drilling the wellbore disturbs the state of equilibrium in the rock formations surrounding the wellbore. Consequently, rock failure and loss of well integrity become possible.

Figure 3.2 shows a schematic of the stable and safe mud weight windows during the drilling stage of the well construction phase. The stable mud weight window is defined by the minimum mud weight (mw) and the minimum in-situ stress ($\sigma_3$) (the green line). The safe mud weight window is defined by the formation pore pressure ($P_{pore}$) and formation breakdown pressure ($P_{breakdown}$) (the orange line). These four key parameters defining the mud weight windows are described briefly below (Cook et al. 2012).

- **Kick pressure ($P_{kick}$).** The minimum mud weight required to balance the formation pore pressure. If the mud weight is lower than the formation pore pressure in the open hole section, an influx of formation fluids (kick) takes place. The consequence of formation fluid influx varies. In some cases, the mud weight is designed to be lower than the formation pore pressure to drill underbalanced. In other cases a kick can be severe, or even disastrous (e.g. British Petroleum 2006 Gulf of Mexico incident), depending on the formation permeability and type of formation fluids.
- **Wellbore instability mud weight ($m_w$).** The minimum mud weight that prevents the formation rock surrounding the wellbore from breaking up and failing. Removing a

column of rock and replacing it with a column of drilling fluid creates a stress concentration in the wellbore wall. Rock failure can take place if the stress concentration is greater than the formation rock strength. The temperature and chemistry of the drilling fluid can stabilise or worsen the rock failure, depending on the difference in thermal and chemical properties between the drilling fluid and formation rock.

- **Minimum in-situ stress ($\sigma_3$).** When there are pre-existing closed natural fractures in the near wellbore region and the drilling fluid pressure is higher than the minimum in-situ stress magnitude, there is a possibility that the closed natural fracture could be re-opened and mud loss induced.
- **Formation breakdown pressure ($P_{breakdown}$).** When the mud pressure in the openhole section is sufficiently high, formation breakdown can take place, resulting in the growth of a hydraulic fracture from the wellbore wall, with associated drilling fluid losses.

It should be noted that the magnitude of the drilling fluid pressure does not necessarily follow the order listed in Figure 3.2. For example, formation breakdown may take place at a lower drilling fluid pressure than the minimum in-situ stress, depending on the regimes of in-situ stresses and the well trajectory in relation to the in-situ stress orientation.

### 3.2.1 Wellbore stability mud weight window

As shown in Figure 3.2, the stability mud weight window is defined by $m_w$ and the minimum principal in-situ stress. When the mud weight or the equivalent circulation density (ECD) mud weight is maintained within the stability mud weight window, no wellbore stability problems are expected to be encountered and the wellbore should be in-gauge. In practice, the mud weight is maintained to be as low as possible within the stability mud weight window for at least two reasons: a) a higher mud weight reduces rate of penetration (ROP), and b) a higher mud weight increases the risk of formation damage when drilling reservoir sections.

Wellbore instability problems can be induced mechanically and chemically. These are reviewed and discussed separately below.

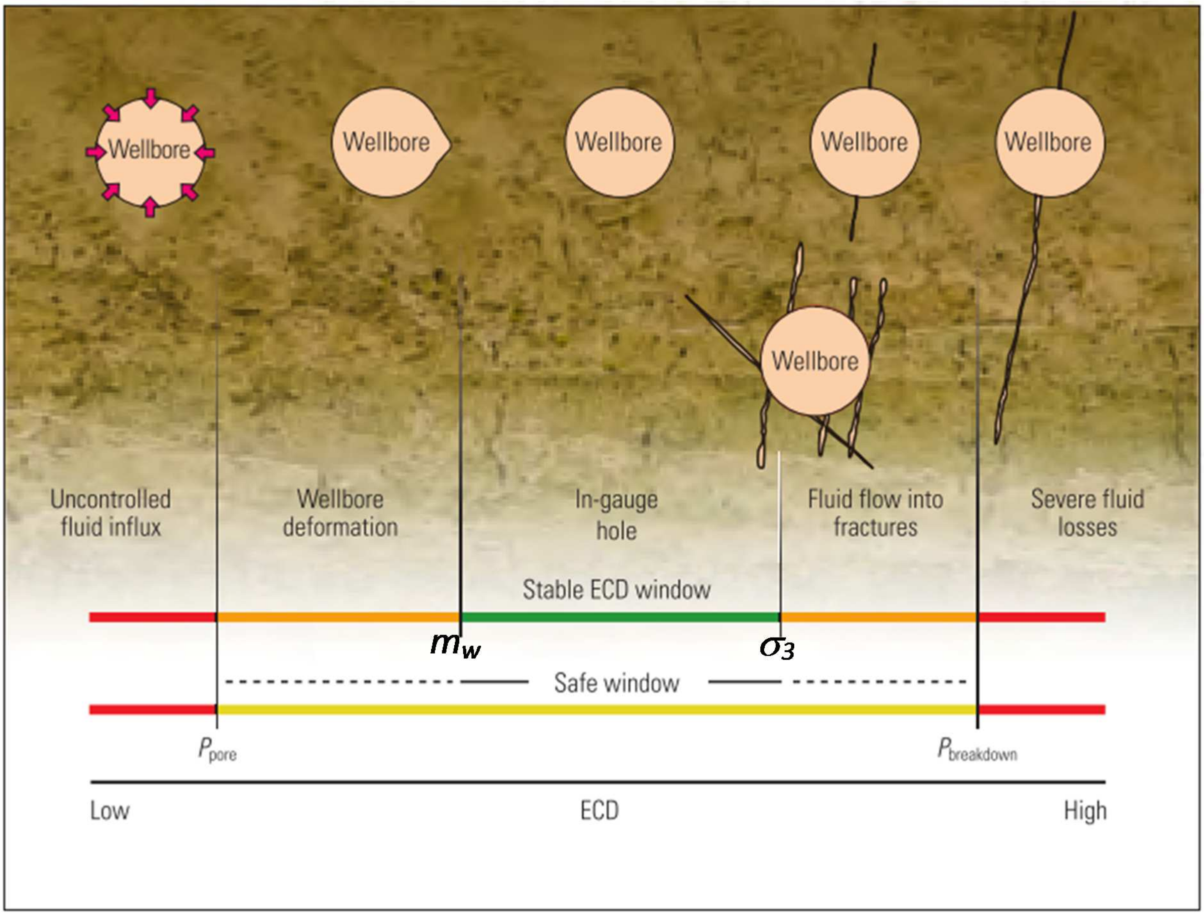


*Source: Cook et al. (2012), Copyright Schlumberger, with permission*

Figure 3.2 A schematic of safe and stable mud weight windows

The stable and hydraulically safe mud weight windows are discussed in detail below.

### 3.2.1.1 Mechanical wellbore instability

Minor instability, such as a small amount of rock breaking off the wellbore wall and falling into the well, is rarely a problem during drilling and can be tolerated in subsequent openhole logging or cementing operations. Major instability is caused by excessive rock failure such that the total volume of cuttings and failed rock materials (both amount and size of cavings) in the hole cannot be circulated out by the drilling fluid (Zoback 2007; Zoback et al. 1985). Wellbore size can be enlarged significantly because of excessive rock failure and, as a result, the circulating velocity of the drilling fluid in the annulus between the wellbore wall and the drill pipe decreases. This, in turn, reduces the hole cleaning ability of the drilling fluid. The combined effect of rock failure and reduced cleaning capacity of the drilling fluid circulation velocity can cause the drilling cuttings and cavings to accumulate at the bottom hole assembly (BHA) where the annulus between the BHA and wellbore wall is likely to be the narrowest. This is often referred to as wellbore collapse, the ramification of which is 'tight hole' or 'stuck pipe' incidents during drilling operations. It should be noted that not all 'tight hole' and 'stuck pipe' incidents are caused by unstable wellbores. Other factors, such as poor hole cleaning as well as poor drilling practice also contribute to tight hole or stuck pipe incidents. The excessive cuttings and cavings, if the size is sufficiently small, can be removed safely from the hole by good drilling practices and hole-cleaning procedures. However, this results in an enlarged hole which could be the main cause for poor openhole logging quality and eventually can result in a poor quality cement sheath between the steel casing and the rock (Cook and Edwards 2009).

A stable wellbore does not need to be one that has experienced no rock failure. The process of wellbore breakout formation and development, due to removal of failed rock on the wellbore wall, is very complex. However, under simplistic conditions and for certain types of rocks, it has been demonstrated experimentally and numerically that a breakout, once formed, does not change in width but tends to develop in depth (Haimson and Herrick 1989; Zheng et al. 1989; Zoback et al. 1985; Zoback 2007). Furthermore, extensive field experience has demonstrated that a wellbore with a limited amount of rock failure can remain stable and be drilled and logged without incident (e.g. Figure 3.3 and Figure 3.4). Figure 3.3 presents an analysis of an acoustic well log from a coal seam gas well in Australia (Johnson et al. 2010a) whilst Figure 3.4 displays an image of wellbore breakout observed on a downhole camera (Tingay et al. 2008; Daneshy 2012). Plasticity and other non-linear mechanisms may also contribute to the post failure stabilisation of wellbores (Morita et al. 2012).

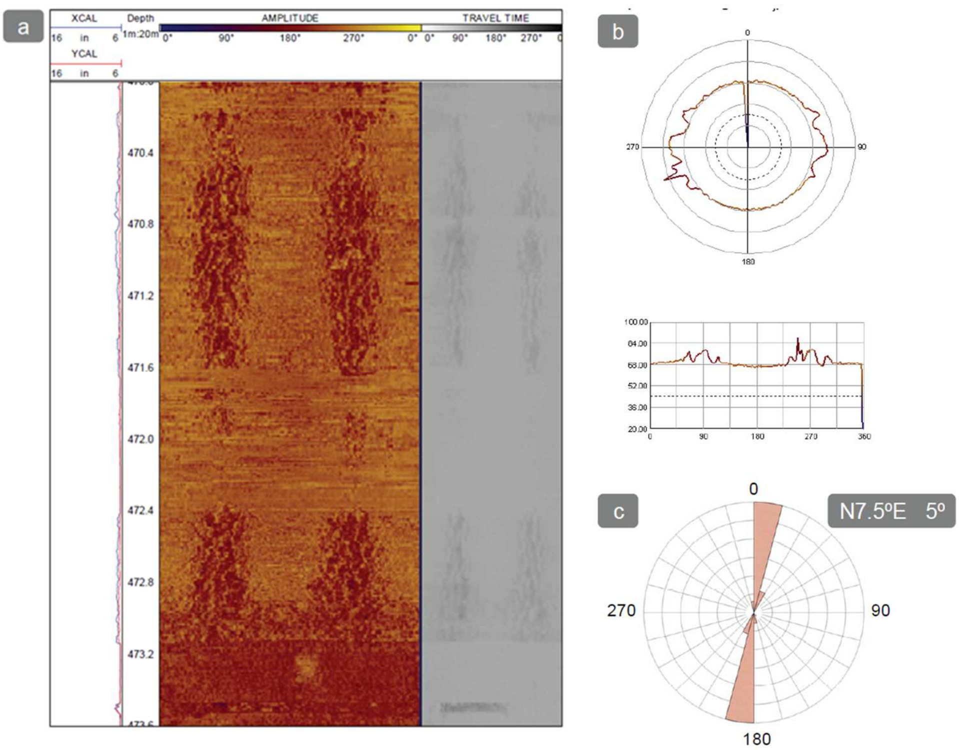


*Source: Johnson et al. (2010a)*[12]

Figure 3.3 Rock failure on wellbore wall from image log data: (a) acoustic image in Ridgewood 4. (b) Cross-sectional view of acoustic image showing shear failure and (c) Rose plot of inferred maximum horizontal stress direction

[12] Copyright 2010, SPE. Reproduced with permission of SPE, further reproduction prohibited without permission.

*From Daneshy (2012), with permission*

Figure 3.4 Wellbore breakout observed on a downhole camera in a shale formation

#### 3.2.1.2 Wellbore instability in coal

Coal is a very complicated organic rock made up of microscopic constituents called macerals. Cleats in coals occur as two mutually perpendicular sets of opening-mode fractures, both of which are perpendicular to coal bedding. Face cleats tend to be continuous and are formed first; butt cleats form subsequently and terminate on face cleats. These three mutually perpendicular planes are considered weaker than the intact coal material (TerraTek 1996).

Coal seams are known to be difficult to drill because of problems with maintaining a stable wellbore. Coals are highly fractured and therefore are of weak strength because of the existence of cleats and natural fractures. For example, consider drilling an in-seam horizontal well. Because of the low permeability of intact coal which impedes initial filtrate loss of drilling fluids (i.e. similar to shale), a filter cake cannot be built on the wellbore wall (Baltoiu et al. 2008). When water / brine solutions are used in drilling the coal section, the coal is subject to an overbalanced condition. The drilling fluids then invade the fracture network resulting in an immediate increase in formation pressure, which is essentially equal to the bottom hole pressure in the vicinity of the wellbore. Therefore, the pressure on a coal block contained within the fracture network equalises, resulting in failure along the cleats / fractures or creation of new fractures. The coal bounded by failure surfaces is easily detached from the wellbore wall because of forces from drilling fluid flow and / or drill string / bottom hole assembly vibration. Typically, the more fluid lost to the formation, the deeper the pressure equalisation, and the greater likelihood for sloughing of coal cavings. Such cavings are usually blocky, with square edges, and can be quite large, up to 10 to 15 cm across. Sloughing happens in a relatively short period of time and in very large volumes. Increased mud density could be detrimental, in this case, to wellbore stability.

Experiments were conducted to simulate cavity completion mechanisms, a type of stimulation process used in some high permeability coal seam gas wells. After the coal block (approximately 400 mm per side) was stressed to simulate in-situ effective stress conditions, high pressure gas was injected into the coal block and then de-pressurised in a fraction of a second to induce failure around the wellbore and create a cavity. A failure zone is clearly shown around the wellbore (see Figure 3.5). Such rapid de-pressurisation could be induced in drilling horizontal wells in coal seams by swab and surge pressures.


*Figure 3.5x CSIRO (unpublished experimental study)*

Figure 3.5 Photo of a cross section of a coal block after a series of laboratory gas cavitation experiments conducted by CSIRO.

The failure mechanisms of horizontal wells, as described above, have been demonstrated in a numerical modelling study (Moos 2011). Table 3.1summarises the input parameter of the finite element analyses. As shown in Figure 3., the zones surrounding the well with cleat failure grows with time as the drilling fluids penetrate into the fracture network. The well is drilled along the minimum horizontal stress direction in a normal fault in-situ stress regime and cleats strike 150° to the minimum horizontal stress direction. The failed zones become progressively deeper but they don't appear to increase significantly in width.

One solution to decrease the amount of coal failure is to raise the drilling fluid density. Figure 3. compares failure immediately after drilling with a higher mud weight to the failure developed with a lower mud weight a few hours after drilling. Almost no failure is predicted immediately after drilling, as shown on the left of Figure 3.. After a few hours, the drilling mud pressure has penetrated into the fracture network, and as a result, the formation pressure in the vicinity of the well is increased. As shown on the right of Figure 3., the failed zone has grown in size until, after a few hours, it is virtually identical to the failure zone size for the case shown in Figure 3., for which overbalanced drilling conditions are smaller. This demonstrates that it makes little sense to increase mud weight unless steps are also taken to prevent drilling fluid penetration into the fracture network.

Table 3.1 Properties used in the numerical modelling study shown in Figure 3..

| | **Coal matrix** | **Cleats** | **Vertical Stress** | **Maximum Horizontal Stress** | **Minimum Horizontal Stress** | **Azimuth Maximum Horizontal Stress** |
|---|---|---|---|---|---|---|
| Unconfined Compressive Strength | 20 MPa (MegaPascal) | 2 MPa | - | - | - | - |
| Friction | 0.6 | 0.5 | - | - | - | - |
| Stress | - | - | 23 MPa | 18 MPa | 14 MPa | 90 |

| | Coal matrix | Cleats | Vertical Stress | Maximum Horizontal Stress | Minimum Horizontal Stress | Azimuth Maximum Horizontal Stress |
|---|---|---|---|---|---|---|
| Pore pressure | 10 MPa | - | - | - | - | - |
| Mud weight | 13 MPa | - | - | - | - | - |

*Source: Moos (2011), with permission*

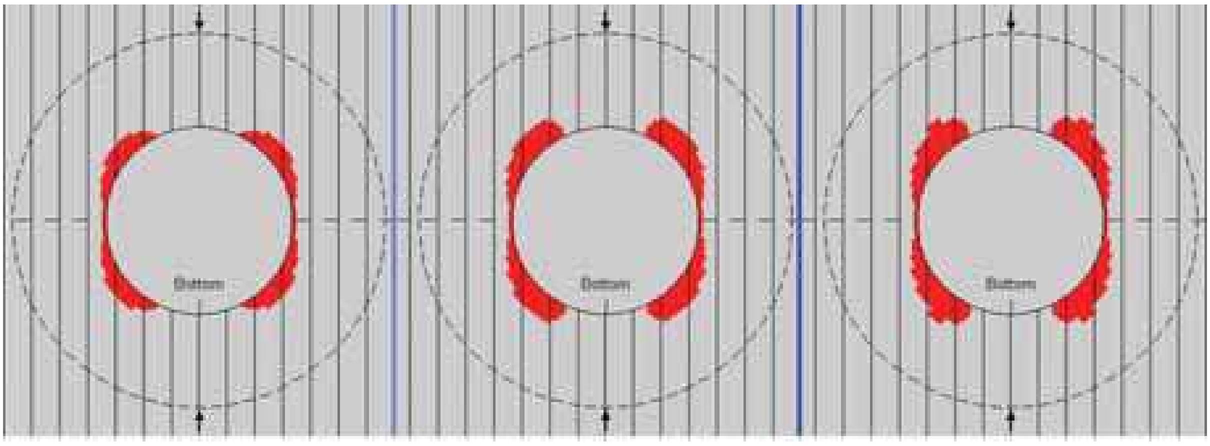


*Source: Moos (2011), with permission. From left to right is shown the zone of failure immediately after drilling, one minute after drilling, and 100 minutes after drilling.*

Figure 3.6 The growth of zones with cleat failure surrounding a horizontal well

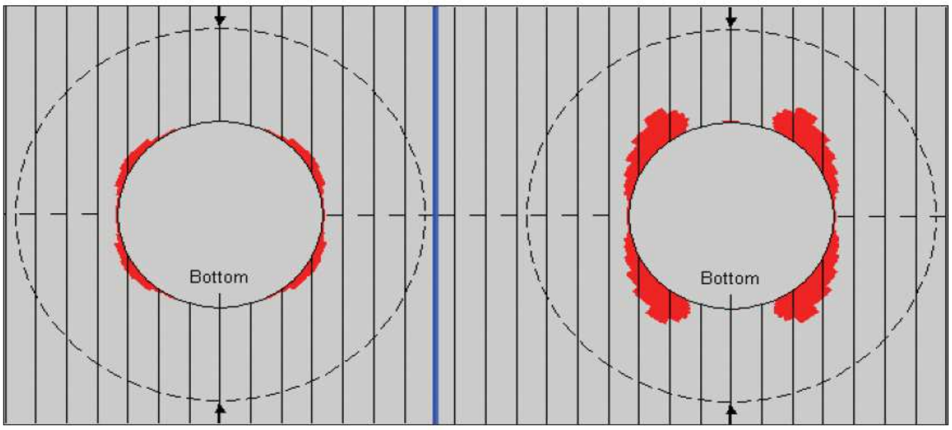


*Source: Moos (2011), with permission*

Figure 3.7 An increase in mud weight significantly reduces the cleat failure zone temporally (the failure zone development immediately following drilling, left), but the enhancement almost disappeared after a few hours due to mud pressure invasion into the fracture network

The modelling study (Moos 2011) also included an investigation into cleat failure zone development for the underbalanced drilling condition, where the bottom hole pressure is less than the formation pressure. The results are presented in Figure 3.7. The bottom hole pressure is less than the formation pressure by 1 ppg (3.3 kPa). A larger failure zone developed immediately after drilling, in comparison with the case for overbalanced conditions. However, as the influx of formation pore fluid into the well occurs, the formation pressure in the vicinity of the well is actually reduced and the well becomes more stable (Figure 3.).

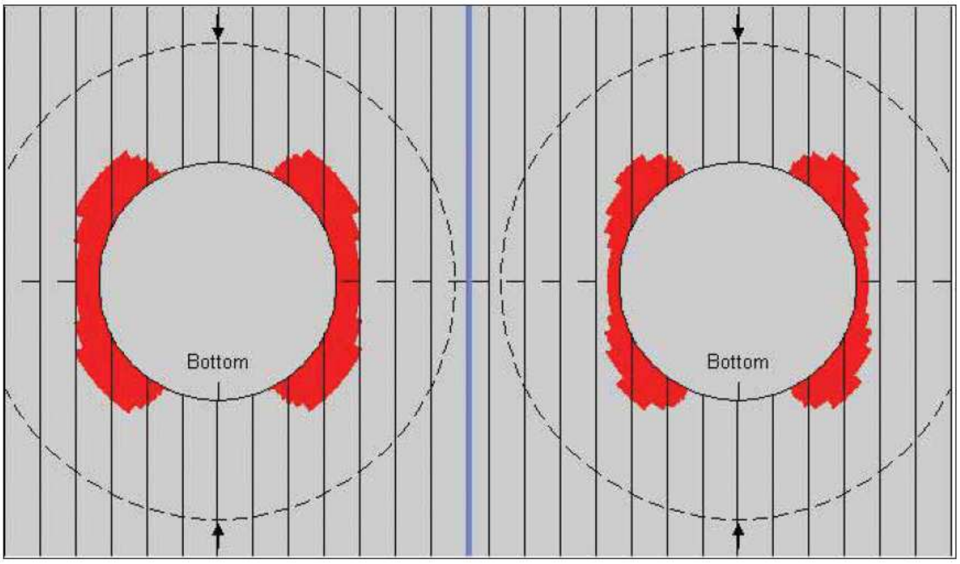


*Source: Moos (2011), with permission*

Figure 3.8 Failure zone immediately after drilling (left) and a few hours later (right) in an underbalanced condition

It should be noted that the numerical modelling assumed the coal materials inside the failure zone remained part of the wellbore wall and the process of removal of the coal materials from the failure zone was not modelled. Detachment of the coal within the failure zone could be induced by drilling fluid flow as well as mechanical vibration of the drill string and bottom hole assembly. Further increase in failure zone size would be expected following the removal of the coal materials from the failure zone.

#### 3.2.1.3 Effect of water-based drilling fluids on wellbore instability

Shales make up more than 75 per cent of drilled formation column in oil and gas well drilling (Steiger et al. 1992). The amount of shale encountered by a coal seam gas well will depend on the basin and targeted seam depth. Shale is a fine-grained, clastic sedimentary rock rich in clay minerals containing fine bedding planes and with extremely low permeability. The inherent physical and chemical properties of shale make it one of the most troublesome formations to drill while maintaining wellbore stability, especially when water-based drilling fluids are used. It has been observed that approximately 90 per cent of wellbore instability takes place in shale formations (Steiger et al. 1992). Figure 3. shows an example of wellbore instability problems in shale formation where the wellbore size was enlarged by failure from the bit size of 8.5 inches to 25 inches as measured on calliper logs (van Oort 2003). In contrast, in the sandstone section, the hole is almost in-gauge or slightly under-gauge because of drill fluid filter cake formed on the wellbore wall.

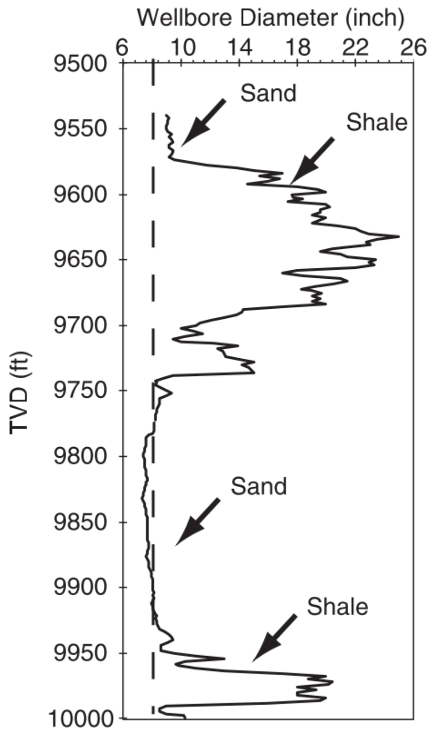


*Source: van Oort (2003)*[13]

Figure 3.9 Example of wellbore instability in shale formation

Water-based drilling fluids are the most commonly used fluid for drilling coal seam gas wells in Australia (NSW Government 2012). The stability mud weight window presented in Figure 3.2 does not differentiate mud types and is solely governed by the magnitude of the drilling fluid density, which is applicable to the initial wellbore stability in shale. However, due to drilling fluid and shale interactions, having the correct drilling fluid density does not necessarily guarantee the stability of the wellbore over time.

A comprehensive review of water-based drilling fluid and shale interaction is given in van Oort (2003). When a shale formation is exposed to water-based drilling fluids, there are potentially four forces driving direct and coupled flows in shale. Table 3.2 provides an overview of the driving forces and transport in shale. The well-known direct flows are Darcy flow of water, driven by hydraulic gradient, and diffusion of solutes/ions, driven by chemical potential gradient between the drilling fluid and the shale.

Assuming the shale is drilled overbalanced in order to maintain mechanical wellbore stability, mud filtrate (water) flows into the shale driven by the hydraulic pressure gradient. The Darcy flow of virtually incompressible water into a high-stiffness shale matrix will have a profound effect on pore pressure. Because of their low permeability, shales cannot dissipate pore pressures quickly to the far field. As a result of mud filtrate invasion, pore pressure will be elevated in an extended zone around the wellbore. Thus, drilling with a water-based mud at overbalance will ‘charge’ the near wellbore pore pressure over time, as shown in Figure 3..

[13] Reprinted from Journal of Petroleum Science and Engineering, 38, van Oort, On the physical and chemical stability of shales, 214, Copyright (2003) with permission from Elsevier

Table 3.2 Overview of flows in shale driven by gradients in hydraulic pressure, chemical potential, electric potential and temperature.

| **Driving force flow** | **Hydraulic pressure gradient** | **Chemical potential gradient** | **Electric potential gradient** | **Temperature gradient** |
|---|---|---|---|---|
| Fluid (water) | Convection (Darcy's Law) | Chemical osmosis | Electro-osmosis | Thermo-osmosis |
| Solutes/ions | Advection | Diffusion (Flick's Law) | Electro-phoresis | Thermal diffusion (Soret Effect) |
| Current | Streaming current | Diffusion current | Electric conduction (Ohm's Law) | Thermo-electricity (Seebeck Effect) |
| Heat | Isothermal heat transfer | Dufour effect | Peltier effect | Thermal conduction (Fourier's Law) |

*Source: adapted from van Oort (2003)*[14]

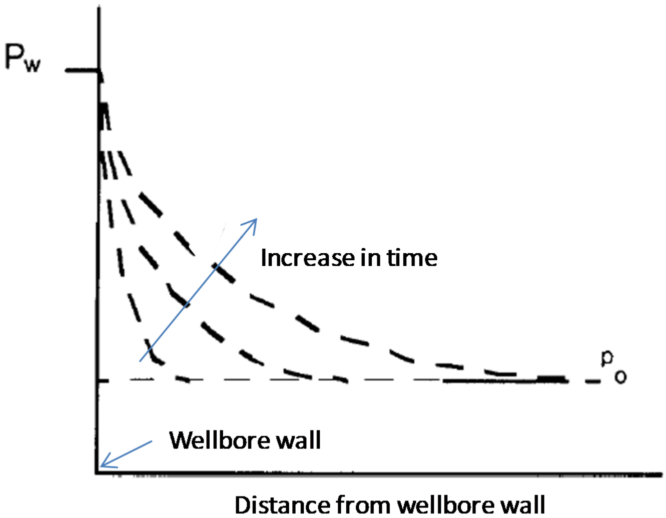


*Source: modified from Lal and Amoco (1999)*[15]

Figure 3.10 Pressure diffusion from wellbore wall with time

Shale and water-based drilling fluid systems exhibit characteristics of '*leaky osmotic membranes*' (van Oort et al. 1996; van Oort et al. 1995). It is possible to stimulate osmotic backflow of shale pore water towards the wellbore by using high-salinity drilling fluid to partially offset the hydraulic inflow of mud filtrate. If the ion content in the drilling fluid exceeds that of the shale pore fluid, diffusion of ions from the drilling fluid to the shale will occur. All the direct and coupled flows give rise to exchange of water and solutes/ions that will change the swelling pressure, water content and pore pressure in the near wellbore region.

---

[14] Reprinted from Journal of Petroleum Science and Engineering, 38, van Oort, On the physical and chemical stability of shales, 217, Copyright (2003) with permission from Elsevier

[15] Copyright 1999, SPE. Reproduced with permission of SPE, further reproduction prohibited without permission.

Diffusion is a more prominent and faster process than Darcy flow in low permeability shales. For shales with permeability in the nano-Darcy range, ion diffusion is one to two orders of magnitude faster than hydraulic flow. Furthermore, the pore pressure front is expected to exceed the ion diffusion front by one to two orders of magnitude (Figure 3.). Figure 3.12 depicts schematically the fronts of the three processes, i.e. mud filtration invasion, ion diffusion and pore pressure diffusion. A good rule of thumb is that where bulk water invasion proceeds at mm per day, ion diffusion will diffuse in the range of cm per day and pressure will diffuse over dm per day (van Oort 2003).

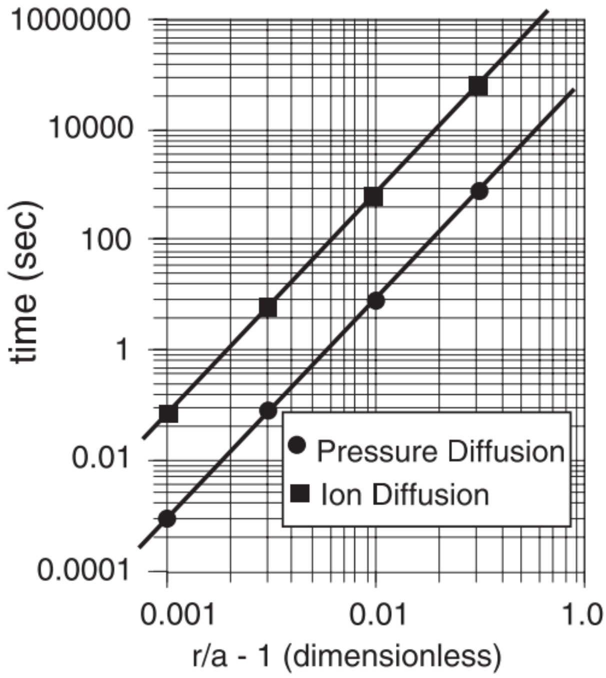


*Source: van Oort (2003)*[16]

Figure 3.11 Pore pressure penetration and ion diffusion in shale, assuming a diffusion constant of $10^{-8}$ $m^2/s$ for pore pressure diffusion and $10^{-10}$ $m^2/s$ for ion diffusion

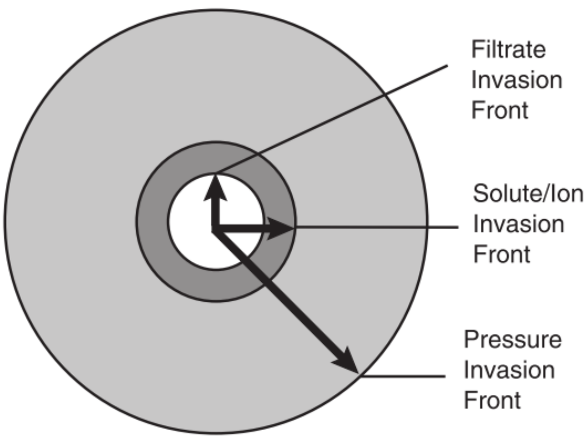


[16] Reprinted from Journal of Petroleum Science and Engineering, 38, van Oort, On the physical and chemical stability of shales, 218, Copyright (2003) with permission from Elsevier

*Source: van Oort (2003)[16]*

Figure 3.12 Schematic overview of the development of filtrate invasion front, solute/ion invasion front and pressure invasion front

There are basically three pressure and chemical mechanisms that originate from the shale and drilling fluid interactions that could lead to wellbore instability:

- elevation of pore pressure due to mud pressure penetration, thereby reducing effective stresses in the shale formation surrounding the well
- elevation of swelling pressure (e.g. due to unfavourable cation exchange at clay sites), reducing effective stresses, and
- chemical alteration and weakening of the cementation bonds in shale.

The opposite can also be true. For example, a more stable well situation may arise when pore pressure or swelling pressure is reduced, or if chemical alteration strengthens the shale.

Figure 3.13 shows how wellbore stability conditions can deteriorate with time from an initially stable condition, because of the drilling fluid and shale interactions. The effective stress state will move towards the failure envelope of native shale due to the increase in pore pressure and / or swelling stress. When a specific point around the wellbore reaches the strength envelope, failure occurs (see solid curve in Figure 3.13). On the other hand, the strength of shale can be reduced due to the chemical alteration and weakening effect of the cementation bonds in shale induced by mud filtrate invasion. To maintain well stability, one of the options readily available to the driller is to increase mud weight in order to change the stress state (i.e. shift the Mohr circle back to the right) and keep the hole open. This, however, is only a temporary fix as the mud pressure penetration will continue to move the stress state on the wellbore wall towards failure envelope. Moreover, a higher mud weight reduces the stable and safe mud weight window (difference between fracture gradient and mud weight required for well control and wellbore stability), ultimately leading to exceeding the fracture gradient, tensile wall fracturing and mud losses.

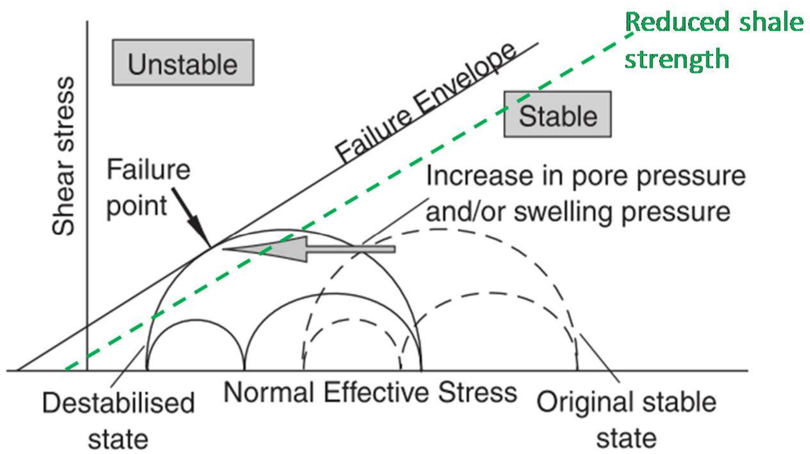

*Source: modified from van Oort (2003)*[17]

Figure 3.13 Mohr-Coulomb representation of shale failure

As mentioned earlier, water-based drilling fluid is currently the most commonly used fluid in drilling coal seam gas wells in Australia (NSW Government 2012). Potassium chloride (KCl) is used as a weighting agent to increase mud weight and to control swelling clays (APPEA factsheet, no date). KCl is probably the best-known inhibitor for shale stability in the conventional oil and gas industry. Its popularity derives mainly from its ability to reduce swelling pressures in smectite clays. It has been applied very effectively in drilling young, reactive 'gumbo-type' shales that contain extensive amounts of smectite clays. Together with partially-hydrolysed polyacrylamide (PHPA), a system is formed that is highly effective in stabilising shale cuttings (Clark et al. 1976). The main performance shortcoming of KCl is its inability to prevent mud filtrate invasion and mud pressure penetration in shales. The viscosities of KCl solutions are close to that of water, even at salt-saturation levels. KCl cannot plug pore throats or modify shale permeability, which is required to reduce mud filtrate invasion and mud pressure penetration into shales. In addition, osmotic pressures generated by concentrated KCl solutions are moderate (typically < 20 MPa) and membrane efficiencies are low (typically 1-2 per cent) due to the relatively high mobility of KCl in shale. Thus, osmotic backflow of shale pore fluid induced by KCl muds (with effective osmotic pressures in the range 0.1–1.0 MPa) will be negligible. As a result, KCl-based mud systems usually are not suitable for drilling older, less-reactive shales. These shales will normally fail due to the effects of mud pressure penetration at prolonged exposure to the invading mud filtrate. In summary, KCl is recommended primarily for cuttings-stabilisation of relatively young, more reactive shale types that contain a significant amount of smectites.

### 3.2.2 Safe mud weight window

As shown in Figure 3.14, the lower limit of the safe mud weight window is defined by the formation pore pressure (or pore pressure gradient) and the upper limit by formation breakdown pressure (or formation fracture gradient). The mud weight must be maintained within the safe mud weight window at all times during drilling of the entire interval to avoid issues related to well integrity, such as influx of formation fluids into the wellbore or loss of drilling mud into the formations. The correct prediction of how pore pressure gradient and fracture gradient varies through the intervals to be drilled is critical to designing an appropriate casing program. Figure 3.14 shows an example where casing depth is limited by the safe mud weight window (Vignes and Aadnoy 2010). Formation pore pressure and fracture gradients are reviewed and discussed separately below.

[17] Reprinted from Journal of Petroleum Science and Engineering, 38, van Oort, On the physical and chemical stability of shales, p. 219, Copyright (2003) with permission from Elsevier

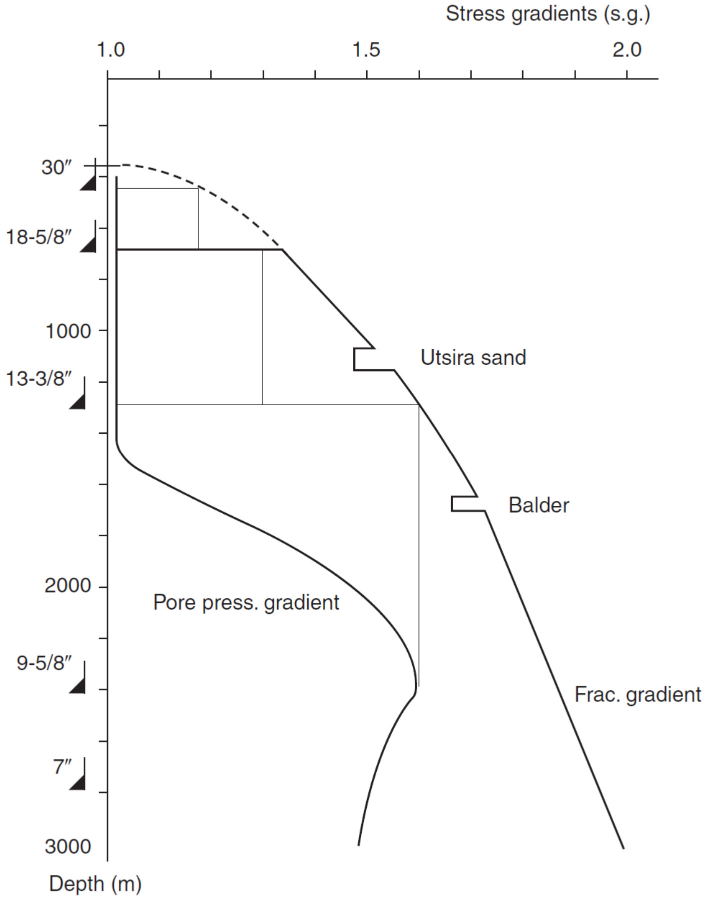


*Source: Aadnoy (2010), with permission*

Figure 3.14 Casing depth limited by safe mud weight window

### 3.2.2.1 Formation pore pressure gradient

For coal seams, the reservoir pore pressure has been reported to vary from near normal water pressure gradient (Cunnington and Hedger 2010; Johnson et al. 2010a; Meng et al. 2011) to highly overpressured (Decker and Horner 1987; Kaiser and Ayers Jr 1994; Logan 1993). Shown in Figure 3.15 is a formation pressure gradient map in the Fruitland formation of the San Juan Basin, US. The pore pressure gradient ranges from 0.30 to 0.40 psi/ft (underpressured) in the south to 0.44 to 0.63 psi/ft (overpressured) in the north central part of the basin. The overpressuring is reported to be artesian in origin; it is not a fossil geopressure. Overpressure is adapted to the present day geomorphology and not to the basin's structural axis or its most thermally mature area (Kaiser and Ayers Jr 1994).

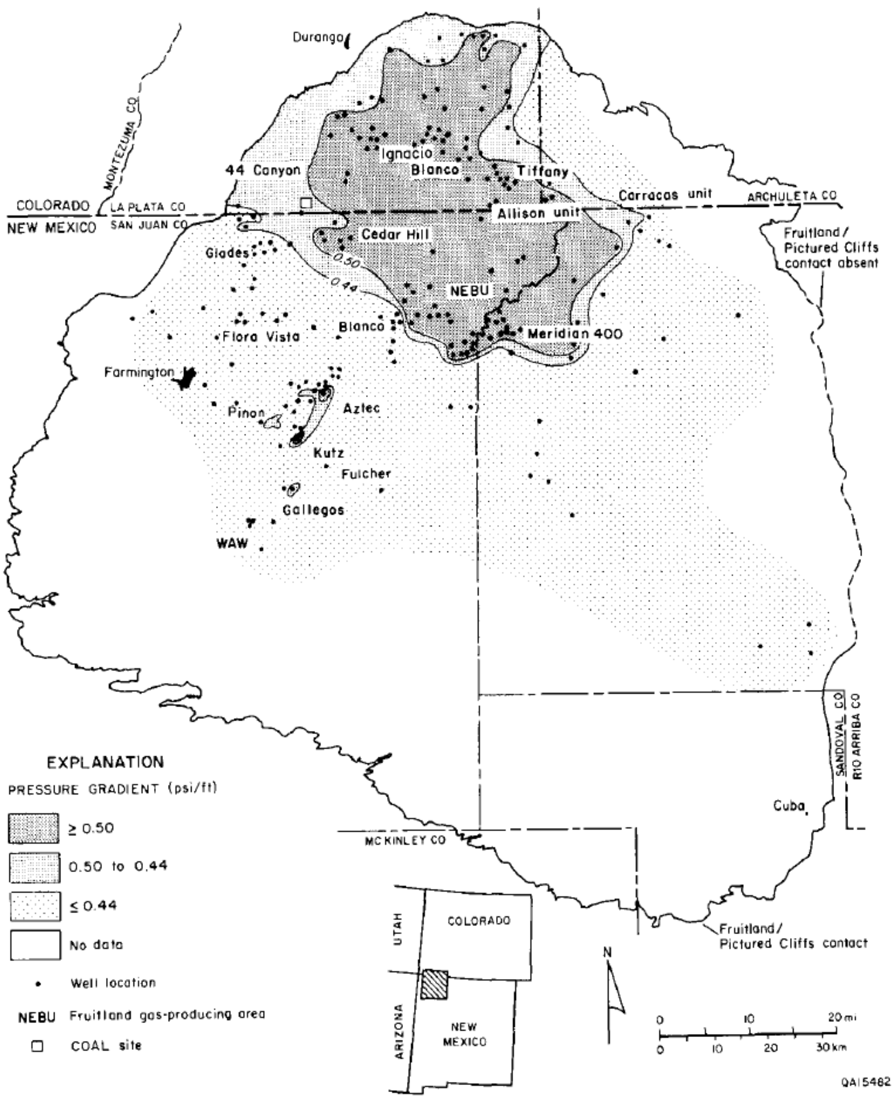


**Fig. 5—Fruitland formation pressure-gradient map.**

*Source: Kaiser and Ayers Jr (1994)*[18]

Figure 3.15 Fruitland formation pore pressure gradient map, the San Juan Basin

Coal seam reservoir pressure is normally evaluated during drilling from drill string tests (DST) or measured from shut-in wellhead pressures during production. Pre-drilling pore pressure evaluation in coal seams has not been reported so far.

For overburden formations, traditional methods to predict pore pressures using rock properties, such as that by Eaton (1975), are restricted to shale and mudrock formations. The pore pressures in other types of formation are derived by assuming pressure equilibrium with neighbouring shale and mudrock formations or by using other methods such as the centroid method (Finkbeiner et al. 2001). The most likely mechanisms of overpressure generation applicable to the traditional methods are under compaction (undrained shales). During the sedimentation process, as long as the pore fluid at a deep formation is in pressure communication with the surface, the formation pressure will remain hydrostatic and the formation is normally pressured. Pressure communication between the formation and the

[18] Copyright 1994, SPE. Reproduced with permission of SPE, further reproduction prohibited without permission.

surface requires that the fluid can flow rapidly enough in the pore space to equalise the pressure. This depends on the permeability of the sediment and the time scale allowed for pressure equalisation to occur. If the sediment permeability is too low or the sedimentation rate is too high, it will not allow the pore fluid to flow and the pressure communication is lost. As sedimentation continues, the overburden load will continue to increase. As water is highly incompressible and pressure communication is lost, the additional load of the increasing overburden will be carried essentially by the pore water, and not by the more compressible framework of the formation rock. As a result, the formation pore pressure is elevated to above hydrostatic pressure and the formation is overpressured.

An under compacted formation will have a lower effective stress and a higher porosity than a normally compacted and pressured formation. As a result, the magnitude of the pore pressure may be estimated based on the measured porosity indicators such as velocities from seismics (Dutta 2012), sonics, resistivity and density from wireline and / or logging while drilling (LWD) logs. For accurate pore pressure estimations, utilisation of one particular measurement is not very reliable, and a combination of techniques (such as LWD/wireline sonics, vertical seismic profile and seismic velocities) will improve the confidence of the estimation.

Under compaction is the most important and commonly encountered overpressure mechanism found in the major basins being developed. Unlike the under compaction mechanism, the other overpressure mechanisms, such as tectonic compression (lateral stress), formation uplifting, hydrocarbon generation and gas cracking, and smectite to illite transformation (Hower et al. 1976) are either comparatively minor or occur late in the formation burial history. Most of these mechanisms reduce effective stress in the formation below the maximum historical value. Pore pressure prediction for these other mechanisms is far more challenging than for the under compaction mechanism, and will not be discussed further in this report.

#### 3.2.2.2 Formation fracture gradient

The formation fracture gradient represents the upper limit of the safe mud weight window beyond which significant well integrity issues result with uncontrolled mud losses into the formation of the openhole section. The fracture gradient is not defined precisely; some identify the fracture gradient as the pressure at which a fracture is initiated, others may select the value of fracture closure pressure (nominal minimum in-situ principal stress) which may be more conservative than the fracture initiation pressure depending on the in-situ stress regime in the field and well trajectory, and some select a value for fracture gradient between these two (Cook et al. 2012).

Leak-off tests (LOT) have been traditionally used to measure formation fracture gradient. In the early stage of a field development, in particular the exploration and appraisal stages, LOT tests are routinely conducted prior to drilling a new hole section. After cementing the casing, approximately 3 m (10 ft) of fresh formation is drilled below the casing shoe. Pressure is applied to the casing and into the freshly drilled openhole at a slow and constant pump rate while the well is shut in to measure the response of the formation. Initially, the pressure builds up linearly as the mud is pumped. The slope of the pressure versus time curve is governed by the pump rate and the compressibility of the system, including the mud in the hole, and the short openhole section and the casing. As pumping continues, the pressure in the wellbore continues to build up until a fracture is induced in the wellbore wall. Once a fracture is created, the slope of the pressure versus time (or volume) curve decreases in response to the increased volume and system compliance associated with the fracture. The point at which the slope changes is traditionally known as the leak-off point (LOP) and is taken to represent the fracture gradient (Figure 3.16). The standard LOT is typically stopped shortly after the LOP is passed.

The process of taking a leak-off test well beyond the LOP point and generating a fracture extending into the formation and then reopening it is often termed an extended leak-off test (Kunze et al. 1992), as shown in Figure 3.16. In this type of test, pumping continues upon reaching the LOP point. The pressure continues to increase and will typically reach a peak (breakdown pressure) and then decline rapidly while the pumping continues. Ultimately, the pressure will settle at a propagation pressure that is normally lower than the breakdown pressure. If pumping is stopped, pressure in the fracture will bleed off to the formation, which will lower pressure in the fracture and allow the fracture to close. The pressure at which the fracture closes completely on itself is the fracture closure pressure ($P_{closure}$). Eventually, the bottom hole pressure will be in equilibrium with the reservoir pressure. When pumping resumes, pressure builds up again and the fracture will reopen at the reopening pressure, ($P_{reopening}$), which is similar in magnitude to $P_{closure}$. The fracture will then resume propagating at a pressure similar to $P_{propagation}$.

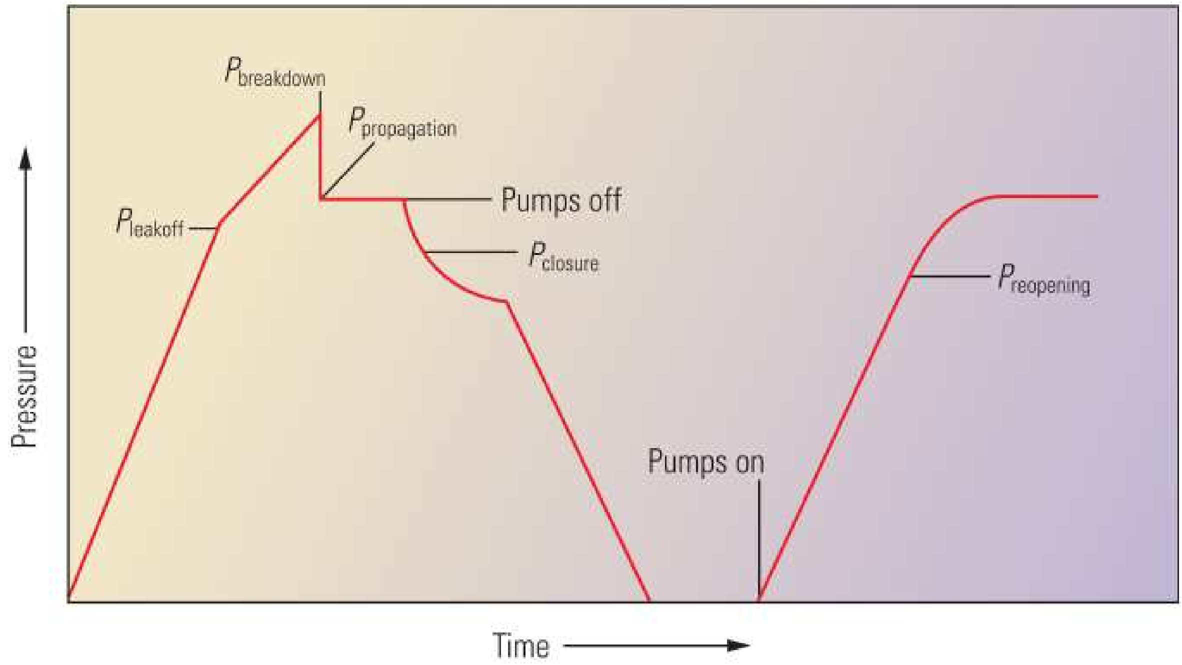


*Source: Cook et al. (2012), Copyright Schlumberger, with permission*

Figure 3.16 Pressure versus time plot for an XLOT. The standard LOT is typically stopped shortly after the LOP is reached

It should be noted that an extended leak-off test (XLOT) curve may not exhibit the exact shape depicted in Figure 3.16 or possess a peak or plateau. The shape is determined by a number of factors, including in-situ stresses, formation pore pressure, rock strength, well trajectory, pre-existing fractures and casing shoe strength.

French and McLean (1993) studied the effect of well trajectory on fracture gradient for drilling high angle development wells. They defined the fracture gradient as the larger of the fracture initiation gradient ($g_{fi}$) and the fracture propagation gradient ($g_{fpr}$).Figure 3.17 shows an example of the variation of $g_{fi}$ and $g_{fpr}$ with increase in wellbore deviation angle. The figure was generated based on linear elasticity stress distribution on an originally intact wellbore wall drilled in a normal fault stress regime with the two horizontal stresses being equal. The fracture gradient is equal to fracture initiation pressure for wellbores with a deviation angle up to 55 degrees, i.e. fracture gradient is mainly affected by the near wellbore stress condition. For higher deviation angles, the fracture gradient is governed by fracture propagation pressure, i.e. far field minimum principal in-situ stress.

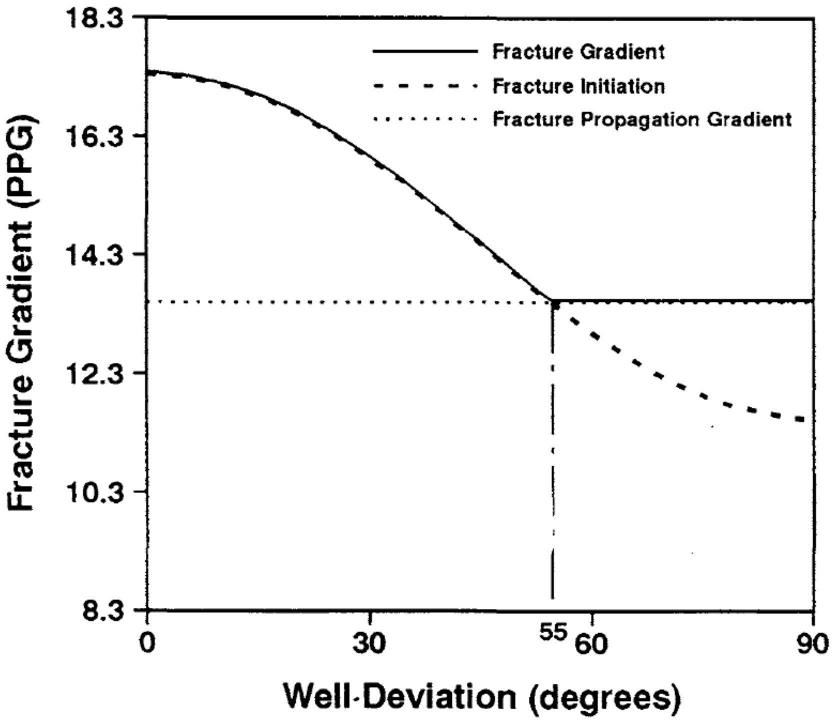


*Source: French and McLean (1993)*[19]

Figure 3.17 Variation of fracture gradient with well deviation angle

The above discussion is related to fracture gradients for intact formations. In the case of pre-existing fractures that are sufficiently long to bypass the disturbed zone in the near wellbore region, drilling fluid can penetrate into the pre-existing fractures during pressurisation of the fracture, and the LOT is likely to be closer to the re-opening pressure in Figure 3.16. For formations with pre-existing natural fractures with high fluid conductivity, the LOT pressure or the fracture gradient would be very close to the formation pore pressure.

One challenge with respect to drilling coal seam gas wells in Queensland is encountering loss zones during drilling and cementing operations (Tan et al. 2012). In one well, minor to moderate dynamic losses were encountered while drilling the high angle (70°-85°) 8.5-inch (215.9 mm) production hole section using an 8.8 ppg water-based mud system (in comparison with the fresh water gradient of 8.345 ppg). As soon as a drilling fluid loss is detected, a lost circulation material (LCM) is added to the drilling fluid. LCM is a cellulose material and prevents fluid loss by blocking the pores and fractures in the formation rock with cellulose particles. In cases where drilling fluid loss is too severe and the LCM does not work, the hole is completely sealed with a cement plug, before being re-drilled.

## 3.3 Risks and mechanisms of losing well integrity related to casing and cement

Once a coal seam gas well is drilled to the designed depth, a steel casing string is run into the well and cemented into the ground (Figure 3.). Poor cementing, leaking through casing connections, and cement degradation and casing corrosion are some of the risks that will compromise well integrity. Furthermore, the integrity and bonding of the cement sheath to the

[19] Copyright 1999, SPE. Reproduced with permission of SPE, further reproduction prohibited without permission

casing and / or formation can be damaged by certain operations in the well's history. This section reviews some of the critical aspects of well integrity related to casing and cementing.

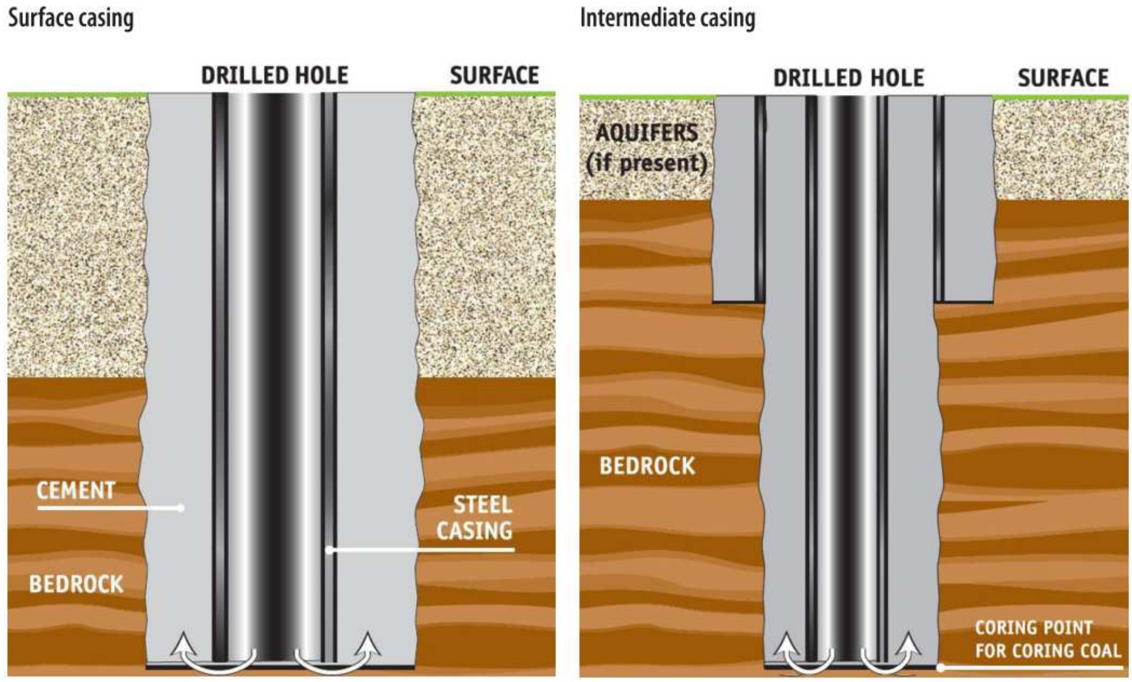


*Source: APPEA (no date)*

Figure 3.18 Cement pumped up the hole between the rock (gravel etc.) and casing – indicative diagram only

### *3.3.1 Challenges in cementing coal seam gas wells*

As shown in Figure 3., cement fills and seals the annulus between the casing strings or between the casing string and the formation. In general, the cement has three basic functions (Taoutao, 2010):

- to provide zonal isolation and segregation
- to protect casing from corrosion by formation fluids
- to support casing and formation.

Cementing coal seam gas wells is largely comparable to cementing conventional oil and gas wells, and the code of practice on construction of coal seam gas wells in Queensland (2011) requires good oil field practice to be applied in cementing coal seam gas wells. Good oil field practice in cementing includes optimum slurry flow rates, conditioning of the hole and centralisation of the casing. Furthermore, while the coal seam gas well may be drilled underbalanced with air or lightweight fluid systems, the cementing operation must be slightly overbalanced to prevent free gas migration in the cement column after placement is accomplished (Halliburton 2007).

The unique challenges present when cementing coal seam gas wells due to the nature of the coal seams include cement invasion into coal seams, slurry losses during pumping, low fracture gradients and annulus pack off (Mohammad and Shaikh 2010). Several seams of coal could exist along a coal seam gas well. The challenges are exacerbated when the wells are deviated or approach horizontal, or have a low temperature at the bottom of the wellbore, resulting in a longer cement setting time.

The coal seams are naturally fractured (cleats); as such they are prone to cement slurry invasion and losses. It has been reported that many loss zones are encountered during drilling and cementing operations of coal seam gas wells in Queensland (Tan et al. 2012). Slurry losses into coal seams are undesirable. In addition to plugging the coal cleats that causes a reduction of well productivity, they result in a reduced cement sheath height and leave some formations open, hence compromising well integrity (Huff and Merritt 2003). To reduce or eliminate cement slurry losses, a number of methods have been developed, including use of low-density cement, foam cement, and adding lost circulation materials to the cement slurries (Tan et al. 2012).

In some cases, vertical coal seam gas wells are drilled with air or inhibited water with a small amount of polymer. Removal of the cuttings before or during the cementation process poses challenges. Presence of excessive cuttings tends to pack off at some restricted areas along the openhole annulus and block the flow path. This results in an incomplete cement sheath, compromising zonal isolation and reducing the protection from corrosion afforded to the casing.

### 3.3.2 Well integrity issues in conventional oil and gas wells

Poor well integrity is a significant problem in oil and gas production operations. A number of studies have been carried out that indicate there is not full integrity in a significant percentage of all wells.

- In the US Gulf of Mexico, approximately 10 per cent of wells have sustained casing pressure (SCP) within one year of being completed and approximately 50 per cent of wells after 15 years of production have SCP (Figure 3.) (Bannerman et al. 2005). The SCP is defined by the Minerals Management Service (MMS) as a pressure measurable at the casing head of a casing annulus that rebuilds when bled down, is not due solely to temperature fluctuations and is not a pressure that has been deliberately applied.
- In offshore Norway, 18 per cent of the wells surveyed in a pilot study (more than 400 wells) had integrity failure, issues or uncertainties, and 7 per cent of these are shut in because of well integrity issues according to the National Petroleum Safety Authority (Vignes and Aadnoy 2010).
- In Canada, 4.6 per cent of 316,439 wells in the database collected by Energy Resources Conservation Board (ERCB) have leakage issues, with gas migration (GM) outside casing or surface casing vent flow (SCVF) from wellbore annuli (Watson and Bachu 2009) (Figure 3.14).

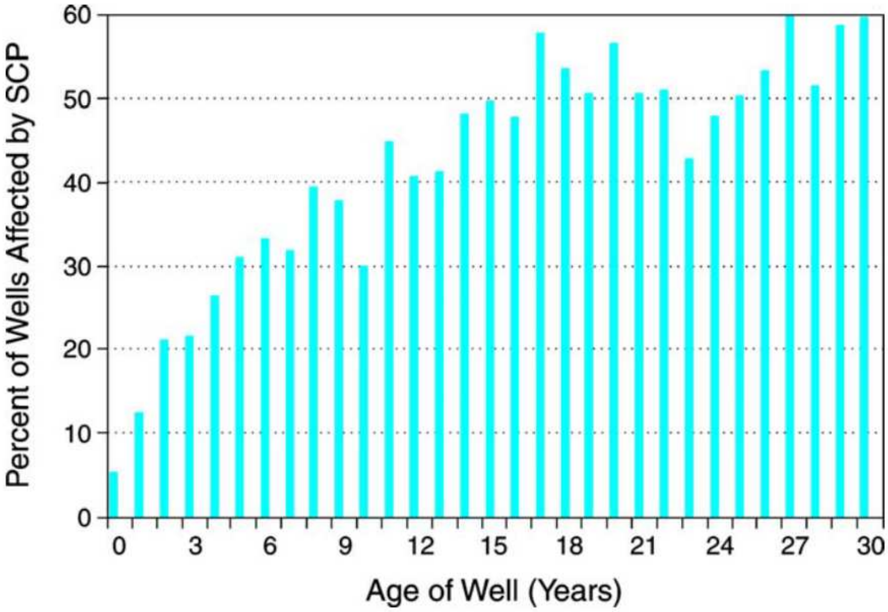


*Source: Bannerman et al. (2005)*[20]

Figure 3.19 MMS records on percentage of wells exhibiting sustained casing pressure in the outer continental shelf area of the Gulf of Mexico, grouped by age of the wells

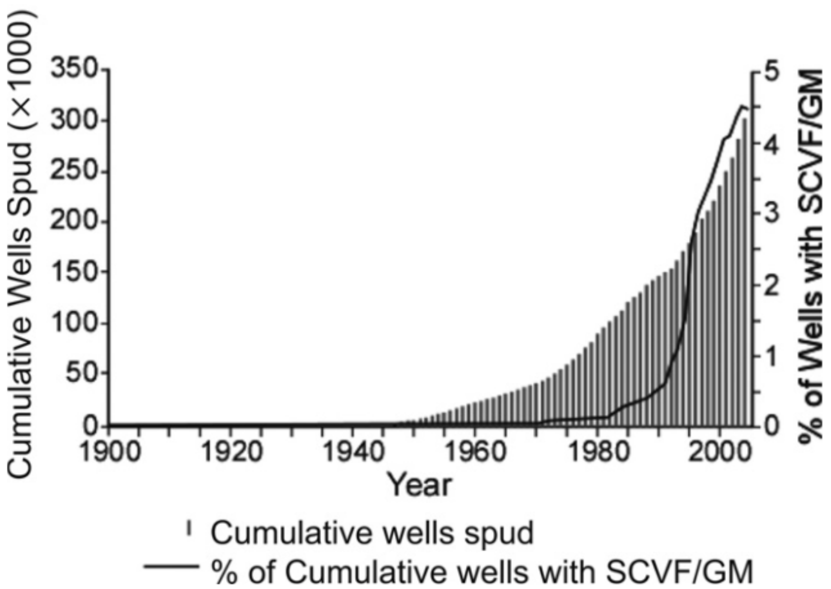


*Source: Watson and Bachu (2009)*[21]

Figure 3.20 Historical levels of drilling activity and SCVF/GM occurrence in Alberta, Canada by cumulative wells

[20] Copyright 2005, SPE. Reproduced with permission of SPE, further reproduction prohibited without permission.
[21] Copyright 2009, SPE. Reproduced with permission of SPE, further reproduction prohibited without permission.

A more comprehensive description on well barrier and well integrity failure for conventional oil and gas wells on land and offshore can be found in a recent publication by King and King (2013).

It should be noted that completed and producing conventional oil and gas wells are constructed with multiple well barriers. Individual well barrier failure rates are often one to two orders of magnitude higher than well integrity failure rates where all barriers in a protection sequence fail and pollution to environment can or does happen (King and King 2013).

### 3.3.3 Potential well leakage pathways

For a leak to occur in a well, whether the leak is to surface or cross flow subsurface between different formations, three elements must exist (Watson 2004):

- a source formation where gas or liquid hydrocarbons or other fluids exist in the pore space
- a driving force between the source formation and surface in case of leakage to surface, or between different formations in case of subsurface cross flow. Such a driving force could be the difference in pressure, temperature or salinity
- a leakage pathway between the source formation and surface or between different formations.

Watson and Bachu (2009) attributed well leakage to poorly cemented casing/hole annulus, casing failure and abandonment failure, and Gasda et al. (2004) identified interfaces between cement and formation rock and / or casing, and casing and plug for abandoned wells as the preferential pathways for fluid flow. In the cement sheath, migration of fluid could also occur through fractures, channels and the pore space. In the latter case, fluid flow would occur only when the cement sheath was degraded or did not form properly during the cementation process (Zhang and Bachu 2011). Figure 3.21 shows a schematic of the potential leakage pathways along an abandoned well.

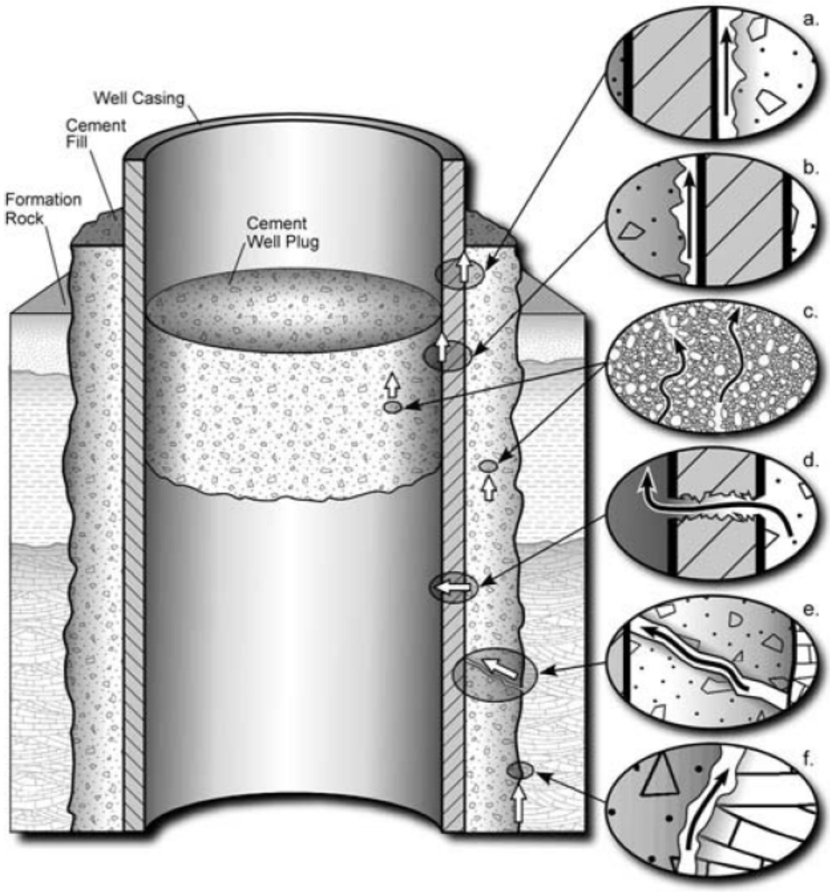


*Source: Celia et al. (2004), with permission*

Figure 3.21 Potential leakage pathways along an existing well: between cement and casing (paths a and b), through the cement (c), through the casing (d), through fractures (e), and between cement and formation (f)

## *3.3.4 Factors affecting cement sheath and cement bond integrity*

### 3.3.4.1 Wellbore condition

Successful zonal isolation is not only dependent on selecting the right slurry, but also involves preparation of the wellbore for cementing. A good cementable wellbore is a prerequisite for a successful cementing job. The ideal cementable wellbore and its requirements are shown in Figure 3.22 (Smith, 1990).

Ideally, the wellbore to be cemented should be in-gauge or nearly in-gauge with a smooth well surface. The wellbore-formation flow should be static with no formation fluid influx or lost circulation. The casing should be centralised in the openhole section with a sufficiently wide annulus, and the mud in the hole should be properly conditioned and free of cavings from sloughing shales. Breakouts are to be avoided or minimised by use of proper mud weight and chemistry during drilling.

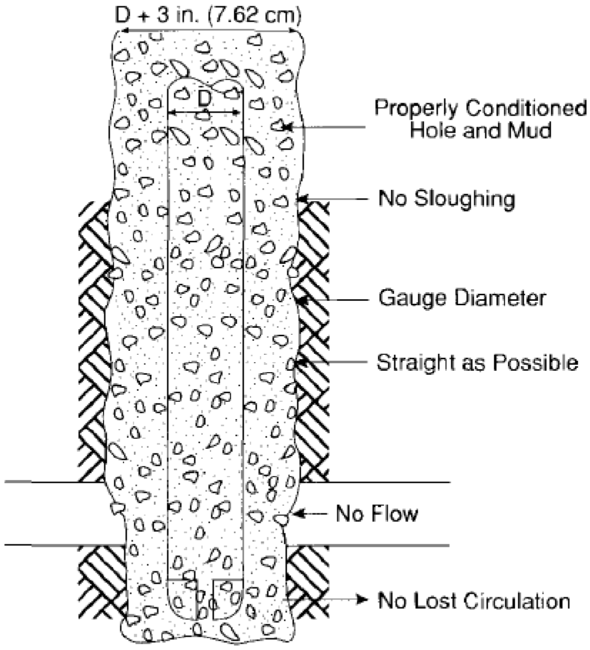


*Source: Smith (1990)*[22]

Figure 3.22 Ideal cementable wellbore requirements

It should be noted that not all rock failure on the well surface will present as breakouts or washouts. Under certain conditions, the rock that has failed due to mechanical stress concentration may still attach to the wellbore wall. This type of rock failure may not be detectable from caliper logs or ultrasonic image logs, but could show up in resistivity logs. This type of rock failure should also be avoided or minimised since the mechanical damage is unlikely to be sealed with cement. This leaves a damaged zone behind the cement sheath with a significantly enhanced permeability which could be a potential pathway for fluid migration outside of the cement sheath.

Figure 3.23 shows a photograph of a cross section of a failed model wellbore in shale tested by CSIRO, illustrating mechanical damage inside shale can develop beyond wellbore breakout or washout zones. The wellbore was modelled by drilling a borehole in the centre of a cylindrical shale sample. The diameters of the borehole and shale sample were 25 mm and 80 mm, respectively. Wellbore failure was induced by applying an external boundary stress to the cylindrical shale sample. In addition to the breakouts, shear failure was developed inside the shale sample. These shear failure surfaces have a significantly enhanced permeability in comparison with intact shale. They may be difficult to fill and seal during cementing of a casing string into a wellbore.

[22] Reprinted from Developments in Petroleum Science, 28, Robert C Smith, Well Cementing ed. Erik B Nelson, Figure 1 Page I, Copyright (1990) with permission from Elsevier

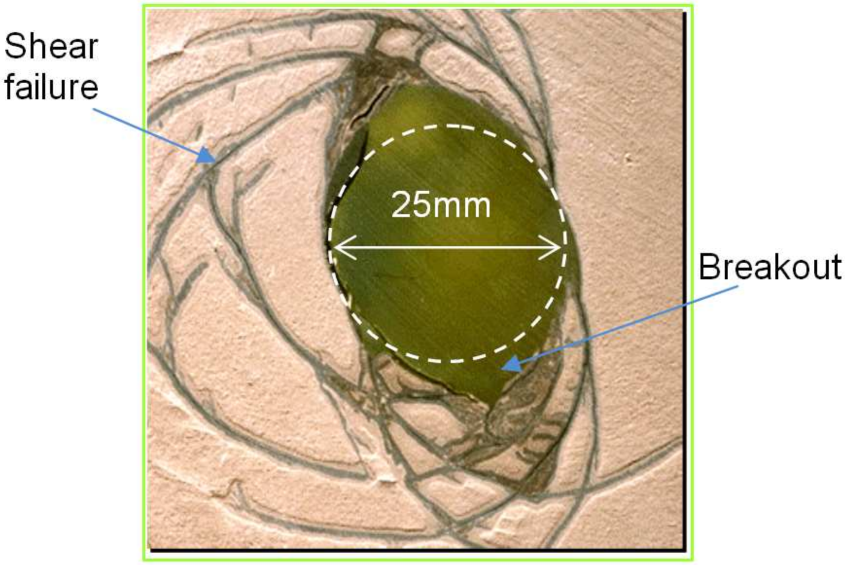


*Source: CSIRO (unpublished experimental study)*

Figure 3.23 Failure of model well in shale, illustrating mechanical damage due to shear failure inside the shale

### 3.3.4.2 Mud conditioning and displacement

Effective mud displacement and mud filter cake removal is a primary requisite to prevent gas or fluids migrating inside a cement sheath or along the interface between cement and formation. The main objective is to provide a relatively clean casing pipe and well surface to which the cement sheath can bond (Watson et al. 2002).

If channels of mud remain in the annulus, they may provide a preferential migration pathway inside the cement sheath (Bonett and Pafitis 1996). Furthermore, a mud filter cake is likely to develop on the well surface in permeable formations due to overbalanced drilling. If the filter cake is not removed from the well surface prior to cementing, it could dehydrate after the cement sets, resulting in an annulus at the formation and cement interface. Incomplete mud removal often occurs in deviated wells (Keller et al. 1987), where a continuous mud channel may remain along the narrow section of the cemented annulus. Figure 3.24 shows drilling mud channels in the cemented annulus due to incomplete displacement of the drilling mud (Watson 2004).

It is important that the drilling mud must be properly conditioned by breaking the gel strength and removing as much as possible of the filter cake (Ravi et al. 1992). Horizontal/high-deviation coal seam gas wells will require a more viscous mud for cuttings removal and an adequate spacer must be used to ensure complete mud removal. To aid mud removal, centralisation of the casing is critical and annular velocities should be as high as the well will allow. Reactive spacers are commonly run to aid in prevention of loss circulation. By coating the wellbore with a fluid that reacts with cement, a small filter cake helps prevent cement from invading into the formation. A non-reactive spacer should then be run between the reactive spacer and cement slurry to prevent premature setting of the slurry (Mohammad and Shaikh 2010). It is preferred for the spacer and cement slurry to be in turbulent flow, if possible, to enhance mud removal and to minimise fluid channelling. If turbulent flow cannot be achieved for various reasons, effective laminar flow displacement may also be quite successful (Brady et al. 1992).

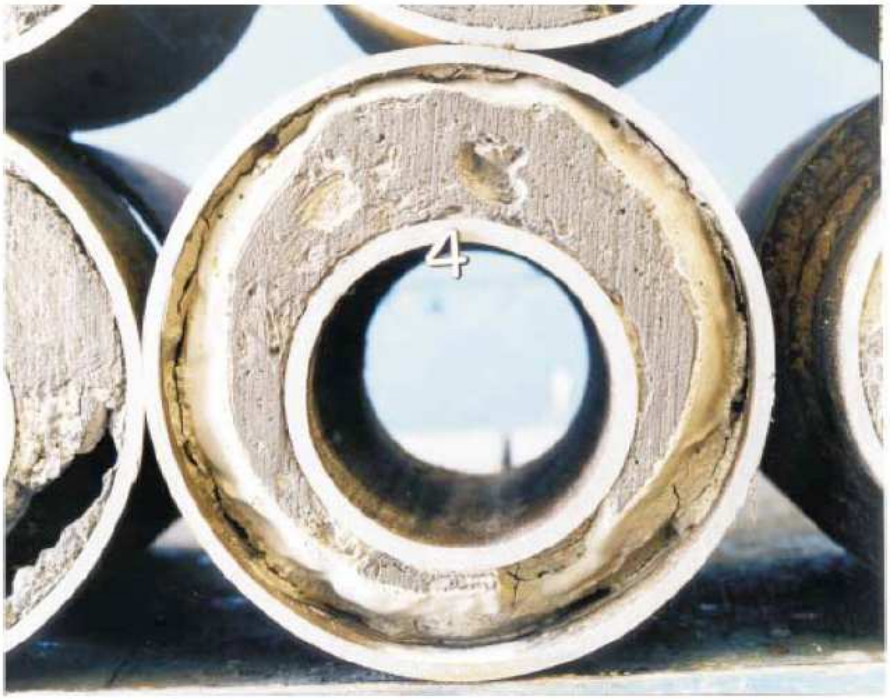

*Source: Watson (2004)*[23]

Figure 3.24 Incomplete displacement of drilling mud and the resulting cement and drilling mud channels. Over time, the gels in the drilling mud will shrink, forming a fluid migration pathway in the annulus

### 3.3.4.3 Gas migration

Cement slurry density is an important factor in cement design for preventing gas migration during cement placement. The density of cement slurry must be high enough to generate a hydrostatic pressure that exceeds the formation gas pressure in order to prevent gas from entering the annulus. However, even for properly designed cement slurry that initially provides sufficient hydrostatic pressure, the pressure within the annulus begins to fall as a result of cement gelation (Bonett and Pafitis 1996; Wojtanowicz 2008). As illustrated in Figure 3.25, gas invasion into the cement-filled annulus could occur during the cement setting process, resulting in gas channelling (Wojtanowicz 2008). During this period, the cement slurry transforms from a fully liquid pumpable state into a fully set rock-like material with extremely low permeability. At the same time, the fluid pressure in the annulus decreases from the initial full hydrostatic pressure of the cement slurry to a pressure that can be significantly lower than the formation pore pressure. When the well becomes underbalanced, formation fluid invasion into the annulus can take place if the cement is not sufficiently set. Various mechanisms have been proposed to explain the fluid pressure reduction and gas migration. Among them, fluid loss, slurry gelation, cement hydration, and bulk shrinkage are of primary importance (Bonett and Pafitis 1996; Parcevaux et al. 1990).

---

[23] Copyright 2004, SPE. Reproduced with permission of SPE, further reproduction prohibited without permission.

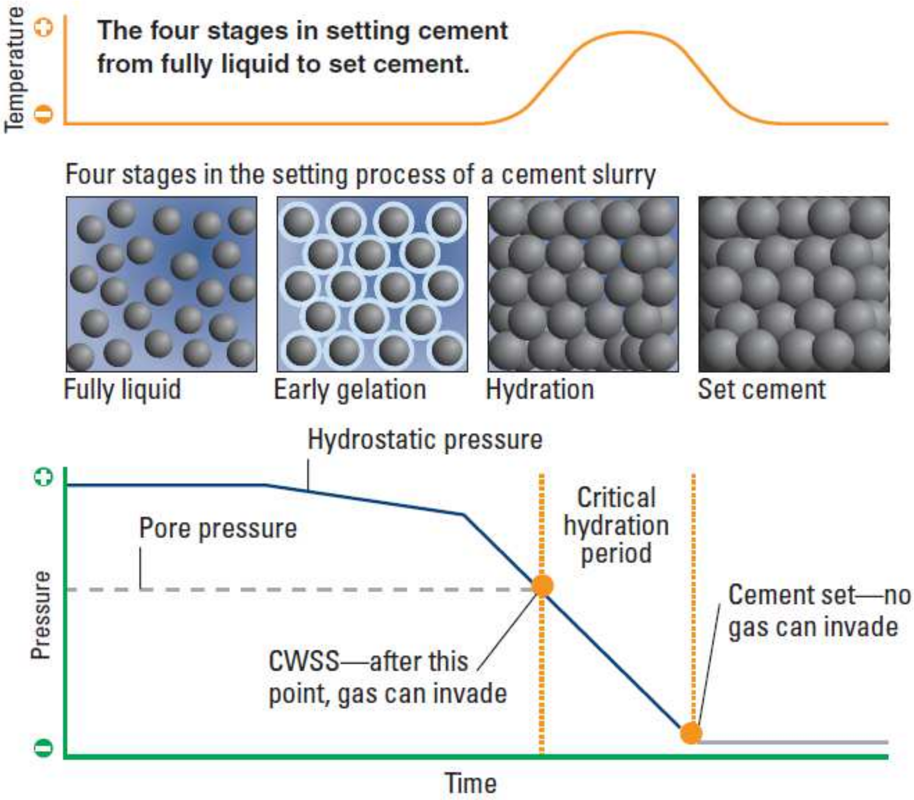


*Source: Kolstad et al. (2004)*

Figure 3.25 Cement setting process from fully liquid to set cement

### 3.3.4.4 Cement sheath and bond failure

After setting, the cement sheath becomes a solid of very low permeability (at the microdarcy or $10^{-18}$ $m^2$ level), (Parcevaux et al. 1990) and bonds to the casing and formation surfaces. As a result, fluids can no longer migrate within or through the sheath. However, downhole pressure and temperature can change due to various operations in the well's history, such as production, shut in, leak-off tests / formation integrity tests (LOT / FIT tests), and reservoir stimulation. These changes can induce deformation and failure in the casing and cement sheath, resulting in de-bonding on the interfaces between cement sheath and casing / formation, creating radial fractures (Figure 3.26) and microannuli migration pathways (Watson et al. 2002).

Goodwin and Crook (1992) reported a laboratory study on cement sheath failure due to casing expansion as a function of internal casing pressure or temperature in a flowing well. It was observed that loss of annular zonal isolation occurred due to radial stress cracks in the cement sheath, which were created by casing expansion. Similar laboratory experiments were conducted by Jackson and Murphey (1993). Gas flow through the annulus was detected after the casing pressure was reduced from 69 to 14 MPa. A pressure decrease occurs in the wellbore during normal well production operations, which causes stress redistribution in casing and cement. This may lead to the failure of the wellbore structure, especially in the perforation section. Loading from far-field formation stresses, such as tectonic stress, subsidence and formation creep, could cause pressure increase on the external surface of the cement. A change of pore pressure or temperature during reservoir production can also result in a change in formation stress (Dusseault et al. 2001).

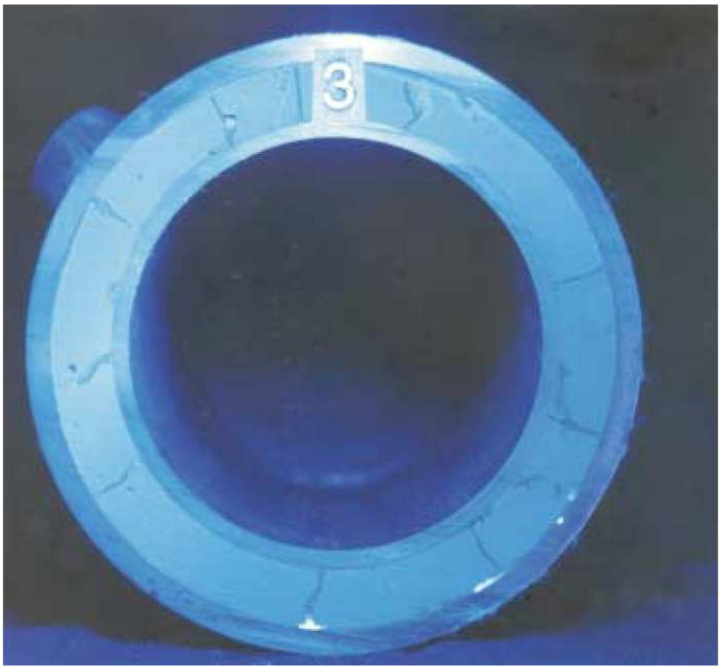


*Source: Watson (2004)*[24]

Figure 3.26 Cement sheath failure, resulting cracks developed from pressure cycling on the internal casing

### 3.3.4.5 Casing corrosion

Corrosion attacks every metal component including casing and tubing at all the stages in the life of an oil and gas field (Brondel et al. 1994). Corrosion induced casing and tubing damage and loss of well integrity have been widely reported (e.g. Bazzari 1989; Vignes and Aadnoy 2010; Watson and Bachu 2009). Corrosion encountered in petroleum production involves several mechanisms. These can be grouped into electrochemical corrosion, chemical corrosion and mechanical and mechanical/corrosive effects. A detailed description of these mechanisms can be found in (Brondel et al. 1994).

Both the inside and outside of the casing can be damaged by corrosion. The corrosion on the outside of the casing can be caused by corrosive fluids or formations in contact with the casing or by stray electric current flowing out of the casing into the surrounding fluids or formations. Severe corrosion may also be caused by sulfate-reducing bacteria. Corrosion damage on the inside of the casing is usually caused by corrosive fluids produced from the well, but the damage can be increased by high fluid velocities (Lyons and Plisga 2004).

The cement sheath and bonding quality on the interfaces play a critical role in protecting the casing from external corrosion. Cement provides favourable geochemical conditions (i.e. a high pH ranging from 12 to 13), which retard corrosion due to passivation of the steel. When the pH drops below approximately nine to 10, passivation is lost and corrosion may commence. An analysis of well logs for casing inspection and cement bond quality in 142 wells (total logged well length of 129 773 m) in Alberta, Canada by Watson and Bachu (2009) found that:

- the majority of significant corrosion occurs on the external wall of the casing

---

[24] Copyright 2004, SPE. Reproduced with permission of SPE, further reproduction prohibited without permission.

- a significant portion of wellbore length is uncemented
- external corrosion is most likely to occur in areas where there is no or poor cement.

In terms of well leakage, it was observed that the top 200 m of the cemented annulus is generally of poor quality and vast majority of SCVF/GM originates from formations not isolated by cement. Furthermore, the majority of casing failure is in the regions of poor or no cement in the annulus.

The study by Bazzari (1989) on casing leaks discovered that the type of cement used is also important to the extent of casing corrosion. Severe corrosion occurred in wells where construction and permeable light cement were used, instead of the usual Portland class G cement with additives. Leakage rates were higher in shallow zones where high sulfate concentrations caused the construction cement – which is non-sulfate resistant – to break down, exposing the exterior of the casing to the corrosive aquifer water.

#### 3.3.4.6 Leakage through casing joint connection

Casing strings with a typical length of 12 m are jointed together by threaded connections. Two major types of connections are American Petroleum Institute (API) connections and proprietary connections. API connections are manufactured according to specifications and tolerances provided by the API. Proprietary or premium connections are designed and manufactured by commercial manufacturers (Lewis and Miller 2009).

As deeper wells are drilled, leak resistance and tensile capacity of the connection become more important. The internal pressure that a given casing and connection can tolerate is the lowest of the internal yield pressure of the casing, internal yield pressure of the connection or the internal pressure leak resistance at the connection critical cross section (Lewis and Miller 2009). Thread tolerances, surface treatment, tension, and pipe dope application and type can all affect leak resistance.

A leak path exists in both eight round and buttress thread casing (BTC) connections due to the thread-cutting process. The leak path must be plugged with solid particles in the thread compound. API thread compound consists of base organic grease with lead, graphite, and other solids to provide lubrication between the threads to prevent galling during makeup and to plug the helical path. One of the problems with thread compound is deterioration with time and temperature, resulting in loss of sealability through the thread leak path. High temperature (> 250°F or 121°C) can cause the compound to evaporate, dry out and shrink. Gas can penetrate the organic grease, and the base grease can react with well fluids, resulting in loss of the seal.

Hydraulic fracturing is often applied to stimulate coal seam gas reservoirs with low permeability. This exposes the casings and connections to the high pressure generated during the treatment. Once a leakage is established through the connection, the high pressure can be transmitted to the cement sheath behind casing. Microcracking and hydraulic fracturing along the interface between the casing and cement sheath can be induced (Dusseault et al. 2000). It is important to apply recommended torque from the casing manufacturer when making up a casing connection. Too much torque may over-stress the connection and result in failure of the connection. Too little torque may result in leaks at the connection (Department of Employment Economic Development and Innovation 2011).

## 3.4 Effect of de-watering and coal seam gas production on well integrity

Coal seam gas production requires initial pumping and removing of water to sufficiently reduce the hydrostatic pressure in coal seam gas reservoirs so that methane can be desorbed from the coal. Coal seam gas is produced at a well pressure that is close to atmospheric pressure (Ely et al. 1990; Schraufnagel 1993). The ratio of water pumped to methane produced is initially high and declines with increasing coal seam gas production (Figure 3.27).

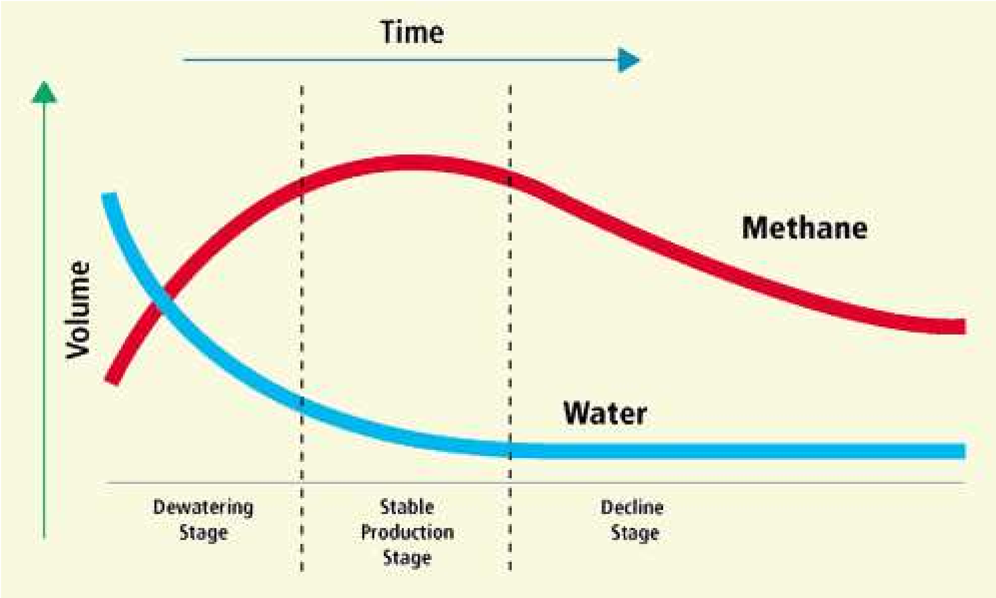


*Source: Walton and McLennan (2013)*

Figure 3.27 Water and gas production over time

The de-watering process reduces reservoir pressure and creates a highly depleted zone surrounding a coal seam gas well. Within such a zone the reservoir pressure is expected to be similar to the bottom hole pressure for highly permeable coal seams, which is close to the atmospheric pressure. Typical depths of coal seam gas reservoirs in Australia range from 300 to 1 000 m and the reservoir pressure is expected to be in the range of approximately three to 10 MPa. Coal seam compaction may be expected due to de-watering for highly fractured and compressible coal seams. This has implications on the integrity of the cement sheath and cement bonds to the casing and formation, as well as overburden formation deformation and potential fault activation. There is currently a lack of literature reporting de-watering induced well integrity issues for coal seam gas wells. The effect of de-watering on coal seam deformation is similar to reservoir compaction arising as a result of production seen in conventional oil and gas fields, which has had widely reported impacts on well failure and integrity. This section briefly reviews the oil and gas production induced reservoir compaction and subsidence, and reported impacts on oil and gas wells.

### 3.4.1 Mechanisms for reservoir compaction and surface subsidence

Doornhof et al. (2006) presented a comprehensive review on the physics of reservoir compaction and subsidence due to conventional oil and gas production. They describe the induced well damage and failures, and the mitigation methods used for several oil / gas fields.

It is well known the weight of sediments above an oil and gas reservoir is supported partially by the rock matrix and partially by the pressurised fluid or gas within the rock pore space (e.g. Bruno 1990; Du and Olson 2001). According to the theory of poroelasticity, the effective stress on a porous material, $\sigma_m^e$, is equal to the total stress (external stress applied to the material) $\sigma_m^t$ minus the pore pressure $p$ of the fluid, i.e. $\sigma_m^e = \sigma_m^t - \alpha p$, where $\alpha$ is Biot's constant. For geologic formations, the vertical external stress is the weight of the overburden while the horizontal stress depends on the lateral deformation response of the rock subject to the vertical compression from the weight of the rock itself and the tectonic stresses. As the total vertical stress generally remains constant, when fluid is withdrawn, pore pressure declines, and more of the load is transferred to the rock matrix (i.e. increase in the vertical effective stress). An increase in the vertical effective stress leads to reservoir formation compression. When the effective stress state reaches the compressive strength of the formation material, plastic deformation occurs and permanent reservoir compaction starts.

If subsurface formation compaction is significant, it will induce both vertical surface displacements (subsidence) and horizontal surface displacements. The amount of surface subsidence is primarily related to the magnitude of the reservoir compaction, its lateral extent, and the reservoir thickness and depth. Deeply buried reservoir compaction of limited areal extent will induce almost no surface subsidence, while laterally extensive or relatively shallow reservoirs can induce surface subsidence nearly equal to the subsurface compaction. The lateral extent of surface subsidence is also related to the depth of the subsurface compaction zone (Du et al. 2009).

In most cases, the thickness of the reservoir undergoing compaction is far less than the lateral dimensions, and lateral deformation is constrained by surrounding rock materials while the surface above the reservoir is completely free to deform. Therefore, the compression associated with pressure decline occurs predominantly in the vertical direction. With the uniaxial strain assumption (i.e. the reservoir is compressed in the vertical direction whilst its deformation in the horizontal direction is limited) a simple 1D analytical estimate of reservoir compaction can be derived as $\epsilon_z = \Delta H/H = C_m \Delta p$, where $H$ is the original reservoir thickness, $C_m$ is the uniaxial compaction coefficient of the reservoir materials. This relationship assumes uniform formation thickness, uniform pressure decline, uniaxial strain/compaction in the thickness direction, and homogeneous elastic isotropic material behaviour. The 1D solution provides a useful order of magnitude estimate for reservoir compaction for a given pressure decline and compressibility.

More accurate analysis on reservoir compaction and surface subsidence requires numerical solutions such as finite element modelling. Rigorous analysis requires a coupled geomechanical model which considers the multiphase flow in the reservoir, material inhomogeneities and elastoplastic deformations in a field-scale domain including the reservoir, overburden, sideburden and underburden (Settari 2002). Most of such models use an iterative coupling method. Settari and Walters (Settari and Walters 2001; Settari et al. 2008) have discussed those models in detail.

### 3.4.2 Impact of reservoir compaction and surface subsidence on wells

Currently there are very limited publicly available subsidence data for Australian coal seam gas developments, though subsidence monitoring is widely proposed for Australian coal seam gas developments (Commonwealth of Australia 2014b). This section examines international experience for a range of geologic settings and well types, because basic principles of well deformation and failure may apply. It should be noted, however, that subsidence from coal seam gas extraction may be different from subsidence from conventional gas extraction. There is a need to exercise caution in extrapolating observations of conventional oil and gas production to coal seam gas production in Australia.

Reservoir compaction and surface subsidence have been observed in a number of conventional oil fields worldwide (Geertsma 1973; Massonnet et al. 1997; Roeloffs 1988; Segall 1985). Some well-known cases include the Willmington oil field in California and the Ekofisk gas field in the North Sea, because of the magnitude of subsidence as well as the cost for extensive remedial work (Bruno 1990; Nagel 2001; Settari 2002). For the case of Wilmington oil field, the surface above the Wilmington oil field in California subsided almost 10 m during 1935 to 1965 due to oil production. The cost to elevate, protect and repair various facilities exceeded $100 million by 1962. The subsidence caused casing failure in hundreds of wells in the field (Bruno 1990). The seafloor subsidence was measured to be about 4 m by 1987 above the Ekofisk field in the North Sea (Sulak and Danielsen 1988). The entire project to raise platforms and to protect storage facilities at this offshore complex exceeded $400 million (Snyder and McCabe 1988). Casing failures have occurred in more than two-thirds of the wells (Yudovich et al. 1988).

The mechanisms of conventional oil and gas reservoir compaction and surface subsidence-induced well failures have been a subject of intensive study for a number of years (e.g. Bruno 1990, 2001; Dusseault et al. 2001). Significant reservoir compaction can induce compression and buckling type casing damage within the producing well interval. Slip on bedding planes and faults within the reservoir and overburden may also occur, causing severe shear damage to the wells. There are several critical forms of casing damage that have been observed in a variety of structural settings (Bruno 2001; Dusseault et al. 2001; Sayers et al. 2006), namely:

- overburden shear damage on localised horizontal planes
- shearing at the top of production and injection intervals
- compression and buckling damage within the production interval
- tensile failure above the reservoir.

**Overburden shear damage**. Reservoir compaction induced shearing can cause casing damage in overburden formations above the reservoir (Bruno 2001). The larger the reservoir compaction, the greater the casing impairment potential in the overburden (Dusseault et al. 2001).

Because of the continuity of overlying rocks and the general lenticular cross-sectional shape of a reservoir, compaction is a downward and inward motion. This leads to the stress state developed in the overburden formations as illustrated in Figure 3.28 (Dusseault et al. 2001). The crest section experiences an increase in horizontal stress ($\sigma_h$); the remote flanks experience a drop in $\sigma_h$; and the rocks above the shoulders experience an increase in the shear stress, $\tau$. If the shear stress anywhere in the overburden exceeds the strength of the bedding planes, or weak layers of sand and clay, low-angle slip occurs. If there is a potential for reactivation of low-angle thrust faults in the crest region, a thrusting mechanism can develop as the horizontal stresses increase, leading to the condition $\sigma_H = \sigma_1 > \sigma_v = \sigma_3$. Finally, there is the potential for a high-angle normal fault mechanism to develop on the flanks, leading to the condition $\sigma_v = \sigma_1 > \sigma_h = \sigma_3$.

It appears that localised shear deformations at weak layers within the overburden have occurred in almost every field that has been investigated (Bruno 1990; Fredrich et al. 2001, 1996; Poland and Davis 1969; Vudovich et al. 1988).The shear deformations of the damage tend to be localised over a relatively short length of casing, perhaps one metre or less in length, and are often related to weak layers rather than to high induced shear stress (Bruno 2001; Dusseault et al. 2001). Figure 3.29 shows a sample casing deformation pattern noted in caliper logs from a damaged gas well (9.625 inch or 244.5 mm casing) in Southeast Asia (Bruno 2001). The localised shear damage at weak overburden layers can be widely distributed over all portions of the field (Dale 1996; Fredrich et al. 1996; Hilbert et al. 1996, Bruno 2001). Figure 3.24 illustrates the distribution of wells damaged in overburden and within the reservoir at Ekofisk field (Bruno 2001). Damage in overburden was initially concentrated along the flanks of the field where shear stresses are highest.

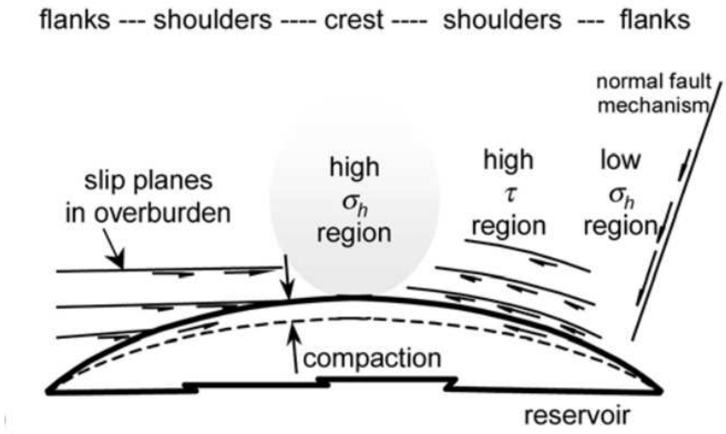


*Source: Dusseault et al. (2001)*[25]

Figure 3.28 Compacting reservoir bedding-plane slip

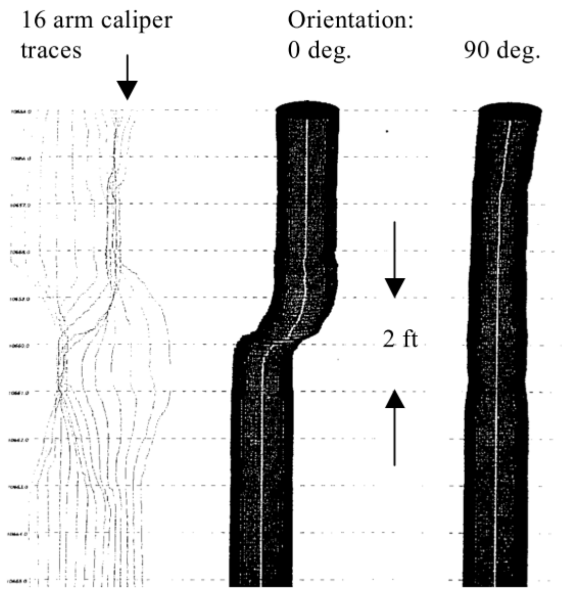


*Source: Bruno (2001)*[26]

Figure 3.29 Sample casing deformation pattern noted in caliper logs for a damaged gas well in Southeast Asia

[25] Copyright 2001, SPE. Reproduced with permission of SPE, further reproduction prohibited without permission.
[26] Copyright 2001, SPE. Reproduced with permission of SPE, further reproduction prohibited without permission.

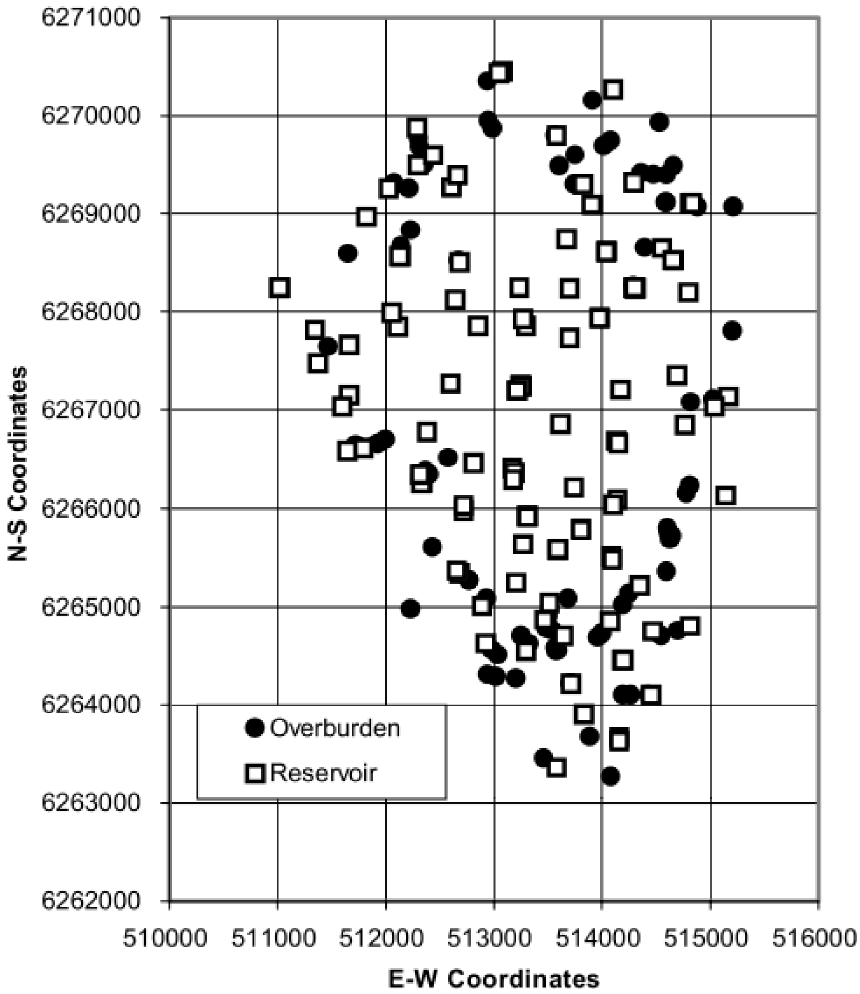


*Source: Bruno (2001)*

Figure 3.30  Distribution of wells damaged in overburden and within the reservoir at Ekofisk

**Shearing at top of production interval.** The second critical casing damage mechanism is localised shear damage near the top of the producing interval (Bruno 2001). This type of damage appears to be the result of a combination of vertical movement of the underlying compacting reservoir and differential lateral contraction and interface slip of the producing reservoir relative to the capping shale. The producing reservoir formations are typically more permeable and soft than the capping shales. The contrast in pressure change and stiffness leads to differential lateral expansion and interface slip. This form of damage is most dominant for relatively shallow reservoirs. For deviated wells, shear damage at the top of the producing interval can be exacerbated by vertical compaction of the producing formation, which can add additional local casing compression or bending (Yadav et al. 2003). This type of well failure is more often associated with injection/water flooding operations.

**Compression and buckling damage with production interval.** The third critical casing damage mechanism is axial compression and buckling within the producing interval (Bruno 2001). This may be caused by vertical deformation. A typical cement and casing completion is illustrated in Figure 3.31. As the reservoir formation compacts as a result of pore pressure reduction, loads are transferred from the formation rock to the cement and finally to the casing. The well casing may fail due to compressive yielding or buckling. The cement sheath may also be damaged from high shear and compressive stresses.

The most likely location for casing compression failure is near the centre of the reservoir where the vertical compaction strain is largest. If no slip occurs between the formation and the cement sheath and between the cement sheath and casing, the compacting reservoir pulls the cemented casing along with it, and may cause compression failure of the casing.

Casing instability or buckling may occur if the axial load becomes large and the reservoir formation provides insufficient lateral restraint. The formation lateral restraint could be lost or reduced if a large vertical section of the casing is very poorly cemented, or cavities surrounding the well develop due to sand/solid production.

Axial buckling is most severe in vertical wells. Observations of this type have been noted most clearly at Ekofisk, Belrdige, Lost Hills and Valhall, and in several Gulf of Mexico formations (Bruno 2001).

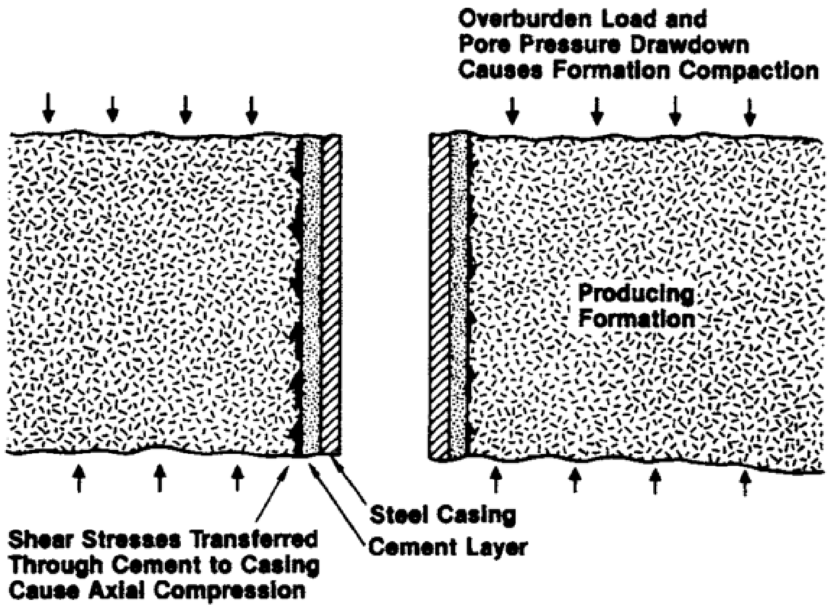


*Source: Bruno (1992)*[27]

Figure 3.31 Typical well completion subject to formation compaction

**Tensile failure above the reservoir.** The compaction of reservoir may result in tensile stresses above the reservoir, which may cause tensile failure of the casing above the reservoir.

Tensile stress and casing stretching above a compacting reservoir have been observed in a number of numerical modelling and time-lapse seismic studies (Kristiansen et al. 2005; Sayer et al. 2006; Hatchell et al. 2003; Furui et al. 2012; Doornhof et al. 2006). Figure 3.32 shows overburden stretch in the Valhall field. Vertical seismic profiles (VSP) were acquired in the two wells 60 m apart in the field in 1982 and 1993, respectively. One-way travel times obtained from the earlier VSP were subtracted from similar measurements from the later VSP, as shown in the right of Figure 3.32. The increasing travel time is thought to be caused by a stretching in the overburden. Furthermore, both the wells were equipped with radioactive markers to monitor formation strain. The results from one of the wells (right insert, Figure 3.32) show that stretching continues from 1993 through to 2002. A loosely coupled

[27] Copyright 1999, SPE. Reproduced with permission of SPE, further reproduction prohibited without permission.

geomechanical model that was run for the period from 1992 to 2002 confirmed this behaviour (left insert, Figure 3.32).

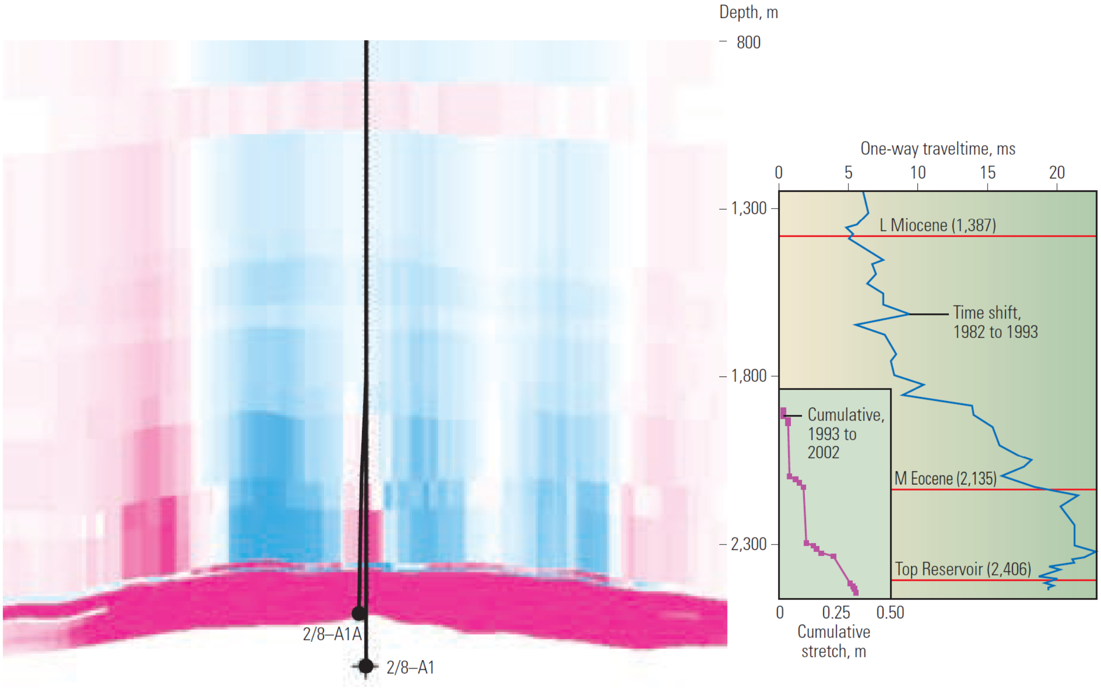


*Source: Doornhof et al. (2006), Copyright Schlumberger, with permission.*

Figure 3.32 Overburden stretch in the Valhall field – time-lapse VSP and radioactive markers measurements (right) and results from a loosely coupled geomechanical model (left)

It should be reiterated that while the critical forms of casing damage due to reservoir compaction and subsidence for conventional oil and gas wells discussed in this section provide valuable learning, their direct relevance to coal seam gas wells in Australia is questionable, due to the differing geological settings and the production processes in extracting coal seam gas in Australia.

## 3.5 Evaluation technologies for zonal isolation

A cement sheath placed between the casing and wellbore is expected to provide zonal isolation throughout and beyond the life of a well. This, however, depends on the proper placement of the cement, the mechanical behaviour of the cement and the stress, and the pressure and temperature conditions in the wellbore. During the life of the well, stress variations are imposed on the casing, cement sheath and formation by various operations inside the well, such as pressure integrity tests, mud weight fluctuation, casing perforation and stimulation, production and shut-in. Any of these operations can damage the cement sheath and its bond with the casing and formation, compromising well integrity.

Since cement hydration is an exothermic reaction (Bellabarba et al. 2008), historically, temperature logs have been used to identify cement tops from heat anomalies generated by cement curing. However, this method reveals little else, in particular, the quality and integrity of the cement sheath.

Hydraulic testing, a common test of zonal isolation, applies internal pressure along the entire casing string. But the pressure inside the casing during the test can expand the casing, causing the cement sheath to experience tensile failure. This may lead to radial cracks and local de-bonding of the cement and casing in areas where the cracks are near the casing wall.

Because of the limitations of the other techniques, acoustic logging has become the industry's tool of choice for detecting cement behind casing and assessing the quality of the bonds between casing, cement and formation (Bellabarba et al. 2008). The state of the art in cement evaluation involves a combination of acoustic cement bond log (CBL), variable density log (VDL), ultrasonic and flexural wave logs.

### 3.5.1 Cement bond log (CBL)

The cement bond log (CBL) has been around since the 1960s (Grosmangin et al. 1962). It is based on the principle that a sonic signal transmitted through a casing unsupported by cement will ring strongly and the waveform will attenuate slowly; while that same signal will ring weakly and attenuate quickly when transmitted through a well casing supported by cement. The measurement is omni-directional, responding to the average of contributions from around the circumference of the casing, and is made at a relatively low frequency of 10.20 kHz (kilohertz) at a transmitter-to-receiver spacing of 0.3 to 1 m. The measurement is normally accompanied by a variable density log (VDL) that is made at a longer transmitter-to-receiver spacing (1.5 m). This VDL may also yield an indication of cement bond to the formation. The cement bond logs (CBLs) and variable density logs (VDLs) are acquired using a sonic logging tool (Figure 3.33). Measurements are displayed on the CBL log in millivolts (mV) or decibel (dB) attenuation, or both. Increased attenuation indicates better quality bonding of the cement to the outer casing wall. In simple cases, the interpreted log response can provide good information about cement quality.

The CBL logging is still used today for cement evaluation, either independently or in combination with an ultrasonic measurement. The measurement responds well to solidity, works well in most fluids in the hole, is unaffected by internal casing condition and provides an indication of cement-formation bond. Latest generation tools also include mapping features that can indicate broad channels in the cement sheath.

The CBL is sensitive to fast formations (i.e. formation with fast sonic velocity), and extremely sensitive to both eccentricity of the casing (called eccentering) and a liquid microannulus. The omni-directional nature of the measurement and the low frequency at which it is taken render the standard CBL ineffective in identifying channels or contaminated cements. Furthermore, the old generations of CBL-VDL logs do not have the capacity to evaluate the casing integrity; also they are greatly affected by heavy mud and thick casing, which in combination significantly attenuate the sonic signals used for cement quality measurement (Tian et al. 2011).

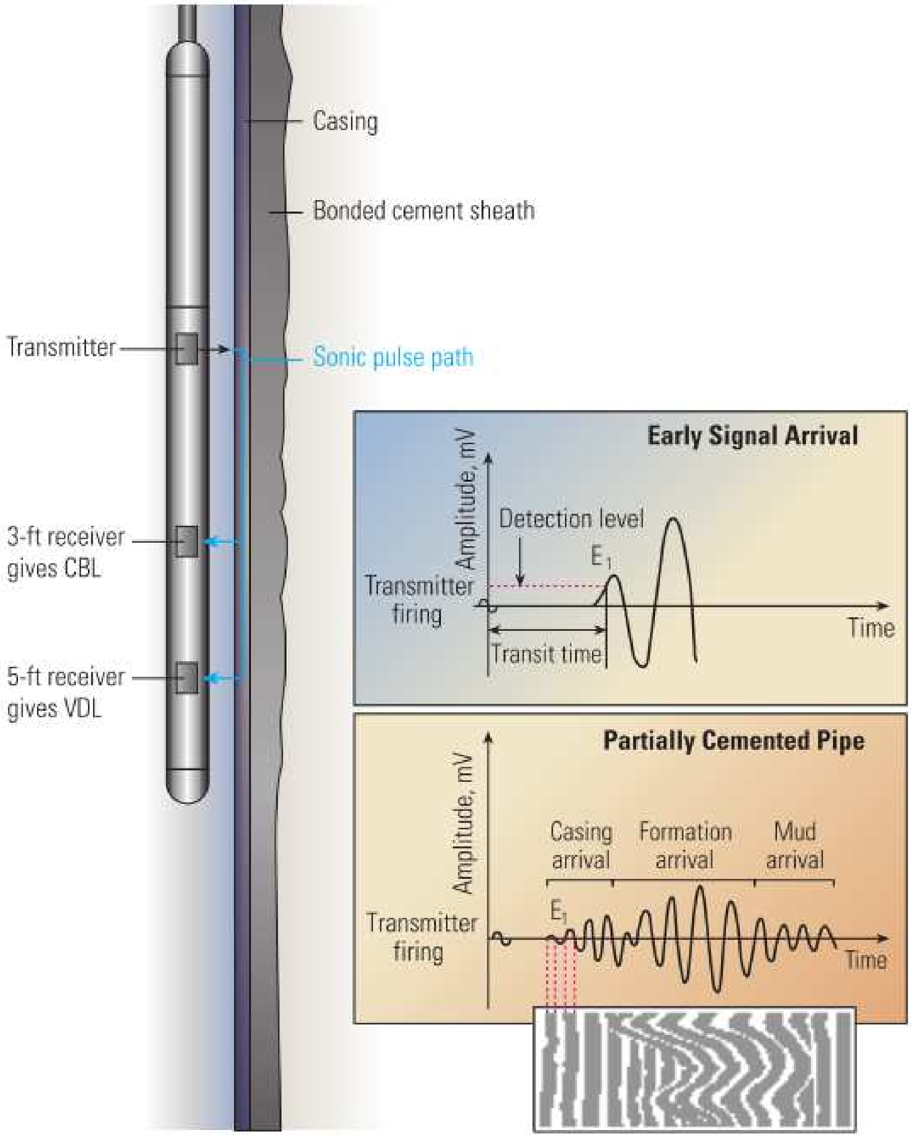


*Source: Bellabarba et al. (2008), Copyright Schlumberger, with permission*

Figure 3.33 Sonic CBL measurement fundamentals

### 3.5.2 Ultrasonic imaging (USI)

To address the CBL weaknesses to evaluate cement quality azimuthally, the cased hole ultrasonic imaging (USI) tool was developed using a high-frequency pulse-echo technique, (Herold et al. 2006; Morris et al. 2007; Sheives et al. 1986). A single rotating transducer is used and rotated at high speed (7+ rev/s), and operates at high frequencies of between 200 and 700 kHz depending on casing thickness. The tool evaluates cement around the entire circumference of the casing at a resolution of 30 mm, and provides the added benefit of corrosion and wear information on the casing.

The basics of the USI tool are given in Figure 3.34. The rotating transducer sends an acoustic wave generated by a transducer toward the casing to excite the casing into its thickness resonance mode. The tool scans the casing at 7.5 revolutions per second to render an azimuthal resolution of five or 10 degrees. This yields 36 or 72 separate waveforms at each depth. These are processed to yield the casing thickness, internal radius and inner wall smoothness as well as an azimuthal image of the cement acoustic impedance (essentially the quality of the cement sheath). A good casing cement bond results in immediate resonance decay, while free pipe rings (generates echoes) for an extended period.

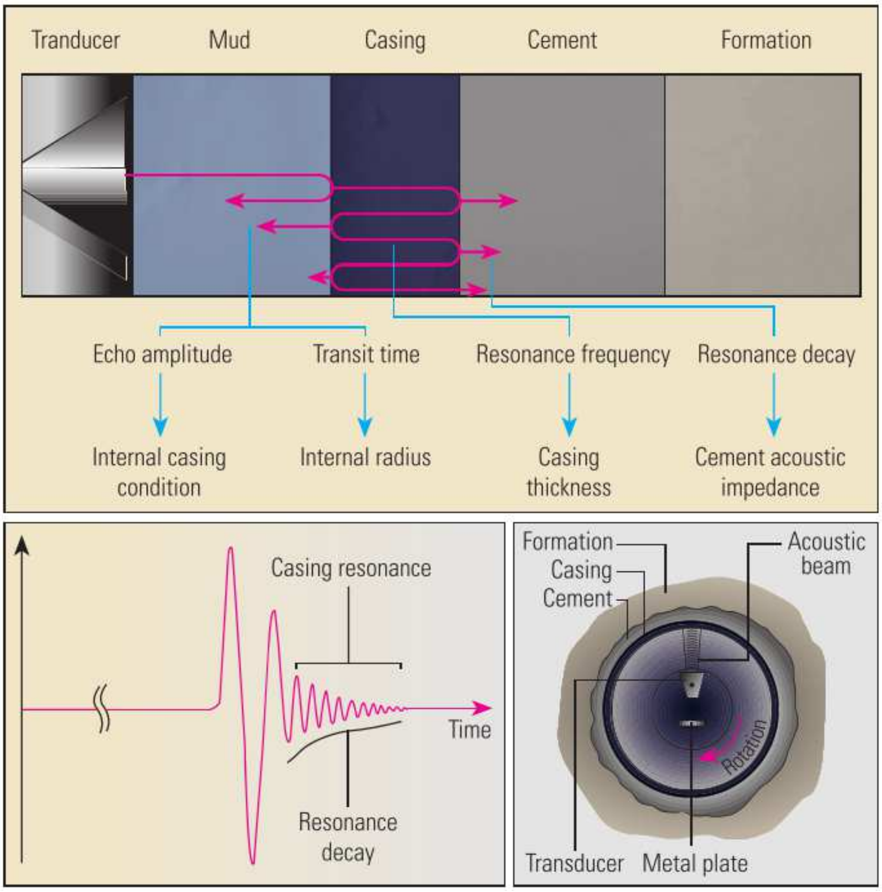


*Source: Bellabarba et al. (2008), Copyright Schlumberger, with permission*

Figure 3.34 Ultrasonic tool basics

The tool provides four main measurements:

- the initial echo amplitude provides an indication of the condition of the internal surface of the casing. A smooth surface will yield high amplitudes when well-centred. Low amplitudes are caused by a rough internal surface and / or eccentering of the tool
- through the knowledge of the mud velocity, the transit time for the first amplitude is converted into an internal radius measurement
- operating the transducer at the casing resonance frequency allows the casing thickness to be measured
- the decay rate of the signal determines the acoustic impedance of the material immediately behind the casing. Acoustic impedance is defined as the product of density and compressional velocity.

While the USI tool addresses the problem of azimuthal coverage, it is susceptible to certain conditions encountered when making the measurement:

- signal to noise ratio reduces with increasing mud weight to the point that a signal cannot be acquired in certain heavy muds. The radial probing power is limited to the cement region adjacent to the casing (Van Kuijk et al. 2005)

- thick casings reduce the operating frequency of the transducer to the point that the frequency falls out of the measuring range of the transducer
- the pulse-echo technique adopted by the USI tool has difficulty in differentiating between a drilling fluid and a lightweight or mud-contaminated cement of similar acoustic impedance. Even under favourable conditions, the acoustic impedance contrast between drilling fluid and cement typically must be larger than 0.5 Mrayl ($10^6$ kg/sm$^2$) for the pulse-echo technique to distinguish between them.

### 3.5.3 Isolation scanner

The isolation scanner addresses the main shortcoming of the USI tool (i.e. the ability to accurately identify low-density cements and contaminated cements). Low-density cements are used to cement casings in formations with low fracture gradients or loss zones, such as deep-water wells and coal seam gas wells (Tan et al. 2012). The acoustic impedance of lightweight and contaminated cements extends into the range of the acoustic impedances common for drilling and completion fluids which may be present in the annulus behind the casing (Table 3.3). The isolation scanner tool combines the classic pulse-echo technique that is used in the USI tool with the latest flexural wave imaging technology to accurately evaluate any type of cement in the annulus.

Table 3.3 Typical annulus material properties

| Material | Density [kg/m$^3$] | Acoustic impedance [Mrayl] |
|---|---|---|
| Gas | 1.3–130 | 0.0004–0.04 |
| Water | 1000 | 1.5 |
| Drilling mud | 1000–2000 | 1.5–3.0 |
| Slurry | 1000–2000 | 1.8–3.0 |
| Light weight cement | 1000–1400 | 2–5 |
| Class G cement | 1900 | 5.0–7.0 |

*Source: Tian et al. (2011)*[28]

The Isolation Scanner maintains the measurement provided by the USI tool (A in Figure 3.35), while adding flexural-wave imaging with one transmitter (B) and two receivers (C) aligned obliquely. The B transducer transmits a high-frequency pulse beam of about 250 kHz to excite a flexural mode in the casing (D). As the wave propagates, this mode radiates acoustic energy into the annulus. This energy reflects at interfaces that present an acoustic contrast, such as the cement/formation interface, and propagates back through the casing predominantly as a flexural wave to reradiate energy into the casing fluid. The two receiving transducers are placed to allow optimal acquisition of these signals. Processing of the signals provides information about the nature and acoustic velocity of the material filling the annulus, the position of the casing in the hole and the geometrical shape of the hole, and information on the third interface (cement/formation).

[28] Copyright 2011, SPE. Reproduced with permission of SPE, further reproduction prohibited without permission.

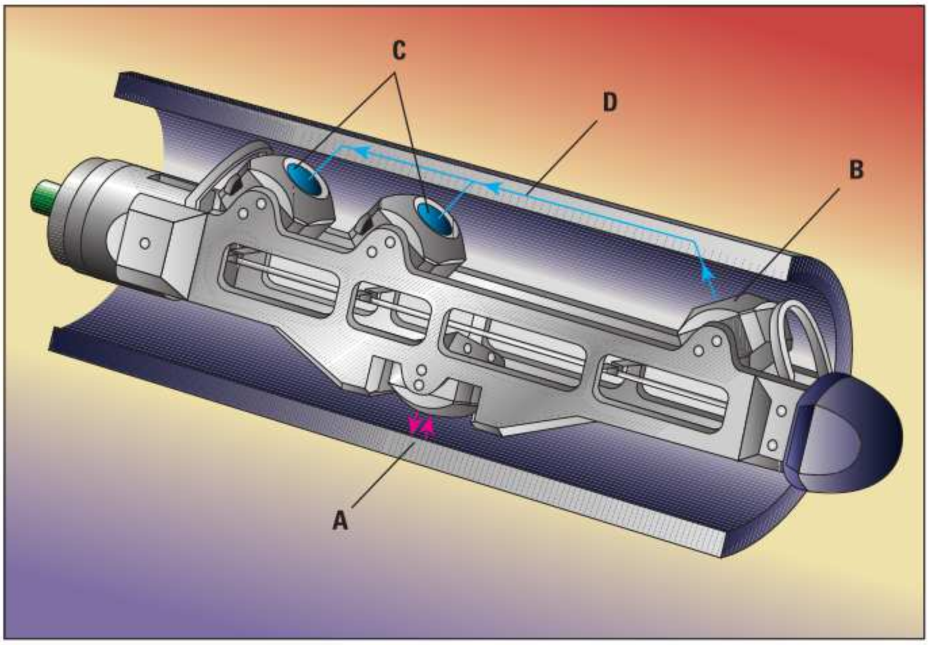


*Source: Bellabarba et al. (2008), Copyright Schlumberger, with permission*

Figure 3.35 Schematic view of an isolation scanner

The output of the isolation scanner log is a solid-liquid-gas (SLG) map displaying the most likely material state behind the casing. The material state is obtained for each azimuth by locating the two measurements on a crossplot of flexural attenuation and acoustic impedance for a given cement (Figure 3.36).

Figure 3. shows an example of isolation scanner and CBL-VDL measurements (Bellabarba et al. 2008). The 9 $^{5}/_{8}$ inch (244.5 mm) casing was cemented in a 12¼ inch (311.1 mm) hole using the low-density LiteCRETE slurry system. The CBL (Track 1) and VDL (Track 2) show a nearly free-pipe response with strong casing arrivals in the VDL and high CBL amplitude. The pulse-echo impedance map (Track 5) shows fluid with patches of solid. Obtaining an adequate interpretation from both measurements was made difficult by the low-impedance LiteCRETE cement. The flexural-wave attenuation map (Track 4), on the other hand, provides a correct diagnosis of the solid behind casing. It also reveals the existence of a fluid-filled channel between X,465 and X,485 m. The solid-liquid-gas (SLG) map (Track 3) supports and simplifies this information. The azimuthal and axial extent of the channel is reported in Tracks 6 and 7.

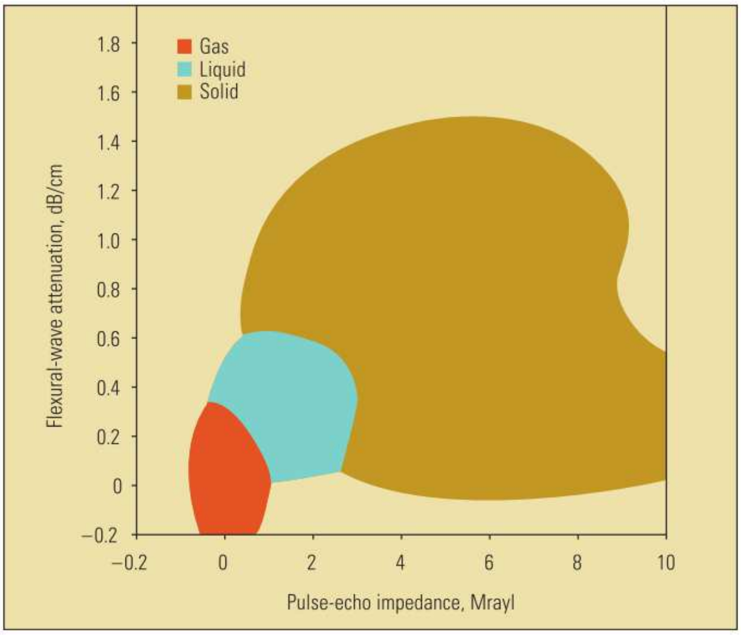


*Source: Bellabarba et al. (2008), Copyright Schlumberger, with permission*

Figure 3.36 Solid-liquid-gas mapping of the measurement plane for a Class G cement

Different cement evaluation techniques are available, such as CBL, USI, etc. The Isolation Scanner integrates the conventional pulse-echo technique (USI) with flexural wave propagation to fully characterise the cased well annular environment while evaluating the casing condition. It is able to differentiate high-performance lightweight cements from liquids, and map annulus material as solid, liquid, or gas. Table 3.4 summarises measurements and limitations of the different cement evaluation techniques.

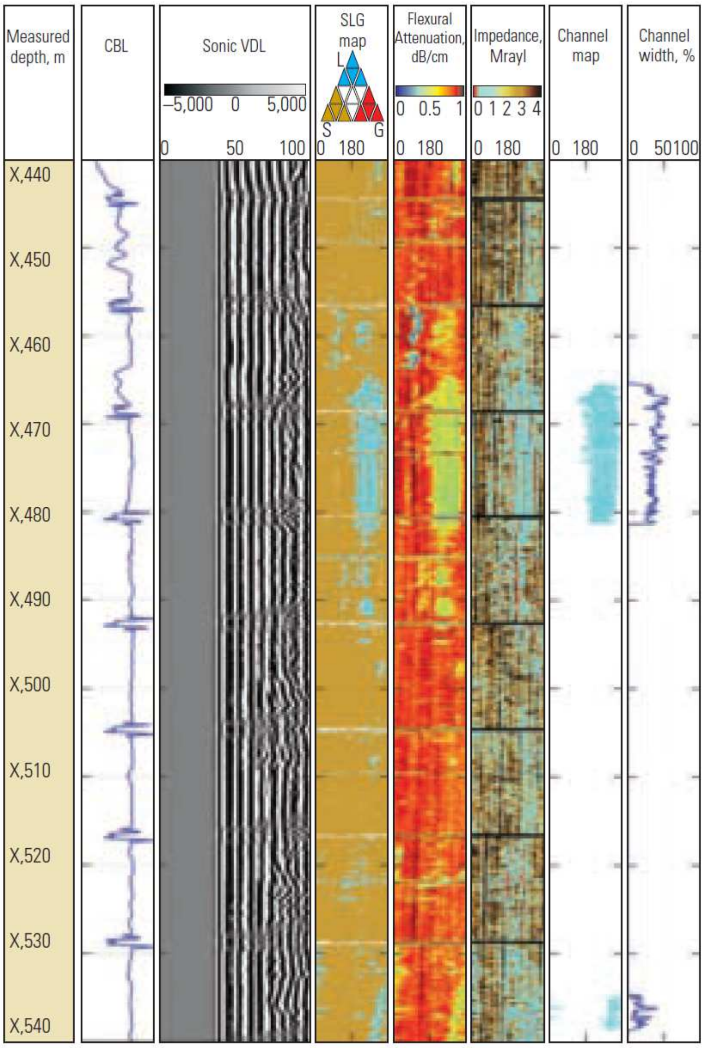


*Source: Bellabarba et al. (2008), Copyright Schlumberger, with permission*

Figure 3.37 Example of an isolation scanner and CBL-VDL measurements inside a casing cemented using the low-density (low impedance) LiteCRETE slurry system

Table 3.4 Summary of measurements and limitations of cement evaluation techniques

| **Cement evaluation technique** | **Measurements** | **Limitations** |
|---|---|---|
| CBL-VDL | Bonding quality of the cement to casing; indication of cement bond to formation; and information on cement quality in simple cases | Sensitive to fast formation and both casing eccentering and liquid microannulus; affected by heavy mud and thick casing; ineffective in identifying channels or contaminated cements |
| Ultrasonic imaging | Azimuth measurements on casing internal surface condition, casing thickness; and acoustic impedance of the material immediately behind the casing | Signal to noise ratio reduces with increase in mud weight; work poorly in evaluating cement quality behind thick casing; difficult to differentiate between drilling fluid and a lightweight or mud-contaminated |

| Cement evaluation technique | Measurements | Limitations |
|---|---|---|
| | | cement of similar acoustic impedance |
| Isolation scanner | Accurately identify material states behind casing – differentiating lightweight/contaminated cements and drilling fluids; evaluating casing conditions; information on cement bond to formation | Currently arguably most comprehensive cement evaluation technique |

## 3.6 Well abandonment

Coal seam gas well abandonment is undertaken to ensure the environmentally sound and safe isolation of the well, protection of groundwater resources, isolation of the productive formations from other formations, and the proper removal of surface equipment. This involves sealing the hole completely from the base to the surface using a series of cement plugs, which provide a seal preventing any cross flow of water and gases (APPEA 2012). To reduce the cost of filling the entire well with cement, a series of cement plugs are placed over the target aquifers to seal the well. The well head is then removed and the steel casing (filled with cement) is cut off at least 1.5 m below ground level, sealed with a metal identification plate and buried (APPEA 2012). The cement used in well construction and abandonment is designed to have a long life span.

Risk of leakage through abandoned wells is a function of the rules and regulations that apply to drilling and abandonment and as enforced at the time of well plugging. The quality of the abandonment operation and the materials used in sealing the well are important factors (Nicot 2009). As rules, regulations and requirements evolve with time, there is a high probability that wells abandoned after more stringent abandonment regulations were introduced are properly plugged (Watson and Bachu 2009). However, inadequate bonding has been detected at the interface between cement and formation/casing by bond logs and other tools (Nicot 2009). In this case, the quality of execution of the plugging operation was considered to be more of a problem than the quality of the materials used. Watson and Bachu (2009) ascribed the abandonment practice as one of the key factors that could potentially result in well leakage.

## 3.7 Remediation technologies

Once the cause for a loss of well integrity is identified, suitable technology is used for remediation. Squeeze cementing, liquid sealant, swelling elastomer and expandable tubular casing patch are some of the remediation technologies for well integrity.

Squeeze cementing, defined as the process of forcing a cement slurry under pressure through perforation holes or cut slots into the casing/wellbore annular space, has long been a common operation (Marca 1990). When the slurry is forced against a permeable formation, the solid particles filter out on the formation face as the aqueous phase (cement filtrate) enters the formation matrix. A properly designed squeeze job causes the resulting cement filter cake to fill the opening(s) between the formation and the casing. Upon curing, the cake forms a nearly impenetrable solid (Suman and Ellis 1977). Squeeze cementing has been applied to repair failed primary cement jobs (due to the mud channelling or insufficient cement height in the annulus) and casing leaks due to corroded or split casing pipe (Cirer et al. 2012; Milanovic and Smith 2005).

While many casing leaks have been repaired successfully in this manner, the casing leak sometimes is so restrictive to fluid injection that it does not lend itself to repair by conventional squeezing methods. This type of casing leak may be too small to allow penetration of cement particles and, in many cases, requires several cementing operations for successful repair. Even worse, many of these tight leaks cannot be repaired and result in well abandonment. In response to this problem, small particle size cement was developed (Meek et al. 1993). Whilst the conventional Portland Class G has a maximum and average particle size of 90 and 21 microns (µm), respectively, the small particle size cement has maximum and average particle size of 15 µm and 5 µm, respectively. The small particle size cement allows for far tighter leaks to be repaired.

Squeeze cementing to repair corroded casing often requires multiple squeeze operations, provides a temporary fix and does not address the cause of corrosion leaks. A technology using expandable tubulars was developed in early 2000s for entire casing interval repair (Braddick and Jordan 2005; Daigle et al. 2000; Innes et al. 2003; Siemers et al. 2003; Storaune and Winters 2005; Wright et al. 2003). The technology has the potential to provide a first-time effective repair of the entire casing interval that is subject to corrosion. In comparison with squeeze cementing, the expandable technology is cost competitive with a reliable pressure seal and longevity of repair achieved.

The expandable casing repair technology needs a workover rig to be used since the tubing needs to be removed from the well. Pressure activated sealant technology can repair small casing leaks without removing the tubing and requiring a workover rig. This technology is used in both injection and production wells (Chivvis et al. 2009; Johns et al. 2006). The pressure activated sealant is unique in that a differential pressure causes the liquid sealant to polymerise into a flexible solid which can plug a leak. The liquid sealant only polymerises at the point of differential pressure which can be created by a pressure drop through a leak. As the polymerisation reaction proceeds, the hardened sealant plates-out on edges of the leak to gradually seal it off. The resulting seal is a flexible plug across the leak site. Both oil-based and water-based pressure activated sealants are employed depending on the fluids in the system and the temperature and pressure conditions. By adjusting the specific gravity and viscosity of the sealant, a procedure is developed to place the sealant exactly at the leak site. Once positioned, the pressure differential across the leak can be manipulated to activate the sealant to solidify and plug the leak. Excess sealant that is not exposed to the pressure differential will remain in the fluid state. It can be left in the well or flushed from the well if desired.

## 3.8 Conclusions

The wellbore provides a possible pathway along which fluids can move between zones in a coal seam gas well or from the subsurface to the surface. Application of correct drilling and completion practice effectively limits the risk of such fluid movement. Data from overseas indicate that well integrity may be a general problem, reinforcing the idea that the wellbore is the main potential leakage pathway between the reservoir and the surface.

Characterisation of the stress and rock properties is required as part of the well design process. The drilling operation and drilling fluids used can then be designed to limit the risk of lost fluids or wellbore breakout.

Casing cementing operations must be designed to account for oversized and damaged sections of the wellbore to ensure removal of drilling fluids during cement displacement. The integrity of the cement and casing sheath can be verified by geophysical logging tools. Remediation of poorly cemented sections can be carried out.

Plugging and abandonment procedures must be designed and carried out using good engineering practice. Pre-existing wells and wellbores that have not been plugged correctly pose a risk for vertical fluid movement and gas venting at the surface.

# 4 Critical review of US EPA coal seam gas risk assessments

The US EPA has recently conducted two major studies of the US coal seam gas industry that are relevant to this report. The most recent of these, published in 2010 (US EPA 2010) provides an overview of methods of coal seam gas extraction and impacts, focusing in particular on surface water and aquatic environments. As such, produced water and the impacts related to improper surface handling comprise the main features. Hydraulic fracturing-derived potential impacts are difficult to delineate from this report.

On the other hand, the US EPA published a report in 2004 that specifically addresses impacts to underground sources of drinking water (USDWs) by coal seam gas-related hydraulic fracturing activities (US EPA 2004). The main conclusion of this report is that:

> *'…injection of hydraulic fracturing fluids into CBM [CSG] wells poses little or no threat to USDWs…'* (US EPA 2004: ES.16).

Table 4.1 and Table 4.2 present a summary of the relevant coal seam gas-producing basins, the citizen reports, and investigation outcomes. In examining the US EPA findings, we note the following major conclusions drawn by the report.

- Increased coal seam gas production activity, not necessarily unfavourable geology, was associated with an increase in complaints.
- Water loss from drinking water wells is perhaps the most common complaint. However, wells dry up in these regions for a variety of reasons, and only in the Powder River Basin, where coal seam gas activities occupy the same aquifer and have caused up to 60 m drawdown, is there a likely direct connection.
- Complaints of contamination occur at a relatively high rate in areas with historically high methane/hydrogen sulfide ($H_2S$) in the water and in areas with high iron content in the water that sustains iron-reducing bacterial activity, i.e. in many (if not the vast majority of) cases, naturally occurring degradation of water quality is blamed on the local coal seam gas activities.
- Best practice well completion and remediation of old wells can reduce methane contamination rates of water wells.
- In the few cases of soap contamination (possibly from escaped drilling fluid), increases in sediment/milky appearance, and increased petroleum odour in the water are, in fact, contamination associated with coal seam gas activities (though not necessarily hydraulic fracturing itself). The overall rate of industry contamination is still approximately only one water well per 1000 coal seam gas wells that are drilled.

We conclude that the experience of the US coal seam gas industry demonstrates that for US conditions, even based on 1990 to 2000 best practice, the rate of water well contamination is very low with at least 99.9 per cent of coal seam gas wells being constructed, stimulated and produced without contamination of any local water wells. However, public perception may well be that the impact is far greater, especially in areas that are prone to drought and / or demand related water loss in wells or that have historically high levels of methane, hydrogen sulfide ($H_2S$), and / or iron-reducing bacteria in the groundwater.

WORKING DRAFT
DO NOT DISTRIBUTE OR CITE

Table 4.1 Summary of 4 largest-producing coal seam gas basins in the US

| | San Juan Basin | Black Warrior Basin | Powder River Basin | Central Appalachian Basin |
|---|---|---|---|---|
| **Number of wells in operation (ca. year 2000)** | 2550 (all vertical and typically hydraulically fractured) | >5800 (98% vertical most of which are hydraulically fractured, horizontal wells are related to mines and not typically hydraulically fractured) | 4270 (rapid growth to more than 8000 by year 2001 with average lifetime production of 300-400 Mcf/well) | Not reported |
| **Production (year 2000)** | 925 Bcf/y<br>(26.2 billion $m^3$/y) | 112 Bcf/y<br>(3.2 billion $m^3$/y) | 147 Bcf/y<br>(4.2 billion $m^3$/y) | 53 Bcf/y<br>(1.5 billion $m^3$/y) |
| **Size** | 7500 $mi^2$<br>(20 billion $m^2$) | 23,000 $mi^2$<br>(60 billion $m^2$) | 25,800 $mi^2$<br>(67 billion $m^2$) | 23,000 $mi^2$<br>(60 billion $m^2$) |
| **Depth of wells** | 550-4000 ft (typically 2400 ft)<br>(170-1200 m typically 730 m) | 350-2500 ft<br>(100-760 m) | 450-6500 ft<br>(140-1700 m) | 500-2000 ft<br>(150-610 m) |
| **Separation from potable aquifer** | 1100 feet (335 m) of shale in the basin's interior, although in some places there is no separation. | None (Pottsville formation is main CSG zone and it is also an unconfined aquifer that satisfies drinking water standards in some areas) | None (many water wells screened in same formation as CSG production – including Gillette, WY municipal water wells) | None (depending on location within the basin), although most water wells are 50-300 ft (15-90 m) deep |
| **Hydraulic fracturing methods** | Slick water, gel, and foam fracture target, relatively thick (20.80 ft or 6.25m) coal beds | Multiple stimulations per well to target thin (a few feet) coal beds, often using limited entry methods and re-fracturing after a few years. About 75% of wells use gel and the rest water or slick water. There is no fracture barrier so hydraulic fractures often experience significant height growth with ~80% of fractures penetrating the | Not widely used because it increases connection with aquifer and increases water production and coal is relatively high permeability without hydraulic fracturing | Foam and water hydraulic fractures target thin (a few feet) coal beds.<br>State of Virginia implemented a voluntary program in which hydraulic fracturing should only occur at 500 ft (150 m) below the deepest water well and the lowest topographic point within a 1500 ft (450 m) radius of the |

| | San Juan Basin | Black Warrior Basin | Powder River Basin | Central Appalachian Basin |
|---|---|---|---|---|
| | | overlying shale beds. T-shape growth is also common. | | extraction well.<br>Also, in the Virginia part of the basin, several weeks often elapse between fracturing injection and flowback due to the need to construct a pipeline system. |
| **Water loss incidents** | Reports of water loss, however these are from an area with typically 2000 ft (610 m) vertical separation between CSG and water wells and county officials qualify statements by saying that a variety of factors can lead to wells going dry in the area | | Gillette, Wyoming has experienced significant drawdown and reduction in water supply, but it is unclear how much of this is due to CSG activity and how much is due to increasing demands from growing population<br>Drawdown related to CSG activities ~200 ft (60 m) in some areas, leading to many complaints of wells drying up (note there are deeper aquifers available and gas companies have drilled new water wells in those layers for private individuals) | Approx. 50 complaints related to water loss.<br>One report claimed “several thousand wells” had “gone dry, overnight”. |
| **Contamination incidents** | Methane and hydrogen sulfide ($H_2S$) contamination estimated at 100s of wells. 34% of domestic wells were methane contaminated according to one study of more than 200 households.<br>Two accounts of appearance of grey sediment a day or two after hydraulic fracturing that | One report of milky white substance and strong odour shortly after hydraulic fracture (HF) event with increasing odour and coal fines contamination over next six months (LEAF v EPA case).<br>One individual reported visible petroleum and sediment contamination, claiming that her | “Some” reports of increased methane levels in drinking water | Approx. 20 complaints lodged related to water quality, including:<br>• “a few” cases of soap contamination (soap is used in the drilling fluid)<br>• a portion of 15-20 residents at a meeting in another area complaining of precipitates, soaps, diesel fuel smells, |

| | San Juan Basin | Black Warrior Basin | Powder River Basin | Central Appalachian Basin |
|---|---|---|---|---|
| | eventually dissipated. | neighbours' water also smelled of petroleum.<br>One individual reported methane contamination and unpleasant odour, which was confirmed by a private consultant. | | increased methane<br>• 'numerous' phone/email complaints including soapy water, diesel odours, iron and sulfur in wells, rashes from showering, gassy taste, murky water.<br>One report of a miner burned by a fluid, possibly HCl from HF activities that infiltrated a mineshaft. |
| **Investigation results** | Gas discharges at the surface, methane and hydrogen sulfide ($H_2S$) contamination, and related explosion incidents pre-date CSG production.<br>Two-thirds of wells tested as of 1998 showed biogenic methane that could not be from the Fruitland coal.<br>Mitigation of old, improperly abandoned wells decreased methane in 27% of wells sampled. | LEAF v EPA investigation concluded that there was no evidence that hydraulic fracturing had contributed to well contamination, but instead that historical records of water quality in the region include sudden onset of iron staining, methane contamination, and presence of foul odoured, white or red-brown, stringy or gelatinous material arising from natural activity of iron-reducing bacteria.<br>Case 2: EPA testing found no petroleum products in individual's well.<br>Case 3: Consistent with historic sudden onset of contamination due to natural processes in the aquifer. | None reported | All complaints investigated by state agency by testing for potential contaminants and comparing with baseline values.<br>Soap contamination acknowledged, but it persists for only a short time.<br>Regional drought conditions likely contributed to water loss. |
| **Conclusions** | Methane/hydrogen sulfide contamination is mainly | Only three cases of contamination reported in spite | Most complaints stem from CSG and water wells occupying | The state of Virginia concluded that none of the complaints |

| | San Juan Basin | Black Warrior Basin | Powder River Basin | Central Appalachian Basin |
|---|---|---|---|---|
| | naturally occurring.<br>Most of that which is not naturally occurring can be avoided through best-practice well completion.<br>Two accounts of grey sediment temporally associated with HF activities apparently not investigated. | of thousands of CSG wells.<br>None of these three cases is inconsistent with historical, natural behaviour of groundwater in the region nor have they been tied to CSG operations. | same aquifer so that drawdown (up to 200 ft or 60 m) causes wells to dry up.<br>Methane contamination occurs but does not seem to be as widespread (report does not mention historical methane contamination). | stemmed from CSG activities.<br>But acknowledged soap contamination does show that drilling fluids can escape to the aquifer. |

*Source: US EPA (2004), unless otherwise noted*

Table 4.2 Summary of producing US basins from which the EPA registered few or no resident complaints

| | **Piceance Basin** | **Uinta Basin** | **Northern Appalachian Basin** | **Western Interior Coal Region** | **Raton Basin** |
|---|---|---|---|---|---|
| **Number of wells in operation (ca. year 2000)** | Not reported | 1255 | Not reported | 377 | Not reported |
| **Production (year 2000)** | 1.2 Bcf/y (34 million $m^3$/y) | 76 Bcf/y (2.2 billion $m^3$/y) | 1.41 Bcf/y (40 million $m^3$/y) | 6.5 Bcf/y (185 million $m^3$/y) | 31 Bcf/y (880 million $m^3$/y) |
| **Size** | 7225 $mi^2$ (19 billion $m^3$) | 14 450 $mi^2$ (37 billion $m^3$) | 43 700 $mi^2$ (113 billion $m^3$) | 87 000 $mi^2$ (225 billion $m^3$) | 2200 $mi^2$ (6 billion $m^3$) |
| **Depth of wells** | Two-thirds of wells >5000 ft (1500 m), nearly all >4000 ft (1200 m) | 1200-4400 ft (370-1340 m) | Most <1000 ft (<300 m) | 600-3700 ft (180-1130 m) | 500-4100 ft (150-1250 m) (based on typical reported overburden thickness) |
| **Separation from potable aquifer** | At least 1500 ft (460 m) separation (water wells range from 500-2000 ft) (150-610 m) | Debateable, but there is perhaps a minimum of 1000 ft (300 m) separation from any producing aquifer since water supplies in this sparsely populated area are derived from surface sources or shallow alluvial aquifers | None, depending on location (water wells 50-400 ft) (15-120 m) | ~500 ft as of year 2000 production, but potential for no separation as region is developed (water wells typically 50-100 ft) (15-30 m) | None (but not clear if there are producing water wells in the CSG zones) |
| **Hydraulic fracturing methods** | 1500-3500 barrels (180-420 $m^3$) of water or cross-linked gel hydraulic fractures used to produce from deep, low permeability coals | Water, gel and foam fractures have all been tested. Not clear what comprises standard practice | Water, gel and foam fractures have all been tested. Not clear what comprises standard practice | Water, gel and foam fractures have all been tested. Not clear what comprises standard practice | Water and gel, often >100 000 barrels (12 000 $m^3$), but not clear if sustained because HF believed to increase water production |

| | **Piceance Basin** | **Uinta Basin** | **Northern Appalachian Basin** | **Western Interior Coal Region** | **Raton Basin** |
|---|---|---|---|---|---|
| **Water loss incidents** | None reported | None reported | None reported | None reported | None reported |
| **Contamination incidents** | None reported | None reported | None reported | None reported | None reported |

*Source: US EPA (2004), unless otherwise noted*

# 5 Discussion

Quite sophisticated numerical models exist and are widely used and generally accepted for design of hydraulic fractures that grow within the desired zone, to the desired length, and with the desired distribution of proppant. Many of these were developed more than 20 to 30 years ago, so there is a substantial history of applying the models to the design and history matching of fracture treatments. Understanding of the processes that affect hydraulic fracture growth continues to improve and models that include new effects are continually being developed. However, fracture modelling is classed as a data limited problem, which means the data required to completely model a given problem are not available. Data limited problems occur frequently in earth and biological sciences and require implementing an iterative method that involves measuring, modelling, and measuring again to continuously test a hypothesised behaviour and test the hypothesis itself with additional data (Starfield and Cundall 1988). In this context, current models are not able to satisfactorily account for three-dimensional growth and interaction of hydraulic fractures with natural fractures.

Better understanding of the processes listed below is fundamental to improving predictions of the growth rate, ultimate size and final shape of the hydraulic fracture and, hence, whether it is likely or unlikely to extend into an aquifer. The third item below provides a tool for making the calculations and predictions of fracture growth based on the understanding obtained from the first two items:

- laboratory and mine-through experiments to better understand the mechanisms that determine when a hydraulic fracture will grow through, as opposed to being arrested by, a natural fracture or lithological contact
- development of numerical models that account for the detailed mechanics of hydraulic fracture interaction with natural fractures
- development of three-dimensional hydraulic fracturing simulators, with a first step being growth on pre-defined planes such as in T-shaped hydraulic fractures. This could include devising efficient approaches that work on a coarse discretisation and avoid computationally costly re-meshing of the domain as the hydraulic fracture grows.

Similarly, there are decades of industry experience associated with monitoring hydraulic fracture growth, including hydraulic fractures in coal. Well-established approaches are able to provide information regarding the orientation, volume and extent of growth. However, microseismic and tiltmeter monitoring, in particular, are sufficiently costly that they are usually deployed only for the first few wells in an area, at most. Work to improve monitoring could focus on measuring fracture growth more accurately with existing monitoring methods and developing new methods that can be used routinely for every fracture treatment. This will provide quality assurance that fracture growth as designed does, in fact, occur during treatment. More specifically, it could be beneficial to:

- maximise the information that can be ascertained from microseismic and tiltmeter monitoring through analysis of microseismic source mechanisms and deploy efficient simulators to extract as much information as possible out of the inversion of tiltmeter data

- develop lower-cost diagnostics and monitoring methods that are able to rely on analysis of pressure records, which are always available, or inexpensive auxiliary equipment, such as a single geophone, for microseismic detection.

# 6 Conclusions

Hydraulic fracturing for coal seam gas production has a 40-year history, with more than 30 years of commercial experience in the US at a scale far exceeding the level to which the Australian coal seam gas industry has grown to date. There has been a commensurate development of numerical models and relevant experimental and field data, especially with respect to predicting height growth of fractures because this is an important consideration that determines the effectiveness of the treatment.

On the one hand, there are a number of commercial and research numerical simulators that are highly sophisticated and for which there is a long track record of use by the industry. On the other hand, even with this sophistication, numerical simulators do not yet handle the three-dimensional nature of hydraulic fracture growth nor do they completely reproduce the mechanics of hydraulic fracture interaction with natural fractures and lithological contacts. For coal seam gas, this limitation is particularly relevant when the hydraulic fracture grows not only vertically in the seam, but also with branches that grow with a horizontal orientation along the contact between the coal and roof/floor rock formations to produce a T-shaped geometry.

There is also a range of methods available for monitoring and diagnosis of hydraulic fracture growth. These include fracturing pressure analysis, injection testing and transient pressure analysis, tracers, microseismic monitoring and tiltmeter monitoring.

The present state of the art, therefore, typically entails using a planar, pseudo 3D numerical model to design a HF treatment to ensure appropriate containment, length growth, and proppant placement. Fracturing pressure analysis, usually including step-rate and mini-fracture tests and analysis, is always available. Other more costly monitoring is typically deployed early in the development of an area to better define the hydraulic fracture growth response in the new area. There are important, open research questions related to both the prediction and monitoring of hydraulic fracture growth. Nonetheless, the experience in North America suggests that the process of stimulation very rarely, if ever, impacts on groundwater. Impacts that have been attributed to hydraulic fracturing can equally be explained in terms of groundwater quality and supply issues that are historically common to a particular gas-producing region or can be attributed to well integrity problems. For example, methane entering a water well is known to occur in wells that are remote from any coal seam gas development and hydraulic fracturing activities (US EPA 2004).

There is evidence that poorly completed wells can lead to migration of contaminants, particularly methane. Like hydraulic fracturing, well completion technology has a long history. Best practice begins during the drilling process by ensuring the drilling fluid is appropriately designed to have the correct composition, density, and rheology so that breakout of the wellbore, which can lead to cementing difficulties, is minimised. Casing and cementing technology is also well-established, and historically wells that leak are often, if not invariably, the product of well construction or abandonment that does not meet current best practice standards.

# 7 References

Aadnoy, B.S, 2010. Modern Well Design, 2nd edition, CRC Press/Balkema, ISBN 978-0-415-88467-9.

Adachi, J.I., 2001. Fluid-driven fracture in permeable rock. PhD Thesis. University of Minnesota.

Adachi, J.I., Detournay, E., 2002. Self-similar solution of a plane-strain fracture driven by a power-law fluid. *International Journal for Numerical and Analytical Methods in Geomechanics* 26, 579–604.

Adachi, J.I., Siebrits, E., Peirce, A.P., Desroches, J., 2007. Computer simulation of hydraulic fractures. *International Journal of Rock Mechanics and Mining Sciences* 44, 739–757.

APPEA, 2012. Environment Protection and Biodiversity Conservation Amendment. Independent Expert Scientific Committee on Coal Seam Gas and Large Coal Mining Development Bill.

APPEA, no date. CSG well construction and bore specifications. Available from: www.appea.com.au/csg/about-csg/fact-sheets.html, Accessed on 30/10/2012.

Baltoiu, L., Warren, B., Natros, T., 2008. State-of-the-Art in Coalbed Methane Drilling Fluids. *SPE Drilling and Completion* 16-18.

Bannerman, M., Calvert, J., Griffin, T., 2005. New API practices for isolating potential flow zones during drilling and cementing operations, in: SPE Annual Technical Conference and Exhibition. Dallas, Texas, pp. 1–12.

Barenblatt, G.I., 1996. Scaling, self-similarity, and intermediate asymptotics: dimensional analysis and intermediate asymptotics, Vol. 14. ed. Cambridge University Press, Cambridge, United Kingdom.

Barree, R., Mukherjee, H., 1996. Determination of pressure dependent leak-off and its effect on fracture geometry, In: SPE Annual Technical Conference and Exhibition, Denver, p. 10.

Barree, R.D., 1983. A practical numerical simulator for three-dimensional fracture propagation in heterogeneous media, In: SPE Reservoir Simulation Symposium. Society of Petroleum Engineers, San Francisco, California, USA.

Barree, R.D., Conway, M.W., Gilbert, J.V., Woodroof, R.A., 2010. Evidence of Strong Fracture Height Containment Based on Complex Shear Failure and Formation Anisotropy, In: *Society of Petroleum Engineers Journal*. Florence, Italy, p. 134142.

Barree, R.D., Winterfeld, P.H., 1998. Effects of shear planes and interfacial slippage on fracture growth and treating pressures, in: SPE Annual Technical Conference and Exhibition. Society of Petroleum Engineers, New Orleans, Louisiana, USA.

Bazzari, J., 1989. Well Casing Leaks History and Corrosion Monitoring Study, Wafra Field. Middle East Oil Show.

Bellabarba, M., Bulte-Loyer, H., Froelich, B., Roy-Delage, S.L, van Kuijk, R., Gulliot, D., Moroni, N., Pastor, S., Zanchi, A., 2008. Ensuring Zonal Isolation Beyond the Life of the Well. *Oilfield Review*, 20(1), 18-31.

Bennett, L., Le Calvez, J., Sarver, D.R., Tanner, K., Birk, W.S., Waters, G., Drew, J., Michaud, G., Primiero, P., Eisner, L., Jones, R., Leslie, D., Williams, M.J., Govenlock, J., Klem, R.C., Tezuka, K., 2005. The Source for Hydraulic Fracture Characterization. *Oilfield Review* 17, 42-57.

Bennett, T., 2012. Innovation of coal seam gas well-construction process in Australia: lessons learned, successful practices, areas of improvement, In: IADC/SPE Asia Pacific Drilling Technology Conference and Exhibition. IADC/SPE 156930. Tianjin, China.

Beugelsdijk, L.J.L., De Pater, C.J., Sato, K., 2000. Experimental hydraulic fracture propagation in a multi-fractured medium, In: Proceedings of SPE Asia Pacific Conference on Integrated Modelling for Asset Management. *Society of Petroleum Engineers*, pp. 1-8.

Bonett, A., Pafitis, D., 1996. Getting to the root of gas migration. *Oilfield Review Spring*, 36-49.

Braddick, B., Jordan, G., 2005. Development and Testing of an Expandable Casing Patch System. *SPE/IADC Drilling Conference*, 1-4.

Brady, S.D., Drecq, P.P., Baker, K.C., Guillot, D., 1992. Recent technological advances help solve cement placement problems in the Gulf of Mexico, In: IADC/SPE Drilling Conference. New Orleans, LA, U.S.A.

Brondel, D., Edwards, R., Hayman, A., Hill, D., Semerad, T., 1994. Corrosion in the Oil Industry. *Oilfield Review* 4-18.

Bruno, M., 1992. Subsidence-induced well failure, In: SPE Drilling Engineering. Society of Petroleum Engineers, Ventura, California, USA.

Bruno, M., 2001. Geomechanical Analysis and Decision Analysis for Mitigating Compaction Related Casing Damage, In: SPE Annual Technical Conference and Exhibition. Society of Petroleum Engineers, New Orleans, Louisiana, USA.

Bunger, A.P., Detournay, E., Garagash, D.I., Clarkson, U., Peirce, A.P., 2007. Numerical Simulation of hydraulic fracturing in the viscosity-dominated regime, In: SPE Hydraulic Fracturing Technology Conference. Society of Petroleum Engineers, College Station, Texas, p. 11.

Bunger, A.P., Zhang, X., Jeffrey, R.G., 2012. Parameters Affecting the Interaction Among Closely Spaced Hydraulic Fractures. *SPE Journal* 292-306.

Celia, M., Bachu, S., Nordbotten, J.M., Gasda, S., Dahle, H., 2004. Quantitative estimation of $CO_2$ leakage from geological storage: analytical models, numerical models and data needs. *GHGT*-7 2–11.

Chen, Z.R., 2012. Finite element modelling of viscosity-dominated hydraulic fractures. *Journal of Petroleum Science and Engineering* 88-89, 136–144.

Chen, Z.R., Jeffrey, R.G., 2009. Tilt Monitoring of Hydraulic Fracture Preconditioning Treatments, In: 43rd US Rock Mechanics Symposium. American Rock Mechanics Association, Asheville, NC.

Cherny, S.G., Lapin, V.N., Chirkov, D.V., and van Reeuwijk, M. 2009. 2D Modeling of Hydraulic Fracture Initiating at a Wellbore with or without Microannulus. *SPE Hydraulic Fracturing Technology Conf*.

Chivvis, R., Julian, J., Cary, D., 2009. Pressure activated sealant economically repairs casing leaks on Prudhoe Bay Wells. SPE Western Regional Meeting.

Choi, S.O., Shin, J.J., 2001. Numerical modelling of hydraulic fracture propagation. Palo Alto, California: Stanford University.

Chuprakov, D., Melchaeva, O., Prioul, R., 2013. Hydraulic fracture propagation across a weak discontinuity controlled by fluid injection [in-press], In: Proceedings of International Conference for Effective and Sustainable Hydraulic Fracturing, 20.22 May 2013. Brisbane, Australia.

Cipolla, C.L., Wright, C.A., 2000. Diagnostic Techniques to Understand Hydraulic Fracturing: What? Why? and How?, In: *SPE/CERI Gas Technology Symposium*. Calgary, Alberta, Canada, pp. 1–13.

Cirer, D., Arze, E., Moggia, J., Soto, H., 2012. Practical Cementing Technique To Repair Severe Casing Damage. *SPE/ICoTA Coiled Tubing and Well Conference*, 27–28.

Clark, R.K., Scheuerman, R.F., Rath, H., Van Laar, H.G., 1976. Polyacrylamide/potassium-chloride mud for drilling water-sensitive shales, in: SPE Annual Technical Conference and Exhibition. Society of Petroleum Engineers, Dallas, Texas, USA, pp. 719–727.

Cleary, M., 1980. Comprehensive Design Formulae for Hydraulic Fracturing, In: Proceedings of SPE Annual Technical Conference and Exhibition. Society of Petroleum Engineers, Dallas, USA, p. 16.

Clifton, R.J., Abou-Sayed, A.S., 1981. A variational approach to the prediction of the three-dimensional geometry of hydraulic fractures, In: SPE/DOE Low Permeability Symposium. Denver, Colorado, USA, pp. 457–463.

Converse, G., Comninou, M., 1975. Dependence on the Elastic Constants of Surface Deformation Due to Faulting. Bulletin of the Seismological Society of America 65, 1173–1176.

Commonwealth of Australia, 2014a. Bore integrity, background review. Australian Government Department of the Environment, Canberra.

Commonwealth of Australia, 2014b. Monitoring and management of subsidence induced by coal seam gas extraction. Australian Government Department of the Environment, Canberra.

Cook, J., Edwards, S., 2009. Geomechanics, Chapter 5 in Advanced Drilling and Well Technology, E.Book. ed. Society of Petroleum Engineers.

Cook, J., Growcock, F., Guo, Q., Hodder, M., van Oort, E., 2012. Stabilising the wellbore to prevent lost circulation. *Oilfield Review*, 23(4), 26–35.

Cooke, M., Underwood, C.A., 2001. Fracture termination and step-over at bedding interfaces due to frictional slip and interface opening. *Journal of Structural Geology* 23, 223–238.

CSIRO (unpublished study) 2009. A study of predicted tilt response.

Cunnington, M., Hedger, L., 2010. Introduction of a new well design to the Narrabri coal seam gas project. SPE Asia Pacific Oil and Gas Conference and Exhibition October 2010.

Daigle, C., Campo, D., Naquin, C., 2000. Expandable tubulars: Field examples of application in well construction and remediation. SPE Annual Technical Conference and Exhibition.

Dale, B., 1996. Dinoflagellate cyst ecology: Modeling and geological applications. Palynology: Principles and Applications, Vol 3. American Association of Stratigraphic Palynologists Foundation.

Damjanac, B., Gil, I., Pierce, M., Sanchez, M., 2010. A New Approach to Hydraulic Fracturing Modeling in Naturally Fractured Reservoirs, in: 44th US Rock Mechanics Symposium. Salt Lake City, p. 7.

Daneshy, A., 2003. Off-balance growth: A new concept in hydraulic fracturing. *Journal of Petroleum Technology*, 55(4), 78–85.

Daneshy, A.A., 1973. On the design of vertical hydraulic fractures. Journal of Petroleum Technology, 25(1), 84–97.

Daneshy, A.A., 2009. Factors controlling the vertical growth of hydraulic fractures, In: SPE Hydraulic Fracturing Technology Conference. The Woodlands, Texas, USA, pp. 19–21.

Davis, P.M., 1983. Surface deformation associated with a dipping hydrofracture. *Journal of Geophysical Research,* 88, 5826.

De Pater, C.J., Cleary, M.P., Quinn, T.S., Barr, D.T., Johnson, D.E., Weijers, L., 1994. Experimental verification of dimensional analysis for hydraulic fracturing. SPE Production and Facilities, 9(4), 230–238.

De Pater, C.J., Deroches, J., Groenenboom, J. and Weijers, L., 1996. Physical and Numerical Modeling of Hydraulic Fracture Closure. *SPE Production and Facilities* (May): 122–128.

De Pater, C.J., Dong, Y., 2009. Fracture Containment in Soft Sands by Permeability or Strength Contrasts, In: SPE Hydraulic Fracturing Technology Conference. The Woodlands, Texas, pp. 19–21.

Decker, A., Horner, D., 1987. Source rock evaluation: a method of predicting dominant reservoir mechanisms of deeply buried, low-permeability coal reservoirs. Low Permeability Reservoirs Symposium.

Department of Employment Economic Development and Innovation, 2011. Code of practice for constructing and abandoning coal seam gas wells in Queensland.

Dershowitz, W.S., Cottrell, M.G., Lim, D.H., Doe, T.W., 2010. A Discrete Fracture Network Approach for Evaluation of Hydraulic Fracture Stimulation of Naturally Fractured Reservoirs, In: 44th US Rock Mechanics Symposium. American Rock Mechanics Association, Salt Lake City, Utah, USA.

Detournay, E., 2004. Propagation regimes of fluid-driven fractures in impermeable rocks, *International Journal of Geomechanics*, 4(1), 35–45.

Diamond, W.P., Oyler, D.C., 1987. Effects of stimulation treatments on coalbeds and surrounding strata, US Bureau of Mines, RI.

Doornhof, D., Kristiansen, T., Nagel, N.B., Pattillo, P.D., Sayers, C., 2006. Compaction and Subsidence. *Oilfield Review*, 18(3), 50-68.

Du, J., Olson, J.E., 2001. A poroelastic reservoir model for predicting subsidence and mapping subsurface pressure fronts. *Journal of Petroleum Science and Engineering*, 30(3), 181–197.

Du, J., Philip, Z., Warpinski, N.R., Mayerhofer, M., 2009. Surface Deformation-based Reservoir Monitoring in Inhomogeneous Media, In: 43rd US Rock Mechanics Symposium. Asheville, NC, p. 7.

Dusseault, M., Gray, M., Nawrocki, P., 2000. Why oilwells leak: cement behavior and long-term consequences, In: SPE Oil and Gas Conference and Exhibition. Beijing, China.

Dusseault, M.B., Bruno, M.S., Barrera, J., 2001. Casing Shear: causes, cases, cures, In: SPE International Oil and Gas Conference and Exhibition. Society of Petroleum Engineers, Beijing, China, pp. 98–107.

Dutta, N.C., 2012. Geopressure prediction using seismic data: Current status and the road ahead, *Geophysics*, 67(6) , 2012–2041.

Eaton, B., 1975. The Equation for Geopressure Prediction from Well Logs, In: Fall Meeting of the Society of Petroleum Engineers of AIME. Dallas Texas.

Economides, M.J., Nolte, K., 2000. Reservoir stimulation, Third. ed. John Wiley and Sons Ltd, West Sussex, England.

Elder, C., Deul, M., 1975. Hydraulic Stimulation Increases Degasification Rate of Coalbeds. Bureau of Mines.

Ely, J.W., Zbitowski, R.I., and Zuber, M.D. 1990. How to develop a coalbed methane prospect: a case study of an exploratory five-spot well pattern in the Warrior basin, Alabama. Proceedings of the 65th Annual Technical Conference, New Orleans, USA, pp. 487.496.

Energy Information Administration, 2011. Australia Energy Data, Statistics and Analysis.

Enever, J.R., Jeffrey, R.G., Casey, D.A., 2000. The relationship between stress in coal and rock, In: American Rock Mechanics Symposium. pp. 409–414.

Evans, K., 1983. On the Development of Shallow Hydraulic Fractures as Viewed Through the Surface Deformation Field  Part I Principles. *Journal of Petroleum Technology*, 35(2), 406–410.

Finkbeiner, T., Zoback, M. Flemings, P. and Stump, B., 2001. Stress, pore pressure, and dynamically constrained hydrocarbon columns in the South Eugene Island 330 Field, Northern Gulf of Mexico. *AAPG Bulletin*, 85(6), 1007-1031.

Fisher, M., Heinze, J., Harris, C., 2004. Optimizing horizontal completion techniques in the Barnett shale using microseismic fracture mapping. In: SPE Annual Technical Conference and Exhibition.

Flewelling SA and Sharma M 2014, ‘Constraints on upward migration of hydraulic fracturing fluid and brine’, *Groundwater,* 52(1), pp 9-19.

Fredrich, J.T., Argoello, J.G., Thorne, B.J., Wawersik, W.R., Deitrick, G.L., De Rouffignac, E.P., Myer, L.R., Bruno, M.S., 1996. Three-Dimensional Geomechanical Simulation of Reservoir Compaction and Implications for Well Failures in the Belridge Diatomite, In: SPE Annual Technical Conference and Exhibition. Denver, Colorado.

Fredrich, J.T., Fossum, A.F., Bruno, M.S., JF Hollad, F.H, 2001. One-way coupled reservoir – geomechanical modeling of the lost hills oil field, California, In: DC Rocks 2001. The 38th US symposium on Rock Mechanics (USRMS).

French, F.R, Mclean, M.R, 1993. Development drilling problems in high-pressure reservoirs. *Journal of Petroleum Technology*, 45(8), 772-777.

Fung, R.L., Vijayakumar, S., Cormack, D.E., 1987. Calculation of Vertical Fracture Containment in Layered Formations. *SPE Formation Evaluation*, 2(4), 518–522.

Furui, K., Fuh, G.F., Morita, N., 2012. Casing and screen failure analysis in highly compacting sandstone fields. In: SPE Annual Technical Conference and Exhibition. Society of Petroleum Engineers.

Gasda, S., Bachu, S., Celia, M., 2004. Spatial characterization of the location of potentially leaky wells penetrating a deep saline aquifer in a mature sedimentary basin. *Environ Geol* 46, 707–720.

Geertsma, J., 1973. Land subsidence above compacting oil and gas reservoirs. *Journal of Petroleum Technology*, 25(6), 734–744.

Geertsma, J., De Klerk, F., 1969. A rapid method of predicting width and extent of hydraulically induced fractures. *Journal of Petroleum Technology*, 21(12), 1571–1581.

Geoscience Australia, 2012. Australian Gas Resource Assessment.

Gidley, J.L., Holditch, S.A., Nierode, D.E., Veatch, R.W., 1989. Recent Advances in Hydraulic Fracturing. Society of Petroleum Engineers, Richardson, Texas, USA.

Goodwin, K., Crook, R., 1992. Cement sheath stress failure. *SPE Drilling Engineering,* 854, 291–296.

Grosmangin, M., Kokesh, F.P., Majani, P., 1962. A sonic method for analyzing the quality of cementation of borehole casings. *Journal of Petroleum Technology*, 13(2), 165-171.

Gu, H., Siebrits, E., 2008. Effect of Formation Modulus Contrast on Hydraulic Fracture Height Containment. *SPE Production and Operations,* 23, 170–176.

Gu, H., Siebrits, E., Sabourov, A., 2008. Hydraulic Fracture Modeling With Bedding Plane Interfacial Slip, In: SPE Eastern Regional/AAPG Eastern Regional Section Joint Meeting. Pittsburgh, Pennsylvania.

Gudmundsson, A., Brenner, S.L., 2001. How hydrofractures become arrested. *Terra Nova* 13, 456–462.

Haimson, B.C., Herrick, C.G., 1989. Borehole breakouts and in situ stress, In: 12th Annual Energy-Sources Technology Conference and Exhibition, Drilling Symposium. American Society of Mechanical Engineers, New York.

Halliburton, 2007. Coalbed methane: principles and practices, Halliburton, Available from: http://www.halliburton.com Accessed on 05-06-2013.

Han, Y., Damjanac, B., Nagel, N., 2012. A Microscopic Numerical System for Modeling Interaction between Natural Fractures and Hydraulic Fracturing, In: 46th US Rock Mechanics / Geomechanics Symposium. Chicago, p. 7.

Hatchell, P. J., van den Beukel, A., Molenaar, M. M., Maron, K. P., Kenter, C. J., Stammeijer, J. G. F., van den Velde, J. J. and Sayers, C. M. 2003. Whole earth 4D: monitoring geomechanics, In: 73rd SEG Meeting, Dallas, USA, Expanded abstracts, 1330-1333.

Helgeson, D.E., Aydin, a., 1991. Characteristics of joint propagation across layer interfaces in sedimentary rocks. *Journal of Structural Geology* 13, 897–911.

Herold, B., Marketz, F., Froelich, B., 2006. Evaluating expandable tubular zonal and swelling elastomer isolation using wireline ultrasonic measurements, In: IADC/SPE Asia Pacific Drilling Technology Conference and Exhibition.

Hilbert, L.B.J., Fredrich, J.T., Bruno, M.S., Deitrick, G.L., De Rouffignac, E.P., 1996. Two-dimensional nonlinear finite element analysis of well damage due to reservoir compaction, well-to-well interactions, and localization on weak layers, In: 2nd North American Rock Mechanics Symposium.

Holditch, S. a., Holcomb, D.L., Rahim, Z., 1993. Using Tracers To Evaluate Propped Fracture Width. *Proceedings of SPE Eastern Regional Meeting* 323–330.

Hower, J., Esligner, E. V., Hower, M. E., Perry, E. A. (1976). Mechanism of burial metamorphism of argillaceous sediment: 1, Mineralogical and chemical evidence, *Geological Society of America Bulletin*, 87(5), 725-737.

Huckabee, P., 2009. Optic fiber distributed temperature for fracture stimulation diagnostics and well performance evaluation, In: SPE Hydraulic Fracturing Technology Conference.

Huff, C., Merritt, J., 2003. Coal seam-well cementing in Northeastern Oklahoma. SPE Production and Operations Symposium.

Innes, G., Craig, J., Lavan, S., 2003. The use of expandable tubular technology to enhance reservoir management and maintain integrity. Offshore Technology Conference.

Jackson, P., Murphey, C., 1993. Effect of casing pressure on gas flow through a sheath of set cement. SPE/IADC Drilling Conference.

Jeffrey, R.G., Brynes, R., Lynch, P., Ling, D., 1992. An analysis of hydraulic fracture and mineback data for a treatment in the German creek coal seam, In: SPE Rocky Mountain Regional Meeting. Society of Petroleum Engineers, Casper, Wyoming.

Jeffrey, R.G., Bunger, A.P., 2007. A detailed comparison of experimental and numerical data on hydraulic fracture height growth through stress contrasts, In: Society of Petroleum Engineers Journal. College Station, Texas, pp. 1–14.

Jeffrey, R.G., Bunger, A.P., Lecampion, B., Zhang, X., Chen, Z.R., Van As, A., De Beer, A., Dudley, J.W., Siebrits, E., Thiercelin, M., Mainguy, M., 2009. Measuring hydraulic fracture growth in naturally fractured rock, In: SPE Annual Technical Conference and Exhibition. Society of Petroleum Engineers, New Orleans, Louisiana, pp. 1–18.

Jeffrey, R.G., Meaney, K.T.A.T.A., Doyle, R.P., 1999. History Matching Of Hydraulic Fracture and Production Data from a Vertical $CO_2$ and $CH_4$ Gas Drainage Test Well, In: The 1999 International Coalbed Methane Symposium. Tuscaloosa, Alabama.

Jeffrey, R.G., Settari, A., Smith, N.P., 1995. A Comparison of Hydraulic Fracture Field Experiments, Including Mineback Geometry Data, with Numerical Fracture Model Simulations, In: SPE Annual Technical Conference and Exhibition. Society of Petroleum Engineers, Dallas, Texas.

Jeffrey, R.G., Vlahovic, W., Doyle, R.P., Wood, J.H., 1998. Propped Fracture Geometry of Three Hydraulic Fractures in Sydney Basin Coal Seams, In: Proceedings of SPE Asia Pacific Oil and Gas Conference and Exhibition. Society of Petroleum Engineers, Perth, Western Australia, pp. 1–11.

Jeffrey, R.G., Settari, A., 1998. An Instrumented Hydraulic Fracture Experiment in Coal, In: SPE Rocky Mountain Regional / Low Permeability Reservoirs Symposium. Society of Petroleum Engineers, Denver, Colorado, pp. 43–50.

Jeffrey, R.G., Zhang, X., 2008. Hydraulic Fracture Growth in Coal, In: Southern Hemisphere Rock Mechanics Symposium. Perth, Western Australia.

Johns, J., Blount, C., Dethlefs, J., Julian, J., Loveland, M., McConnell, M., Schwartz, G., 2006. Applied ultrasonic technology in wellbore leak detection and case histories in Alaska North Slope wells. Proceedings of SPE Annual Technical Conference and Exhibition.

Johnson, R.L., Gas Projects Group, Scott, S., Herrington, M., Queensland Gas Co. Ltd., 2006. Changes in completion strategy unlock massive jurassic coalbed methane resource base in the Surat Basin , Australia, In: SPE Asia Pacific Oil and Gas Conference. pp. 1–16.

Johnson, R.L., Glassborow, B., Scott, M.P., Pallikathekathil, Z.J., Datey, A., Meyer, J., 2010a. Current Technologies to Understand Permeability, Stress Azimuths and Magnitudes and their Impact on Hydraulic Fracturing Success in a Coal Seam Gas Reservoir, In: SPE Asia Pacific Oil and Gas Conference and Exhibition. Society of Petroleum Engineers, Brisbane, Queensland, Australia.

Johnson, R.L., Scott, M.P., Jeffrey, R.G., Chen, Z.R., Bennett, L., Vendenborn, C., Tcherkashnev, S., 2010b. Evaluating Hydraulic Fracture Effectiveness in a Coal Seam Gas Reservoir from Surface Tiltmeter and Microseismic Monitoring, In: SPE Annual Technical. Society of Petroleum Engineers, Florence, Italy.

Kaiser, W., Ayers Jr, W., 1994. Geologic and hydrologic characterization of coalbed-methane reservoirs in the San Juan Basin. SPE Formation Evaluation.

Keller, S.R., Crook, R., Haut, R., Kulaofsky, D., 1987. Deviated wellbore cementing: part 1-problems. JPT, August, 955–960.

Khristianovic, S.A., Zheltov, Y.P., 1955. Formation of vertical fractures by means of highly viscous liquid, in: World Petroleum Congress. Rome, Italy.

King, G. E. and King, D. E. 2013. Environmental risk arising from well construction failure: difference between barrier and well failure, and estimates of failure frequency across common well types, locations and well age. SPE 166142, SPE Annual Tech. Conf. Exhib. New Orleans, Louisiana, USA, 30 Sept. – 2 Oct. 2013.

Kolstad, E., Mozill, G., Flores, J., 2004. Deepwater Isolation, shallow-water flow Hazards test cement in Marco Polo. *Offshore*, 64(1), 76.

Kresse, T., Warner, N., Down, A., Hays, P., Vengosh, A., Jackson, R., 2012. Shallow groundwater quality and geochemistry in the fayetteville shale gas-production area , North-central Arkansas, 2011, US Geological Survey Scientific Investigations Report, 5273.

Kristiansen, T., Barkved, O., Buer, K. Bakke, R., 2005. Production-induced deformations outside the reservoir and their impact on 4D seisimic. In: International Petroleum Technology Conference. Doha, Qatar.

Kunze, K.R., Steiger, R.P., Production, E., 1992. Accurate In situ Stress Measurements During Drilling Operations. SPE Annual Technical Conference and Exhibition.

Lal, M., Amoco, B.P., 1999. Shale Stability: Drilling Fluid Interaction and Shale Strength, In: SPE Latin American and Caribbean Petroleum Engineering Conference. Caracas, Venezuela.

Lecampion, B., Jeffrey, R.G., Detournay, E., 2004. Real-time estimation of fracture volume and hydraulic fracturing treatment efficiency, In: Gulf Rocks 2004, the 6th North America Rock Mechanics Symposium (NARMS). American Rock Mechanics Association, Houston, Texas.

Lecampion, B., Jeffrey, R.G., Detournay, E., 2005. Resolving the Geometry of Hydraulic Fractures from Tilt Measurements. *Pure and Applied Geophysics* 162, 2433–2452.

Leguillon, D., 2002. Strength or toughness? A criterion for crack onset at a notch. European Journal of Mechanics . *A/Solids* 21, 61–72.

Lewis, D., Miller, R., 2009. Casing Design, in Advanced Drilling and Well Technology, 1st ed. SPE.

Logan, T.L., 1993. Drilling techniques for coalbed methane, *Hydrocarbons From Coal*, 269-285.

Lyons, W., Plisga, G., 2004. Chapter 4. Drilling and Completions in Standard Handbook of Petroleum and Natural Gas Engineering, 2nd ed. SPE.

Marca, C., 1990. 13 Remedial Cementing, *Developments in Petroleum Science*, 28, 13-1.

Massonnet, D., Holzer, T., Vadon, H., 1997. Land subsidence caused by the East Mesa geothermal field, California, observed using SAR interferometry. *Geophysical Research Letters* 24, 901–904.

Matsunaga, I., Tenma, N., 1995. Characterization of forced flow in a deep fractured reservoir at the Hijiori hot dry rock test site, Yamagata, Japan, In: 8th ISRM Congress. pp. 795–798.

McDaniel, R.R., Borges, J.F., Dakshindas, S.S., 2007. A New Environmentally Acceptable Technique for Determination of Propped Fracture Height and Width, In: SPE Annual Technical Conference and Exhibition. Society of Petroleum Engineers, Anaheim, California.

McGowen, J.M., Gilbert, J.V., Samari, E., 2007. Hydraulic fracturing down under, In: SPE Hydraulic Fracturing Technology Conference. College Station, Texas.

Meek, J.W., Co, O.E., Harris, K., Services, H., 1993. Repairing casing leaks with small-particle-size cement. *SPE Production and Facilities*, 8(1), 45–50.

Meng, C., De Pater, C.J. De, 2011. Hydraulic fracture propagation in pre-fractured natural rocks, In: SPE Hydraulic Fracturing Technology Conference. The Woodlands, pp. 24–26.

Meng, Z., Zhang, J., Wang, R., 2011. In situ stress, pore pressure and stress-dependent permeability in the Southern Qinshui Basin. International *Journal of Rock Mechanics and Mining Sciences* 48, 122–131.

Meyer, B.R., 1989. Three-dimensional hydraulic fracturing simulation on personal computers: theory and comparison studies. Proceedings of SPE Eastern Regional Meeting.

Meyer, B.R., Bazan, L.W., 2011. A Discrete Fracture Network Model for Hydraulically Induced Fractures : Theory , Parametric and Case Studies, In: SPE Hydraulic Fracturing Technology Conference. pp. 1–36.

Milanovic, D., Smith, L., 2005. A Case History of Sustainable Annulus Pressure in Sour Wells – Prevention, Evaluation and Remediation. Proceedings of SPE High Pressure/High Temperature Sour Well Design Applied Technology Workshop.

Mills, K.W., Jeffrey, R.G., 2004. Remote High Resolution Stress Change Monitoring of Hydraulic Fractures, In: MassMin: Proud to Be Miners. Santiago, Chile.

Mills, K.W., Jeffrey, R.G., Zhang, X., 2004. Growth analysis and fracture mechanics based on measured stress change near a full-size hydraulic fracture, In: Gulf Rocks 2004, the 6th North America Rock Mechanics Symposium (NARMS).

Mohammad, H., Shaikh, S., 2010. Coalbed methane cementing best practices-Indian case history. In: International Oil and Gas Conference and Exhibition in China.

Moos, D., 2011. The influence of coal seam discontinuities on wellbore stability and production. SPE-WA. Available from: http://www.spe-wa.org/useruploads/files/09bdDr_spe143_web.pdf Accessed on 05/02/2013.

Morita, N., Fuh, G., Company, C., 2012. Parametric Analysis of Wellbore Strengthening Methods from Basic Rockmechanics. Paper SPE 145765 presented at SPE Annual Technical Conference and Exhibition, Denver, Colorado, 30 October–2 November.

Morris, C., Sabbagh, L., Wydrinski, R., 2007. Application of Enhanced Ultrasonic Measurements for Cement and Casing Evaluation. In: SPE/IADC Drilling Conference.

Mukherjee, H., Paoli, B.F., McDonald, T., Cartaya, H., Anderson, J.A., 1995. Successful control of fracture height growth by placement of artificial barrier, In: SPE Rocky Mountain Regional / Low Permeability Reservoirs Symposium. Denver, Colorado.

Naceur, K. Ben, Touboul, E., 1990. Mechanisms controlling fracture-height growth in layered media. *SPE Production Engineering*, 5(2), 142–150.

Nagel, N., Sanchez, M., Lee, B., 2012. Gas shale hydraulic fracturing: a numerical evaluation of the effect of geomechanical parameters, In: SPE Hydraulic Fracturing Technology Conference and Exhibition. pp. 1–19.

Nagel, N.B., 2001. Compaction and subsidence issues within the petroleum industry: from Wilmington to Ekofisk and beyond. Physics and Chemistry of the Earth, Part A: Solid Earth and Geodesy, 26(1), 3–14.

Nicot, J., 2009. A survey of oil and gas wells in the Texas Gulf Coast , USA , and implications for geological sequestration of CO 2. *Environ Geol* 1625–1638.

Nolte, K.G., 1991. Fracturing pressure analysis for nonideal behavior. *Journal of Petroleum Technology*, 43(2), 210–218.

Nolte, K.G., Smith, M.B., 1981. Interpretation of Fracturing Pressures. *Society of Petroleum Engineers Journal*, 33(9), 1767–1775.

Nordgren, R.P., 1972. Propagation of a Vertical Hydraulic Fracture. *SPE Journal August*, 306–314.

NSI Technologies, 2012. StimPlan Software.

NSW Government, 2012. Code of Practice for Coal Seam Gas: Well Integrity. NSW Government.

Okada, Y., 1985. Surface deformation due to shear and tensile faults in a half-space. *Bulletin of the Seismological Society of America*, 75, 1135–1154.

Okada, Y., 1992. Internal deformation due to shear and tensile faults in a half-space. *Bulletin of the Seismological Society of America*, 82, 1018–1040.

Olson, J., Du, Y., Du, J., 1997. Tiltmeter data inversion with continuous, non-uniform opening distributions: A new method for detecting hydraulic fracture geometry. *International Journal of Rock Mechanics and Mining Sciences*, 34(3), 236.e1.

Origin, ConocoPhillips, Sinopec, 2013. Hydraulic fracture stimulation: A safe way to extract coal seam gas. Available from: http://www.aplng.com.au/pdf/factsheets/Factsheet_Fraccing.APLNG.pdf, Accessed on 30-01-2013.

Palmer, I.D., Sparks, D.P., 1991. Measurement of Induced Fractures by Downhole TV Camera in Black Warrior Basin Coalbeds. *Journal of Petroleum Technology*, 43(3), 270–328.

Parcevaux, P., Rae, P., Drecq, P., 1990. Prevention of Annular Gas Migration. In Well Cementing, Schlumberger Educational Services, Houston.

Peirce, A., Detournay, E., 2008. An implicit level set method for modeling hydraulically driven fractures. *Computer Methods in Applied Mechanics and Engineering* 197, 2858–2885.

Peirce, A.P., Gu, H., Siebrits, E., 2009. Uniform asymptotic Green's functions for efficient modeling of cracks in elastic layers with relative shear deformation controlled by linear springs. *International Journal for Numerical and Analytical Methods in Geomechanics Methods* 33, 285–308.

Peirce, A.P., Siebrits, E., 2001. Uniform asymptotic approximations for accurate modeling of cracks in layered elastic media. *International Journal of Fracture* 110, 205–239.

Perkins, T.K., Kern, L.R., 1961. Widths of Hydraulic Fractures. *Journal of Petroleum Technology* September, 937–949.

Poland, J., Davis, G., 1969. Land subsidence due to withdrawal of fluids. Geological Society of America, INC reviews in Engineering Geology II 187–269.

Pollard, D.D., Holzhausen, G., 1979. On the mechanical interaction between a fluid-filled fracture and the Earth's surface. *Tectonophysics*, 53(1), 27-57.

Prats, M., Maraven, S.A., 1981. Effect of Burial History on the Subsurface Horizontal Stresses of Formations Having Different Material Properties. Society of Petroleum Engineers Journal 658–662.

Press, W.H., Teukolsky, S.A., Vetterling, W.T., Fannery, B.P., 1986. Fortran Numerical Recipes, Second Edited. ed. Cambridge University Press, Cambridge, United Kingdom.

Queensland Government, 2012. Queensland's coal seam gas overview (February 2012). Available from: www.mines.industry.qld.gov.au Accessed on 11/02/2013.

Quinn, T.S., 1994. Experimental Analysis of Permeability Barriers to Hydraulic Fracture Propagation. (Doctoral dissertation, Massachusetts Institute of Technology).

Rahim, Z., Al-qahtani, M.Y., 2001. Using Radioactive Tracer Log , Production Tests , Fracture Pressure Match , and Pressure Transient Analysis to Accurately Predict Fracture Geometry in Jauf Reservoir , Saudi Arabia, In: SPE Annual Technical Conference and Exhibition. Society of Petroleum Engineers, New Orleans, Louisiana.

Ravi, K.M., Beirute, R.M., Covington, R., 1992. Erodibility of partially dehydrated gelled drilling fluid and filter cake, In: Annual Technical Conference and Exhibition. Washington, D.C.

Renshaw, C.E., Pollard, D.D., 1995. An experimentally verified criterion for propagation across unbounded frictional interfaces in brittle, linear elastic materials. *International Journal of Rock Mechanics and Mining Sciences and Geomechanics Abstracts* 32, 237–249.

Roeloffs, E.A., 1988. Hydrologic precursors to earthquakes: A review. *Pure and Applied Geophysics PAGEOPH* 126, 177–209.

Rongved, L., Frasier, J.T., 1958. Displacement discontinuity in the elastic half-space. *Journal of Applied Mechanics* 25, 125–128.

Rongved, L., Hill, N.J., 1957. Dislocation over a bounded plane area in an infinite solid. *Journal of Applied Mechanics* 24, 252–254.

Saulsberry, J.L., Schafer, P.S, Schraufnagel, R.A., 1996. A guide to coalbed methane reservoir engineering. Chicago: Gas Research Institute.

Savitski, A.A., Detournay, E., 2002. Propagation of a penny-shaped fluid-driven fracture in an impermeable rock: asymptotic solutions. *International Journal of Solids and Structures* 39, 6311–6337.

Sayers, C., Boer, L.D., Lee, D., 2006. Predicting reservoir compaction and casing deformation in deepwater turbidites using a 3D mechanical earth model. First International Oil Conf., 1–7.

Schraufnagel, R.A. 1993. Coalbed methane production. Chapter 15 of AAPG Studies in Geology 38, pp. 341.361.

Segall, P., 1985. Stress and subsidence resulting from subsurface fluid withdrawal in the epicentral region of the 1983 Coalinga earthquake. *Journal of Geophysical Research* 90, 6801–6816.

Settari, A., 1988. Quantitative Analysis of Factors Influencing Vertical and Lateral Fracture Growth. *SPE Production Engineering* 3, 310–322.

Settari, A., 2002. Reservoir Compaction. *Society of Petroleum Engineers Journal* 62–69.

Settari, A., Cleary, M.P., 1984. Three-dimensional simulation of hydraulic fracturing. *Society of Petroleum Engineers Journal*, 1177–1190.

Settari, A., Walters, D.A., 2001. Advances in coupled geomechanical and reservoir modeling with applications to reservoir compaction, In: SPE Reservoir Simulation Symposium. Society of Petroleum Engineers, pp. 14–17.

Settari, A., Walters, D.A., Stright, D.H., Aziz, K., 2008. Numerical Techniques Used for Predicting Subsidence Due to Gas Extraction in the North Adriatic Sea. *Petroleum Science and Technology* 26, 1205–1223.

Sheives, T.C., Tello, L.N., V.E., M., Standley, T.E., Blankinship, T.J., 1986. A Comparison of New Ultrasonic Cement and Casing Evaluation Logs With Standard Cement Bond Logs. Proceedings of SPE Annual Technical Conference and Exhibition.

Siebrits, E., and Peirce, A.P., 2002. An Efficient Multi-Layer Planar 3D Fracture Growth Algorithm Using a Fixed Mesh Approach. *International Journal for Numerical Methods in Engineering* 53 (3) (January 30): 691–717. doi:10.1002/nme.308. http://doi.wiley.com/10.1002/nme.308.

Siemers, G., Ukomah, T., Mack, R., 2003. Development and Field Testing of Solid Expandable Corrosion Resistant Cased-Hole Liners to Boost Gas Production in Corrosive Environments. Offshore Technology.

Simonson, E.R., Abou-Sayed, A.S., Clifton, R.J., 1978. Containment of Massive Hydraulic Fractures. *Society of Petroleum Engineers Journal* 6089, 27–32.

Smith, M., Rosenberg, R., Bowen, J.F., 1982. Fracture width-design vs. measurement, In: SPE Annual Technical Conference and Exhibition. p. 9.

Smith, M.B., Ren, N..K., Sorrells, G.G., Teufel, L.W., 1986. A Comprehensive Fracture Diagnostics Experiment: Part 2. Comparison of Fracture Azimuth Measuring Procedures. *SPE Production and Operations* 423–431.

Smith, R., 1990, Nelson, E. (Ed.). Well Cementing (Preface), Elsevier Science. ISBN: 0-444-88751-2 (Vol.28).

Sneddon, I.N., 1946. The Distribution of Stress in the Neighbourhood of a Crack in an Elastic Solid. *Proceedings of the Royal Society A: Mathematical, Physical and Engineering Sciences* 187, 229–260.

Sneddon, I.N., Elliott, H.A., 1946. The opening of a Griffith crack under internal pressure. *Journal of Applied Mechanics* 4, 262–267.

Snyder, R.E. and McCabe, C.R. 1988. Ekofisk Jack-up: The Story behind the Headlines. *Ocean industry*, 23(1), 27-55.

Sousa, J.L., Carter, B., Ingraffea, A., 1993. Numerical simulation of 3D hydraulic fracture using Newtonian and power-law fluids. *International Journal of Rock Mechanics and Mining Sciences* 30, 1265–1271.

Spence, D.A., Sharp, P., 1985. Self-similar solutions for elastohydrodynamic cavity flow, In: *Proceedings of the Royal Society A: Mathematical, Physical and Engineering Sciences*. pp. 289–313.

Standards Norway, 2004. Norsok Standard: Well integrity in drilling and well operations. Lysaker, Norway.

Starfield, A., Cundall, P., 1988. Towards a methodology for rock mechanics modelling. *International Journal of Rock Mechanics and Mining Science*, 25(3), pp.99–106. Available at: http://www.sciencedirect.com/science/article/pii/0148906288922929.

Steidl, P.F., 1993. Evaluation of Induced Fractures Intercepted by Mining, In: International Coalbed Methane Symposium. The University of Alabama, Tuscaloosa, Alabama, pp. 675–686.

Steiger, R.P., Leung, P.K., Production, E., 1992. Quantitative Determination of the Mechanical Properties of Shales. *SPE Drilling Engineering* 181–185.

Stewart, W.J., Barro, L., 1982. Coal seam degasification by use of hydraulic fracturing in vertical wells: Case histories, In: Seam Gas Drainage with Particular Reference to the Working Seam. Illawarra, New South Wales, Australia, pp. 89–98.

Storaune, A., Winters, W., 2005. Versatile expandable technology for casing repair. SPE/IADC Drilling Conference 1–8.

Sulak, R. M. and Danielsen, J. 1988. Reservoir Aspects of Ekosfisk Subsidence. Paper OTC 5618 presented at the 1988 Offshore Technology Conference, Houston.

Suman, G.O.J., Ellis, R.E., 1977. World oil's Cementing Oil and Gas Wells Including Casing handling Procedures. Books on Demand, MI.

Sun, R.J., 1969. Theoretical size of hydraulically induced horizontal fractures and corresponding surface uplift in an idealized medium. *Journal of Geophysical Research* 74, 5995.

Tan, B., Lang, M., Sheth, D., 2012. High-strength, low-density cement pumped on-the-fly using volumetric mixing achieves cement to surface in heavy loss coal seam gas field. SPE Asia Pacific Oil and Gas Conference and Exhibition, 1–10.

Taoutaou, S., 2010. Well integrity - expert view. Oil and Gas Middle East, 6(2), 34.

TerraTek, 1996. GRI.95/0432 Project Final Report.

Thiercelin, M., Roegiers, J.C., Boone, T.J., Ingraffea, A.R., 1987. An investigation of the material parameters that govern the behavior of fractures approaching rock interfaces, In: 6th ISRM Congress. pp. 263–269.

Tian, J., Wang, Q., Guo, Q., Guo, H., Liu, C., 2011. Casing Integrity Evaluation in Deep Well with Extreme Heavy Mud in Tarim Basin. SPE EUROPEC/EAGE Annual Meeting.

Tingay, M., Reinecker, J., Müller, B., 2008. Borehole breakout and drilling-induced fracture analysis from image logs. World Stress Map Project.

Touboul, E., BenNaceur, K., Thiercelin, M., 1986. Variational methods in the simulation of three-dimensional fracture propagation, In: Hartman, H.L. (Ed.), The 27th US Symposium on Rock Mechanics (USRMS). Society of Mining Engineers, Alabama, pp. 659–668.

US EPA, 2004. Evaluation of Impacts to Underground Sources of Drinking Water by Hydraulic Fracturing of Coalbed Methane Reservoirs. US Environmental Protection Agency, Office of Water, Washington, DC.

US EPA, 2010. Coalbed Methane Extraction: Detailed Study Report. US Environmental Protection Agency, Office of Water, Washington, DC.

Van Eekelen, H.A.M., 1982. Hydraulic fracture geometry: fracture containment in layered formations. *Society of Petroleum Engineers Journal*, 22, 341–349.

Van Kuijk, R., Zeroug, S., Froelich, B., 2005. A novel ultrasonic cased-hole imager for enhanced cement evaluation, In: International Petroleum Technology Conference.

van Oort, E., 2003. On the physical and chemical stability of shales. *Journal of Petroleum Science and Engineering*, 38, 213–235.

van Oort, E., Hale, A.H., Mody, F.K., 1995. Manipulation of coupled osmotic flows for stabilisation of shales exposed to water-based drilling fluids, In: SPE Annual Technical Conference and Exhibition. Dallas, Texas, pp. 497–509.

van Oort, E., Ripley, D., Ward, I., Chapman, J.W., Williamson, R., Aston, M., 1996. Silicate-based drilling fluids: competent, cost-effective and benign solutions to wellbore stability problems, In: IADC/SPE Drilling Conference. New Orleans, Louisiana, pp. 189–203.

Vandamme, L., Curran, J., 1989. A three-dimensional hydraulic fracturing simulator. *International Journal for Numerical Methods in Engineering* 28, 909–927.

Vignes, B., Aadnoy, B.S., 2010. Well-integrity issues offshore Norway, In: SPE/IADC Drilling Conference. Orlando, Florida.

Vudovich, A., Chin, L., Morgan, D.R., 1988. Casing deformation in Ekofisk. Offshore Technology Conference 729–734.

Walton, I., McLennan, J., 2013. The role of natural fractures in shale gas production. Effective and Sustainable Hydraulic Fracturing, ISBN: 978-953-51-1137-5, Intech. Available from http://www.intechopen.com/books/effective-and-sustainable-hydraulic-fracturing/the-role-of-natural-fractures-in-shale-gas-production

Warpinski, N., Lorenz, J., Branagan, P., 1993. Examination of a cored hydraulic fracture in a deep gas well. SPE Production and Facilities 150–164.

Warpinski, N.N.R., 1985. Measurement of width and pressure in a propagating hydraulic fracture. *SPE Journal*, 25(1), 46–54.

Warpinski, N.R., 2000. Analytic crack solutions for tilt fields around hydraulic fractures. *Journal of Geophysical Research*, 105(B10), 23463-23.

Warpinski, N.R., 2006. Hydraulic fracture mapping with hybrid microseismic / tiltmeter arrays. *GasTIPS*, 12(3), 17–20.

Warpinski, N.R., 2011. Measurements and Observations of Fracture Height Growth. In: US EPA Technical Workshop for the Hydraulic Fracturing Study: Chemical and Analytical Methods, Arlington, Virginia. Availabe from: <http://water.epa.gov/type/groundwater/uic/class2/hydraulicfracturing>. Accessed on 30-01-2013.

Warpinski, N.R., Teufel, L.W., 1987. Influence of geologic discontinuities on hydraulic fracture propagation. *Journal of Petroleum Technology* 209–220.

Warpinski, N.R., Waltman, C.K., Weijers, L., 2010. An evaluation of microseismic monitoring of lenticular tight-sandstone stimulations. *SPE Production and Operations* 23–25.

Warpinski, N.R. 2013. Understanding hydraulic fracture growth, effectiveness, and safety through microseismic monitoring. proceedings of the international conference for effective and sustainable hydraulic fracturing. Intech. ISBN: 978.953.51.1137.5. Available from: http://www.intechopen.com/books/effective-and-sustainable-hydraulic-fracturing

Watson, T., 2004. Surface casing vent flow repair - A process. In: Canadian International Petroleum Conference.

Watson, T., Bachu, S., 2009. Evaluation of the potential for gas and $CO_2$ leakage along wellbores. *SPE Drilling and Completion* 115–126.

Watson, T., Getzlaf, D., Griffith, J., 2002. Specialized Cement Design and Placement Procedures Prove Successful for Mitigating Casing Vent Flows . Case Histories. Proceedings of SPE Gas Technology Symposium.

Weng, X., Kresse, O., Cohen, C., Wu, R., Gu, H., 2011. Modeling of hydraulic-fracture-network propagation in a naturally fractured formation. *SPE Production and Operations* 368–380.

Weng, X. 1993. Fracture Initiation and Propagation from Deviated Wellbores. SPE Annual Technical Conference and Exhibition. SPE.

Wojtanowicz, A.K., 2008. Chapter 3 Environmental Control of Well Integrity.

Wright, C., Davis, E., Golich, G., Ward, J.., 1998a. Downhole tiltmeter fracture mapping: Finally measuring hydraulic fracture dimensions, In: SPE Western Regional Conference. Bakersfield, California, U.S.A.

Wright, C.A., Davis, E.J., Minner, W.A., Ward, J.F., Weijers, L., Schell, E.J., Hunter, S.P., 1998b. Surface tiltmeter fracture mapping reaches new depths - 10,000 feet and beyond?, In: SPE Rocky Mountain Regional / Low Permeability Reservoirs Symposium. Denver, Colorado, pp. 135–146.

Wright, C.A., Stewart, D.W., Emanuele, M.A., Wright, W.W., 1994. Reorientation of propped refracture treatments in the Lost Hills field, In: SPE Western Regional Conference. Long Beach California, pp. 483–497.

Wright, C.A., Weijers, L., 2001. Hydraulic fracture reorientation: Does it occur? Does it matter? The Leading Edge 1185–1189. http://dx.doi.org/10.1190/1.1487252.

Wright, J., Moore, M., Winters, W., 2003. Expandable tubular casing repairs: four case histories. Proceedings of SPE Annual Technical Conference and Exhibition.

Wu, H., Chudnovsky, A., Dudley, J.W., Wong, G.K., 2004. A map of fracture behavior in the vicinity of an interface, In: Gulf Rocks 2004, the 6th North America Rock Mechanics Symposium (NARMS). Houston, Texas.

Yadav, A., Sharma, A. K. and Walia, A. 2003. Casing impairment/damage in stress-sensitive reservoir – a case study. Paper 2003-133 presented at Petroleum Society's Canadian International Petroleum Conference 2003, Calgary, Alberta, Canada.

Yang, X., Davis, P.M., 1986. deformation due to a rectangular tension crack in an elastic half-space. *Bulletin of the Seismological Society of America* 76, 865–881.

Yudovich, A., Chin, L. Y. and Morgan, D. R. (1988). Casing deformation in Ekofish. Paper OTC 5623 presented at the 1988 Offshore Technology Conference, Houston.

Zhang, M., Bachu, S., 2011. Review of integrity of existing wells in relation to $CO_2$ geological storage: What do we know? *International Journal of Greenhouse Gas Control* 5, 826–840.

Zhang, X., Detournay, E., Jeffrey, R.G., 2002. Propagation of a penny-shaped hydraulic fracture parallel to the free-surface of an elastic half-space. *International Journal of Fracture* 125–158.

Zhang, X., Jeffrey, R.G., Thiercelin, M., 2007a. Effects of frictional geological discontinuities on hydraulic fracture propagation, in: SPE Hydraulic Fracturing Technology Conference. Society of Petroleum Engineers, College Station, Texas, pp. 1–11.

Zhang, X., Jeffrey, R.G., Thiercelin, M., 2007b. Deflection and propagation of fluid-driven fractures at frictional bedding interfaces: A numerical investigation. *Journal of Structural Geology* 29, 396–410.

Zhang, X, Jeffrey, R.G, 2008, Fluid-driven fracture growth. *Journal of Geophysical Research*, 113, 1-16.

Zhang, X., Jeffrey, R.G., Thiercelin, M., 2008. Escape of fluid-driven fractures from frictional bedding interfaces: A numerical study. *Journal of Structural Geology* 30, 478–490.

Zheng, Z., Kemeny, J., Cook, N.G.W., 1989. Analysis of Borehole Breakouts. *Journal of Geophysical Research* 94, 7171–7182.

Zimmer, U., Maxwell, S., Waltman, C., Warpinski, N., 2009. Microseismic monitoring quality-control (QC) reports as an interpretative tool for nonspecialists. SPE Journal.

Zoback, M.D., 2007. Reservoir Geomechanics. Cambridge University Press, Cambridge, United Kingdom.

Zoback, M.D., Moos, D., Mastin, L., Anderson, R.N., 1985. Wellbore breakouts and in situ stress. *Journal of Geophysical Research* 90, 5523.